

The Effect of Local Heating on the Weld Line Formation in Plastic Injection Molding of Acrylonitrile Butadiene Styrene and Glass Fiber Reinforced Polypropylene

Master of Science
in Mechanical Engineering

by
Muhsin Deniz GÜLER
ORCID 0000-0002-2471-1881

February, 2022

This is to certify that we have read the thesis **The Effect of Local Heating on the Weld Line Formation in Plastic Injection Molding of Acrylonitrile Butadiene Styrene and Glass Fiber Reinforced Polypropylene** submitted by **Muhsin Deniz GÜLER**, and it has been judged to be successful, in scope and in quality, at the defense exam and accepted by our jury as a MASTER'S.

APPROVED BY:

Advisor: **Asst. Prof. Dr. Aydın ÜLKER**
İzmir Kâtip Çelebi University

Co-advisor: **Prof. Dr. –Ing Sami SAYER**
Ege University

Committee Members:

Prof. Dr. Çiçek ÖZES
Dokuz Eylül University

Prof. Dr. Kutlay SEVER
İzmir Kâtip Çelebi University

Date of Defense: February 03, 2022

Declaration of Authorship

I, **Muhsin Deniz GÜLER**, declare that this thesis titled **The Effect of Local Heating on the Weld Line Formation in Plastic Injection Molding of Acrylonitrile Butadiene Styrene and Glass Fiber Reinforced Polypropylene** and the work presented in it are my own. I confirm that:

- This work was done wholly or mainly while in candidature for the Master's / Doctoral degree at this university.
- Where any part of this thesis has previously been submitted for a degree or any other qualification at this university or any other institution, this has been clearly stated.
- Where I have consulted the published work of others, this is always clearly attributed.
- Where I have quoted from the work of others, the source is always given. This thesis is entirely my own work, with the exception of such quotations.
- I have acknowledged all major sources of assistance.
- Where the thesis is based on work done by myself jointly with others, I have made clear exactly what was done by others and what I have contributed myself.

Date: 03.02.2022

The Effect of Local Heating on the Weld Line Formation in Plastic Injection Molding of Acrylonitrile Butadiene Styrene and Glass Fiber Reinforced Polypropylene

Abstract

In this study, the effect of local heating on the weld line formation in a plastic injection mold was studied by using acrylonitrile butadiene styrene (ABS) and polypropylene 20% glass fiber (PP GF20) plastic material. An aluminum 6000 insert was fitted into the injection mold to set temperatures for local heating. The three parameters with three levels were selected for injection molding process parameters as insert temperature, mold temperature, and melt temperature and to produce mechanical tests specimens with weld lines and non-weld lines. L₉ orthogonal array was arranged for the Taguchi method.

To verify the mold design, plastic injection molding simulation software Moldex3D was implemented for plastic filling analysis. The tensile and bending test results for specimens were analyzed by using the statistics package Minitab 19.1.

Consequently, the contribution rates of the insert temperature for the weld line tensile and bending strength were calculated as 0.40% and 64.97% for ABS, respectively. The contribution rates of the insert temperature for the weld line tensile and bending strength were calculated as 38.31% and 62.05% for PP GF20, respectively.

Keywords: Plastic injection molding, mold local heating, weld line, acrylonitrile butadiene styrene, glass fiber reinforced polypropylene

Akrilonitril Bütadien Stiren ve Cam Elyaf Takviyeli Polipropilenin Plastik Enjeksiyon Kalıplamasında Lokal Isıtmanın Birleşme İzi Oluşumuna Etkisi

ÖZ

Bu çalışmada, plastik enjeksiyon kalıbında lokal ısıtmanın birleşme izi oluşumu üzerindeki etkisini akrilonitril bütadien stiren (ABS) ve polipropilen %20 cam elyaf (PP GF20) plastik malzemesi kullanılarak incelenmiştir. Yerel ısıtma için sıcaklıkları ayarlamak üzere enjeksiyon kalıbına bir alüminyum 6000 serisi insert parçası yerleştirildi. Enjeksiyon kalıplama proses parametreleri için insert sıcaklığı, kalıp sıcaklığı ve eriyik sıcaklığı olarak üç seviyeli üç parametre seçildi ve birleşme izi ve birleşme izi olmayan mekanik test numuneleri üretildi. Taguchi yöntemi için L₉ ortogonal dizisi düzenlenmiştir.

Kalıp tasarımını doğrulamak için, plastik enjeksiyon kalıplama simülasyon yazılımı Moldex3D programında plastik dolum analizi uygulanmıştır. Numuneler için çekme ve eğilme test sonuçları Minitab 19.1 istatistik programı kullanılarak analiz edildi.

Sonuç olarak, ABS malzemesinde birleşme izi ve birleşme izi olmayan çekme ve eğilme mukavemetleri için lokma sıcaklığının katkı oranı sırasıyla %0.40 ve %64.97 olarak hesaplanmıştır. PP GF20 malzemesinde birleşme izi ve birleşme izi olmayan çekme ve eğilme mukavemetleri için lokma sıcaklığının katkı oranı sırasıyla %38.31 ve %62.05 olarak hesaplanmıştır.

Anahtar Kelimeler: Plastik enjeksiyon kalıplama, lokal kalıp ısıtma, birleşme izi, akrilonitril bütadien stiren, cam elyaf takviyeli polipropilen

The thesis work is to be dedicated to my family...

Acknowledgment

I would like to thank my advisor Asst. Prof. Dr. Aydın ÜLKER, and my co-advisor Prof. Dr. –Ing Sami SAYER for their contributions, supports, and experiences.

I would like to thank my parents Yasemin GÜLER and Abbas GÜLER, my sister Zeynep GÜLER who have always been with me.

The mold for test specimen and plastic raw materials were supplied by the Plastic Technology Laboratory of Ege Vocational High School at Ege University. The mold revisions were machined and the tensile specimens by injection molding were fabricated at Metis Kalıp Makina Elektronik Mühendislik San. ve Tic. A.Ş. The authors would like to thank The Plastic Technology Laboratory of Ege Vocational High School at Ege University and Metis Kalıp Makina Elektronik Mühendislik San. ve Tic. A.Ş. The authors also thank Moldex3D Insource Yazılım in Turkey for licensing the academic version of the software.

Table of Contents

Declaration of Authorship.....	ii
Abstract	iii
Öz.....	iv
Acknowledgment	vi
List of Figures	x
List of Tables.....	xiv
List of Abbreviations.....	xvi
List of Symbols	xviii
1 Introduction.....	1
2 Formations and Types of the Weld Line.....	9
2.1 Formations of the Weld Line	9
2.2 Type of the Weld Line	11
3 Literature Research	14
3.1 Effects of Molding and Injection Parameters on the Properties of Plastics...15	
3.2 Effects of Reinforcement and Filling Materials on the Properties of Plastics	21
3.2.1 Effect of Reinforcement Materials on Plastics	22
3.2.2 Effect of Filler Materials on Plastics	25
4 The Effect of the Plastic Parts and Mold Design on the Weld Line	29
4.1 Improved Plastic Part Design to Reduce the Effect of the Weld Line.....	30
4.1.1 Ribs and Bosses Design.....	30
4.1.2 Hole and Gap Designs	31
4.2 Improved Mold Design to Reduce the Effect of the Weld Line	33

4.2.1	The Gate	34
4.2.2	Air Vent Channel.....	37
4.2.3	Cooling System.....	40
5	Materials and Methods	46
5.1	Materials	46
5.2	Methods.....	46
5.2.1	Plastic Injection Molding.....	46
5.2.2	Tensile Testing Machine	47
5.2.3	Mold Temperature Controller.....	47
5.2.4	Temperature Control Module	48
6	Experiments.....	49
6.1	Design of Experiments.....	49
6.2	The Mold and Plastic Part Design	54
6.2.1	Design of Gates and Runners	61
6.2.1.1	Gates.....	61
6.2.1.2	Runners.....	63
6.2.2	The Cooling Channel Design	64
6.2.3	The Air Vent Channel Design	66
6.3	Tensile Tests and Bending Tests.....	67
6.3.1	Tensile Tests	67
6.3.2	Bending Tests	69
7	Analyses and Results.....	72
7.1	Plastic Injection Filling Analysis	72
7.1.1	Plastic Filling Analysis of ABS.....	73
7.1.2	Plastic Filling Analysis of PP GF20.....	75
7.2	Tensile and Bending Properties	77
7.2.1	Results of ABS	77

7.2.1.1	Results of the Tensile Tests for ABS	77
7.2.1.2	Results of the Bending Tests for ABS.....	81
7.2.2	Results of PP GF20	86
7.2.2.1	Results of the Tensile Tests for PP GF20	86
7.2.2.2	Results of the Bending Tests for PP GF20.....	93
7.3	Effects of Process Parameters on Weld Line Strength – ABS and PP GF20	100
7.3.1	Effect of Insert Temperature.....	100
7.3.2	Effect of Mold Temperature	101
7.3.3	Effect of Melt Temperature	102
8	Conclusion.....	104
9	Future Work.....	108
	References	109
	Appendices.....	114
	Appendix A Publications from the Thesis.....	115
	Curriculum Vitae	116

List of Figures

Figure 1.1	World benchmark plastics / steel between 1950-2015	2
Figure 1.2	World thermoplastics demand: 2015	2
Figure 1.3	Molecular oriented in (a) amorphous and (b) semicrystalline plastics.....	4
Figure 1.4	Polymer pyramid	5
Figure 1.5	Basic units of injection molding machine	7
Figure 1.6	Plastic injection molding processes	7
Figure 1.7	Formation of weld line.....	8
Figure 2.1	The process of weld line forming	10
Figure 2.2	The effect of different gate types on the weld line, (a) The single gate, (b) The two gates	11
Figure 2.3	Formation of weld line types	12
Figure 2.4	Melt line and knit line.....	12
Figure 2.5	Formation of meeting angle.....	13
Figure 3.1	Relationship between melt temperature and strength of weld line and a third-order polynomial trend line.....	15
Figure 3.2	Process parameter levels S/N ratio of weld line strength in PP	17
Figure 3.3	Process parameter levels S/N ratio of weld line strength in GPPS	18
Figure 3.4	Comparison of maximum tensile strength for non-weld line and cold-weld line specimens at 140 °C, 150 °C, and 160 °C mold temperatures	19
Figure 3.5	Effect of mold temperature on (a) Storage modulus (E') and (b) Loss factor (tanδ) of PBT.....	20
Figure 3.6	Orientation of reinforcement material in the weld line region	22
Figure 3.7	Stress-strain graph in the weld line region of fiber reinforced PP composite, (a) Glass fiber, (b) Carbon fiber, (c) Aramid fiber.....	23
Figure 3.8	Weld line and non-weld line strengths of glass fiber parts.....	24

Figure 3.9	Tensile strength of CaCO ₃ , SiO ₂ , and CB fillers added to rubber material with and without the weld line, (a) phr of CaCO ₃ , (b) phr of SiO ₂ , (c) phr of CB	26
Figure 3.10	The density and hardness graph of PP-R at different CaCO ₃ ratios	28
Figure 4.1	The rib dimensions	31
Figure 4.2	Tensile strength of specimens with/without weld line for obstacle edge angle, (a) Melt temperature, (b) Packing pressure	32
Figure 4.3	(a) Diaphragm gate and cross-section (b) Ring gate and cross-section..	35
Figure 4.4	Fan gate.....	36
Figure 4.5	Improved the fan gate design.....	37
Figure 4.6	Cold slug well design	37
Figure 4.7	Air Trap	38
Figure 4.8	Samples of the air trap defect	38
Figure 4.9	The design of the air vent channel	39
Figure 4.10	The effect of the mold temperature on the weld line factor for PP	41
Figure 4.11	In line transverse cooling channel	42
Figure 4.12	In line longitudinal cooling channel	43
Figure 4.13	Spiral cooling channel	43
Figure 4.14	Zig-zag cooling channel	43
Figure 5.1	Arburg Allrounder 470C Golden Edition plastic injection molding machine.....	47
Figure 5.2	RTC 950 series oil type mold temperature controller	48
Figure 5.3	Opkon HCC-4 hot runner control module	48
Figure 6.1	The mold of the tensile test specimen.....	55
Figure 6.2	Design of the cavity side of the mold	56
Figure 6.3	The cavity side of the mold	57
Figure 6.4	Design of the core side of the mold	58
Figure 6.5	The core side of the mold	59
Figure 6.6	The insert design.....	60
Figure 6.7	ABS specimens	60
Figure 6.8	PP GF20 specimens	61

Figure 6.9	The weld line region of PP GF20	61
Figure 6.10	The fan gate design.....	62
Figure 6.11	Dimension of 1. fan gate.....	63
Figure 6.12	Dimension of 2. fan gate.....	63
Figure 6.13	Dimension of 3. fan gate.....	63
Figure 6.14	Runner dimensions, (a) Thin runner, (b) Thick runner	64
Figure 6.15	Cooling channel design of the insert	65
Figure 6.16	Cooling channel design of the cavity.....	65
Figure 6.17	Cooling channel design of the core	66
Figure 6.18	The weld line specimen made of PP GF20 after tensile test	67
Figure 6.19	The non-weld line specimen made of PP GF20 after tensile test.....	67
Figure 6.20	Dimensions of the specimen in DIN EN ISO 527-2 standard	68
Figure 6.21	The tensile testing machine	68
Figure 6.22	The weld line specimen made of PP GF20 after bending testing.....	69
Figure 6.23	Dimensions of the specimen in DIN EN ISO 178-2019 standard.....	70
Figure 6.24	The three-point bending test machine.....	71
Figure 7.1	The plastic filling analysis design in the Moldex3D program.....	73
Figure 7.2	Filling ABS in 50% time	74
Figure 7.3	Filling ABS in 95% time	74
Figure 7.4	Filling ABS in 100% time	75
Figure 7.5	Filling PP GF20 in 50% time.....	76
Figure 7.6	Filling PP GF20 in 95% time.....	76
Figure 7.7	Filling PP GF20 in 100% time.....	77
Figure 7.8	Main effects plot for S/N ratios: insert temperature vs. weld line tensile strength for the weld line for ABS	78
Figure 7.9	Main effects plot for S/N ratios: mold temperature vs. weld line tensile strength for the weld line for ABS	79
Figure 7.10	Main effects plot for S/N ratios: melt temperature vs. weld line tensile strength for the weld line for ABS	79
Figure 7.11	Main effects plot for S/N ratios: insert temperature vs. weld line bending strength for the weld line for ABS	83
Figure 7.12	Main effects plot for S/N ratios: mold temperature vs. weld line bending strength for the weld line for ABS	83

Figure 7.13 Main effects plot for S/N ratios: melt temperature vs. weld line bending strength for the weld line for ABS	84
Figure 7.14 Main effects plot for S/N ratios: insert temperature vs. weld line tensile strength for the weld line for PP GF20.....	87
Figure 7.15 Main effects plot for S/N ratios: mold temperature vs. weld line tensile strength for the weld line for PP GF20.....	87
Figure 7.16 Main effects plot for S/N ratios: melt temperature vs. weld line tensile strength for the weld line for PP GF20.....	88
Figure 7.17 Main effects plot for S/N ratios: mold temperature vs. non-weld line tensile strength for the non-weld line for PP GF20.....	90
Figure 7.18 Main effects plot for S/N ratios: melt temperature vs. non-weld line tensile strength for the non-weld line for PP GF20.....	91
Figure 7.19 Main effects plot for S/N ratios: insert temperature vs. weld line bending strength for the weld line for PP GF20.....	94
Figure 7.20 Main effects plot for S/N ratios: mold temperature vs. weld line bending strength for the weld line for PP GF20.....	95
Figure 7.21 Main effects plot for S/N ratios: melt temperature vs. weld line bending strength for the weld line for PP GF20.....	95
Figure 7.22 Main effects plot for S/N ratios: mold temperature vs. non-weld line bending strength for the non-weld line for PP GF20	98
Figure 7.23 Main effects plot for S/N ratios: melt temperature vs. non-weld line bending strength for the non-weld line for PP GF20	98

List of Tables

Table 3.1	Parameters and levels of PP in the Taguchi experiments	17
Table 3.2	Parameters and levels of GPPS in the Taguchi experiments	18
Table 3.3	The retention of weld line strength values	25
Table 6.1	The process parameters and levels for ABS	50
Table 6.2	The process parameters and levels for PP GF20.....	50
Table 6.3	L ₉ (3 ⁴) orthogonal array of the parameters and levels of ABS	51
Table 6.4	L ₉ (3 ⁴) orthogonal array of the parameters and levels of PP GF20.....	51
Table 6.5	Plastic injection parameters and levels kept constant for ABS.....	52
Table 6.6	Plastic injection parameters and levels kept constant for PP GF20.....	52
Table 6.7	Part names of the cavity side.....	56
Table 6.8	Part names of the core side	58
Table 7.1	The weld line and the non-weld line tensile strength for ABS	78
Table 7.2	The predicted value of the weld line tensile strength for ABS	80
Table 7.3	Response table for signal-to-noise (S/N) ratios for the weld line tensile strength for ABS	80
Table 7.4	ANOVA results for weld line tensile strength for ABS.....	81
Table 7.5	Fisher test value for F(2,2).....	81
Table 7.6	The weld line and the non-weld line bending strength for ABS.....	82
Table 7.7	The predicted value of the weld line bending strength for ABS.....	84
Table 7.8	Response table for signal-to-noise (S/N) ratios for the weld line bending strength for ABS	85
Table 7.9	ANOVA results for weld line bending strength for ABS	85
Table 7.10	The weld line and the non-weld line tensile strengths for PP GF20.....	86
Table 7.11	The predicted value of the weld line tensile strength for PP GF20	88
Table 7.12	Response table for signal-to-noise (S/N) ratios for the weld line tensile strength for PP GF20	89

Table 7.13	ANOVA results for weld line tensile strength for PP GF20.....	90
Table 7.14	The predicted value of the non-weld line tensile strength for PP GF20.	91
Table 7.15	Response table for signal-to-noise (S/N) ratios for the non-weld line tensile strength for PP GF20	92
Table 7.16	ANOVA results for non-weld line tensile strength for PP GF20	92
Table 7.17	Fisher test values for F(2,4)	93
Table 7.18	The weld line and the non-weld line bending strength for PP GF20.....	93
Table 7.19	The predicted value of the weld line bending strength for PP GF20.....	96
Table 7.20	Response table for signal-to-noise (S/N) ratios for the weld line bending strength for PP GF20	96
Table 7.21	ANOVA results for weld line bending strength for PP GF20	97
Table 7.22	The predicted value of the non-weld line bending strength for PP GF20	99
Table 7.23	Response table for signal-to-noise (S/N) ratios for the non-weld line bending strength for PP GF20.....	99
Table 7.24	ANOVA results for non-weld line bending strength for PP GF20.....	100

List of Abbreviations

ABS	Acrylonitrile Butadiene Styrene
AF	Aramid Fiber
BLM	Boundary Layer Mesh
BMC	Bulk Moulding Compound
CaCO ₃	Calcium Carbonate
CB	Carbon Black
CF	Carbon Fiber
CuBe	Copper Beryllium
f ₁	Degree of Freedom for Variable Factor
f ₂	Degree of Freedom for Error Factor
F-test	Fisher Test
GF	Glass Fiber
GPPS	General-Purpose Polystyrene
HB	Brinell Hardness Number
HRC	Hardness Rockwell C
MFI	Melt Flow Index
NR	Natural Rubber
nWB _p	Predicted Value of Optimum Non-Weld Line Bending Strength
nWT _p	Predicted Value of Optimum Non-Weld Line Tensile Strength
PA	Polyamide
P _A	Contribution Rate for Factor A
PBT	Polybutylene Terephthalate

PC	Polycarbonate
PE	Polyethylene
PET	Polyethylene Terephthalate
phr	Filled Filler Contents
PMMA	Polymethyl Methacrylate
POM	Polyoxymethylene
PP	Polypropylene
PP GF20	Polypropylene 20% Glass Fiber
PP-R	Polypropylene Random Copolymer
PPS	Polyphenylene Sulfide
PVC	Polyvinyl Chloride
S/N	Signal-to-Noise
SAN	Styrene-Acrylonitrile
SCRIMP	Seemann Composites Resin Infusion Molding Process
SEM	Scanning Electron Microscope
SiO ₂	Silica
SMC	Sheet Moulding Compound
SRIM	Structural Reaction Injection Moulding
SS' _A	Net Sum of Squares of Factor A
SS' _T	Total Sum of Squares
TEM	Transmission Electron Microscopy
WB _p	Predicted Value of Optimum Weld Line Bending Strength
WT _p	Predicted Value of Optimum Weld Line Tensile Strength

List of Symbols

A	Cross-sectional area [mm]
b	Width of specimen [mm]
b ₁	Width of narrow portion[mm]
b ₂	Width at ends [mm]
d	The thickness of specimen [mm]
D	Elongation [mm]
E'	Storage modulus [MPa]
E''	Loss modulus [MPa]
F	Force [N]
h	The thickness of specimen [mm]
L	Length of the span between supports [mm]
l	Length of specimen [mm]
l ₁	Length of narrow parallel-sided [mm]
l ₂	Distance between broad parallel-sided portions [mm]
l ₃	Overall length [mm]
L _f	Length after deformed [mm]
L _o	Original length [mm]
r	Radius [mm]
R ₁	Radius of loading edge [mm]
R ₂	Radius of supports [mm]
tan δ	Loss factor
α	Significance level

ε	Strain [mm/mm]
σ	Tensile strength [MPa]
σ_e	Bending strength [MPa]
s_y^2	Variance of y
\bar{y}	Average of test data
y_i	Value of output characteristic for the test

Chapter 1

Introduction

Plastics are commercialized as one of the most usual materials. Some properties of plastics are suitable for mass production, light, flexible, and good corrosion resistance, etc. For this reason, plastics can be found in almost all industries. Areas of usage of plastics have been significantly increased in the last decades. Figure 1.1 shows the increasing trend of plastic use. New plastics, new production methods, and new solutions are emerging to develop this industry. Nevertheless, some shortcomings, imperfections, and faults cannot be completely resolved in all production methods of plastics. For the sake of examples, the plastic injection molding process has some defects or limitations that are weld line, sink mark, shrinkage, and nonhomogeneous fiber orientation, etc. Compression molding has some defects or limitations that are a simple part design on account of high viscosity and longer cycle time etc. The extrusion process has some defects or limitations that are melt fracture, sharkskin and bambooning, etc. [1]. The thermoforming process has some defects or limitations that are ripples and other surface failures, undercuts, and waviness, etc. [2]. The blow molding process has some defects or limitations that are low gloss, surface roughness, wall thickness nonuniform, and warped top and bottom of parts, etc. [3]. Some of these defects can be partially solvable, however, some of them can be just improvable because that is the nature of plastics. So, there are thousands of studies to understand and improve them. Figure 1.2 depicts the usage rate of some thermoplastic grades.

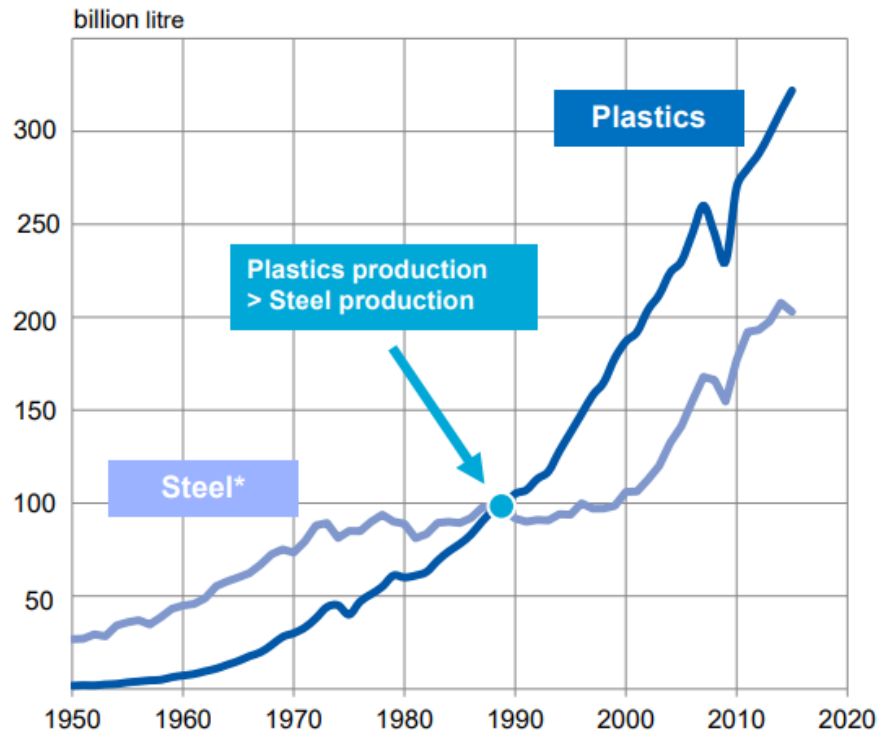


Figure 1.1: World benchmark plastics / steel between 1950-2015 [4]

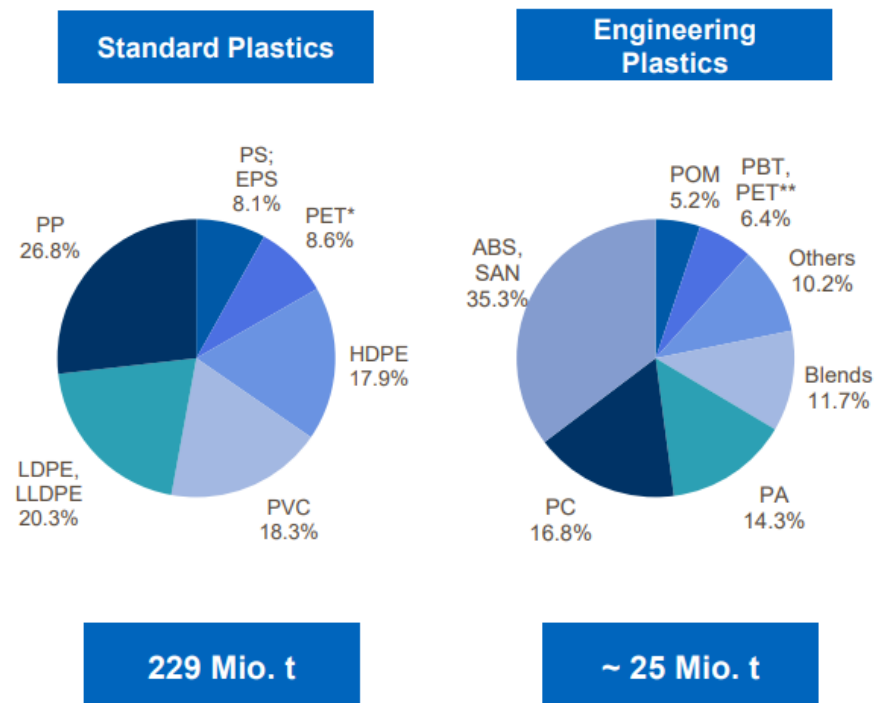


Figure 1.2: World thermoplastics demand: 2015 [4]

A polymer is a substance or material consisting of very large molecules, or macromolecules, composed of many repeating subunits. Plastics are separated as classifications that have different macromolecular structures and numerous temperature-dependent physical properties. This classification of plastics can be carried out like thermoplastics, elastomers, and thermosets. Thermoplastics can be repeatedly melted by thermal and mechanical energy. It is for this reason recycling thermoplastics is easy to do. Thermoplastics are linear or branches of macromolecule chains. When they are energized, it is typically decreased viscosity and is separated chains finally can become fluent. Thermoplastics can be processed in injection molding, blow molding, extrusion, thermoforming, tape winding, compression molding, autoclave, and diaphragm forming. Elastomers cannot be melted by energy so recycling elastomers are more difficult than thermoplastics. Elastomers are usually soft or flexible materials, thereby they have far knit crosslinking. Elastomers can be processed transfer molding, injection molding, extrusion, vulcanization, and compress molding, etc. Finally, another type of plastic is thermosets that cannot be melted by energy, so they are not easily recycled compared to thermoplastics. Thermosets have resistant to heat and hard elasticity, thereby they have narrow knit crosslinking. Thermosets can be processed Sheet Moulding Compound (SMC) molding, Structural Reaction Injection Moulding (SRIM), Bulk Moulding Compound (BMC), Spray-up, injection molding, filament winding, pultrusion, hand lay-up, Autoclave, Seemann Composites Resin Infusion Molding Process (SCRIMP), roll wrapping, bladder molding [5, 6].

One of the most frequently consumed plastics is thermoplastics because of recycling. Thermoplastics are two types that are amorphous and semicrystalline. Properties of them are different from each other. The molecular orientations of amorphous thermoplastics are without any near order. So, the properties of amorphous thermoplastics have brittle, dimensional stability, rigid, and can be transparent. Samples of amorphous thermoplastics are acrylonitrile butadiene styrene (ABS), polycarbonate (PC), polystyrene (PS), polyvinyl chloride (PVC) and polymethyl methacrylate (PMMA), etc. The molecular orientations of semicrystalline thermoplastics are arranged in an orderly fashion that amorphous structure embedded crystalline structure. So, some semicrystalline thermoplastics have flexibility, chemical resistance, fatigue resistance, and opacity. Polypropylene (PP), polyamide

(PA), polyethylene (PE), polyethylene terephthalate (PET), polybutylene terephthalate (PBT), polyoxymethylene (POM) are an example of semicrystalline thermoplastic [5-7]. Figure 1.3 easily demonstrates the difference between an amorphous structure and a semicrystalline structure.

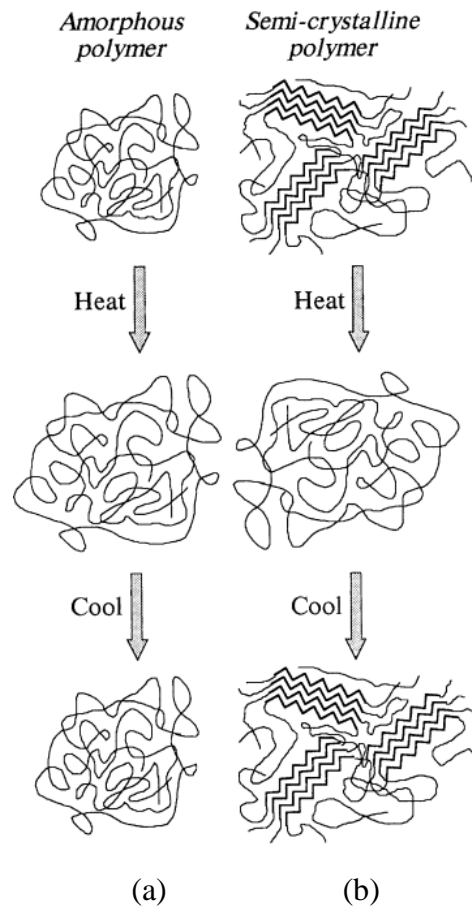


Figure 1.3: Molecular oriented in (a) amorphous and (b) semicrystalline plastics [8]

Amorphous and semicrystalline thermoplastics are divided into three groups among themselves. These are advanced engineering plastics, engineering plastics, and standard plastics. Figure 1.4 is depicted the polymer pyramid. Standard plastics have a low density, low cost, and wide areas of use. Engineering plastics have an impressive mechanical and thermal performance. On the other hand, advanced engineering plastics have high-temperature resistance and significant chemical resistance.

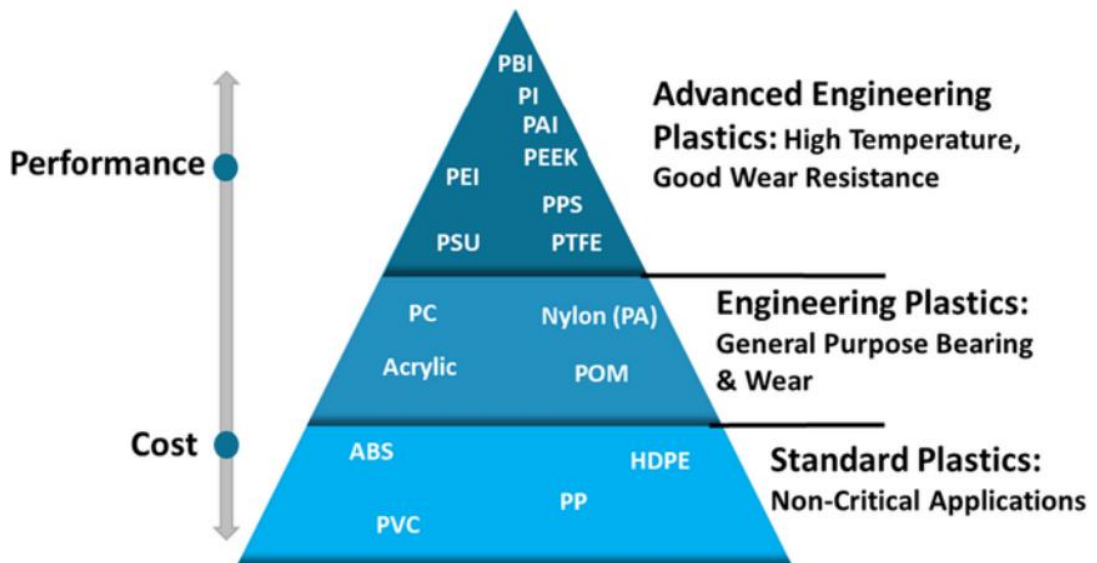


Figure 1.4: Polymer pyramid [9]

ABS is a common thermoplastic polymer typically supplied for injection molding applications. This engineering plastic is popular due to its low production cost.

Desired properties of ABS can be listed below:

- Impact resistance
- Structural strength and stiffness
- Chemical resistance
- Excellent high and low-temperature performance
- Great electrical insulation properties
- Easy to paint and glue

PP is a crystalline thermoplastic made up of a blend of different polypropylene monomers. It is known for its toughness and rigidity. Being resistant to many external factors makes polypropylene one of the most consumed thermoplastics in the plastic manufacturing industry. Polypropylene is broadly utilized in producing many different kinds of products in various industries throughout the world.

Desired properties of PP :

- Semi-rigid
- Translucent
- Good chemical resistance
- Tough
- Good fatigue resistance
- Integral hinge property
- Good heat resistance

The plastic injection molding process is one of the most prevalent methods in the production of plastics. The most significant reasons can be suitability for mass production, complex part design, the low unit price of plastic parts, tight tolerances. It is generally completely automatic and often does not need after-processing [10]. Nevertheless, this process suffers disadvantages that are high initial investment cost, wall thickness should be same all over the part designs, and inability to apply thick walls because of sinking.

Form of plastics is often provided as grains or powders in an injection molding process. Grains or powders fill the hopper that is a section of the injection molding machine. After those plastics are melted by electric resistors in a barrel. The barrel has a screw utilized to mix plastics and to push plastic to the mold cavity. After molten plastic is cooled in the mold cavity, the mold is separated from each other followed by ejection from the mold. Sections of the injection molding machine are illustrated in Figure 1.5. Injection molding processes are shown in Figure 1.6.

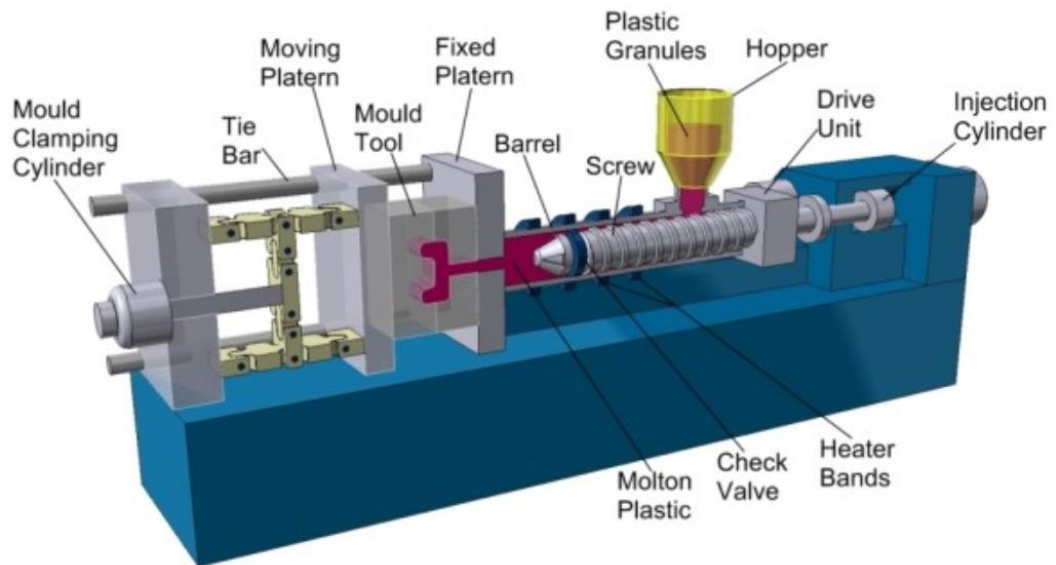


Figure 1.5: Basic units of injection molding machine [11]

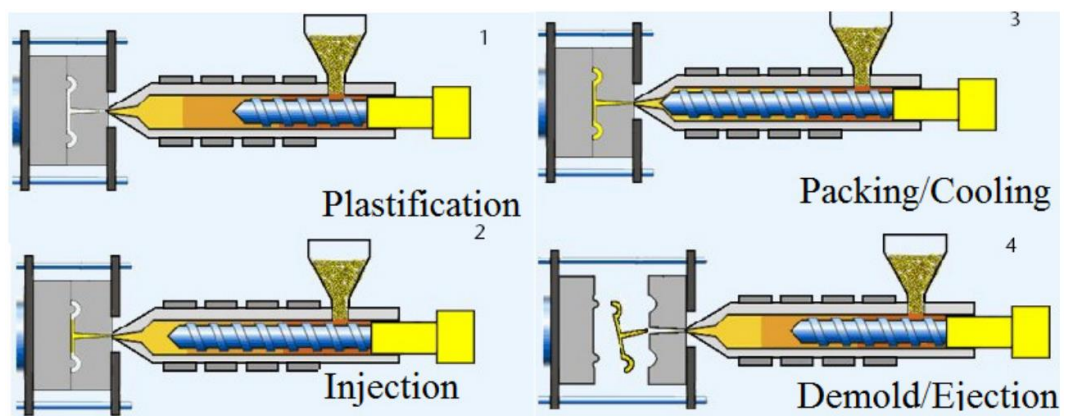


Figure 1.6: Plastic injection molding processes [12]

The plastic injection molding process has some defects affecting adversely the strength of plastic parts. One of them is the weld line (knit line, cold weld line, or stagnating weld line). Weld lines occur with recombination opposite directions of two melted plastics [13]. The formation of the weld line is illustrated in Figure 1.7. Another type of weld line is known as melt line, hot weld line, or flowing weld line. The melt line occurs when two melted plastics emerge in parallel to each other. Melt and weld lines are very similar as a form but there is quite a difference in structure. This is because the point or line where the two melted plastics rejoin has a different angle. Therefore, the result is different mechanical properties and behaviors.

The weld lines generally reduce the mechanical properties of the plastic part. The reason is that the region of the weld line has a lack of interdiffusions, molecular orientations, and V-notch effect [14]. Therefore, weld lines are usually the weakest region of the part. Some parameters that are affected the strength of the weld line region are the type of plastic, type of reinforcement, amount of reinforcement, type of filler, amount of filler, the degree of interfacial adhesion between the fiber and the matrix, the temperature of point or line that is joined melted plastics, mold temperature, melt temperature, injection pressure, injection speed, holding pressure, back pressure, cooling time, holding time, and angle of lines that are joined melted plastics, etc. These parameters are significant for both weld line strength and part strength; moreover, they affect weld line surface quality and part surface quality. For this reason, there are hundreds of studies about the effects of these parameters on weld line and part strength and quality.

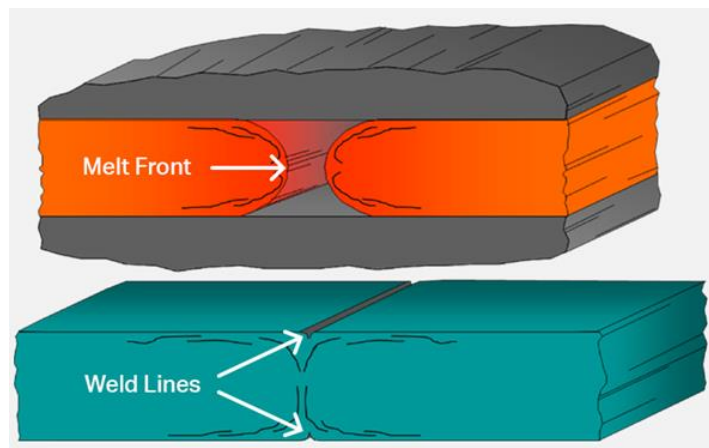


Figure 1.7: Formation of weld line [15]

Chapter 2

Formations and Types of the Weld Line

2.1 Formations of the Weld Line

The plastic injection molded part has two weak regions. One of them is the gate regions of parts and the other is the weld line regions. The reason why the gate region is weak is due to the pressure during injection leaving stress on the part. The reason for the weak welding line is the formation of a notch in that region.

Weld lines are formed to recombine when the molten plastic separates against the obstacle during injection or when the mold has more than one gate. The weld line formation process is illustrated in Figure 2.1. It is not possible to eliminate the weld line with injection settings, cooling systems, and plastic raw materials. These parameters allow the weld line region to improve its strength and visual appearance. There are two different solutions to completely remove the weld line region or to move it to different locations. One of them is to change the gate locations of the mold and the other is to alter the plastic part design. Thus, the weld line can be lost or moved to another region where strength is not required. However, these changes must be made before mold production, otherwise, it may cause too many modifications in the mold. With plastic part filling analysis, it is possible to predict where the weld lines will occur, their junction temperature, and angle. Optimizations performed in this way are a permanent solution for the plastic part design. Unfortunately, due to some mechanical design constraints, it is impossible to eliminate the weld line or even change its regions by plastic part or mold design changes. In this case, optimization should be performed in the strength and visual appearance of plastic parts with injection parameter settings, cooling or heating of the mold, and plastic raw material replacement.

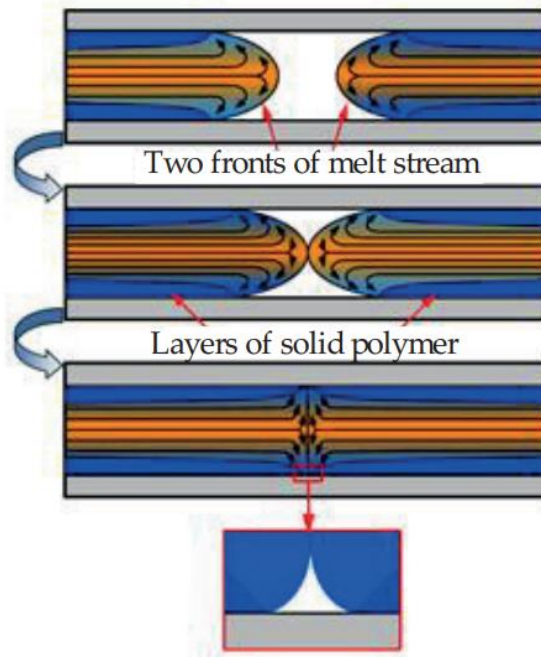


Figure 2.1 The process of weld line forming [16]

The position of the weld line on the part depends on the method of feeding the molten plastic to the cavity and the gate location. With multi-point cavity feeding, some gates can be blocked to limit the number of streams of molten material, which is not always possible. Sometimes, however, it is even advisable to increase the number of injection points to shorten the flow path, and receive collision of melt fronts with a higher temperature and higher flow velocity, and, as a result, provide higher strength of the joining regions [16]. In Figure 2.2, the weld line region has been changed by adding one different gate. Thus, if the weld line in Figure 2.2.a is located on an important region in terms of strength and visual quality, it can be moved to a different location. The part with a single gate in Figure 2.2.a has a longer flow length and two weld lines. However, the part with double gates in Figure 2.2.b has a shorter flow length and three weld lines.

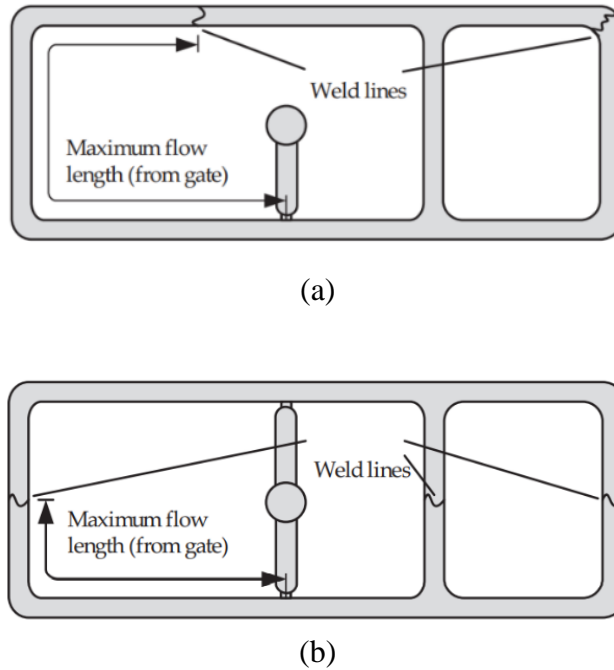


Figure 2.2: The effect of different gate types on the weld line, (a) The single gate, (b) The two gates [16]

2.2 Type of the Weld Line

There are two types of weld lines are depicted in Figure 2.3. Where the flow fronts meet head-on and there is no further melt flow in the weld line, stagnating weld lines are formed. If the flow fronts meet at an angle that allows a continuous flow of the melt and the weld line, flowing weld lines are formed. One of the two types, stagnating weld lines have lower mechanical strength. While the strength values of flowing weld lines are around 75% compared with the standard material, stagnating weld line strengths can be as low as 50% in the case of brittle amorphous thermoplastics. Higher values can be expected for ductile amorphous or partially crystalline thermoplastics [14]. If there is no reinforcement in the plastic material, the strength may not decrease as expected. However, the material loses its ductility too much in the weld line region and the amount of elongation can decrease up to four times. If there is reinforcement in the plastic material, both strength and elongation decrease significantly.

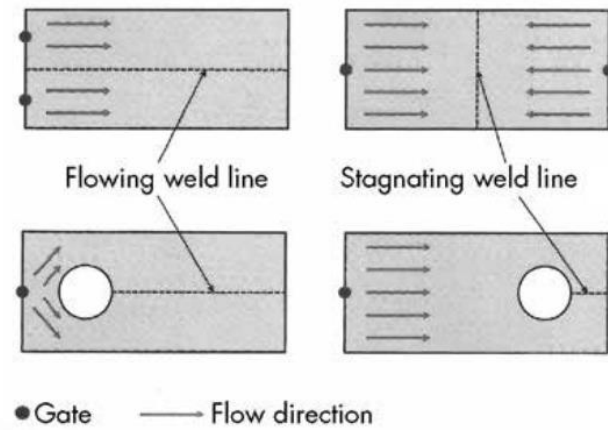


Figure 2.3: Formation of weld line types [14]

In addition, a stagnating weld line is also called a knit line and the flowing weld line is called the melt line. Melt line and knit line are illustrated in Figure 2.4. The weld line forms if the meeting angle of two flow fronts is smaller than 135° . If the meeting angle is more than 135° , the melt line forms. Knit lines are formed in the region of the meeting of two melt fronts that flow from opposite directions. Similarly, melt lines are formed when two melt fronts flow parallel to each other [17].

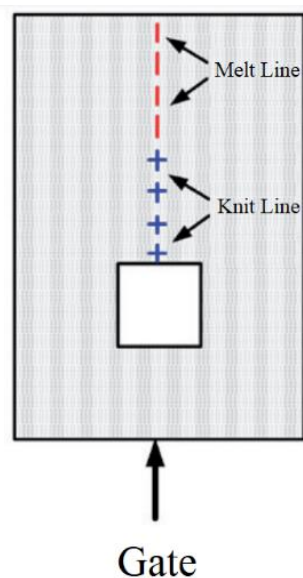


Figure 2.4: Melt line and knit line [17]

The angle of tangents that recombine two molten plastics in different flows is called the meeting angle. The meeting angle will affect the degree of molecular diffusion and fusion across a weld line [18]. The greater this angle, the greater the mechanical properties of the weld line region. When it decreases to zero degrees, there is a stagnating weld line. For this reason, if the mechanical properties and visual quality of the plastic parts are desired, the part and the mold should be designed by considering this angle in the plastic injection filling analysis. Figure 2.5 illustrates the meeting angle.

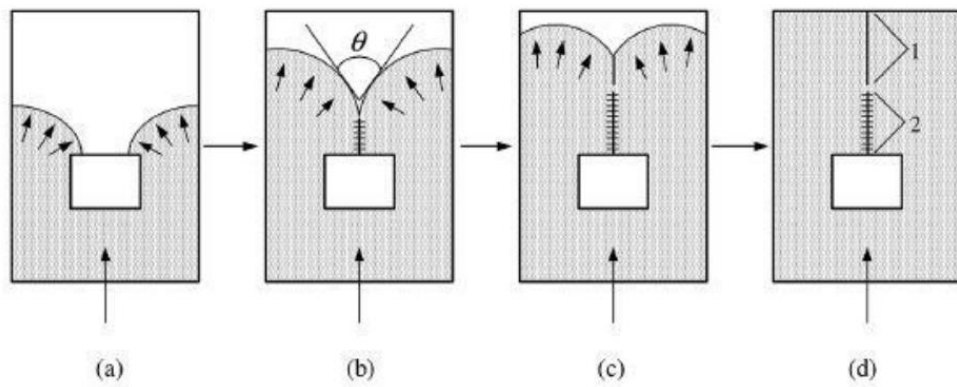


Figure 2.5: Formation of meeting angle [18]

Chapter 3

Literature Research

Many manufacturing factors affect the parts produced in plastic injection. These parameters concern very different fields: Plastic material, part and mold design, mold material selection, and injection process parameters. These factors requiring a separate specialization are not very related to each other. For this reason, there is a lot of work by specialists with different expertise in plastic injection molding. Existing many parameters affecting the plastic part also make it difficult to work on the parameters influencing the weld line. It is really difficult to keep all other parameters constant under the same conditions. Therefore, it takes a lot of experimentation to reduce the error factor.

In the literature, there are many studies on the weld line for diverse parameters such as injection time and pressure, back pressure, melt temperature, mold temperature, material type, filler and reinforcement materials and their ratios, cooling time, holding time and pressure, the geometry of the obstacle forming the weld line and test environment at different temperatures.

However, among these studies, there are a very limited number of studies investigating the effect of applying a different local temperature to the weld line region of the mold without being affected by the core and cavity temperature and its effect on the weld line formation.

Also, there are rare studies on the effect of different runner gate designs on the weld line formation. In other studies, the weld line region could not be heated locally because the mold temperature was also affected. Accordingly, local heating has been made with a unique design with minimal effect on the mold temperature.

3.1 Effects of Molding and Injection Parameters on the Properties of Plastics

Melt and mold temperatures are significant parameters for weld line strength and surface quality because they affect the amount of interdiffusion, intermolecular entanglement, and junction temperature of plastics. The strength of the weld line can be improved by increasing temperature. However, if plastics are processed at very high-temperatures, they can degrade. The degradation may not be noticed in the appearance of plastic parts. Nevertheless, the strength of plastic parts and weld lines can be adversely affected by ultra-high-temperatures. Raz and Sedlacek [19] studied the effect of melt temperature on weld line strength of polypropylene (PP). They had altered melt temperatures by 10 °C between 160 °C and 260 °C, then weld line strength of PP had been investigated. Figure 3.1 illustrates the relationship between the strength of the weld line and melt temperature. They also concluded that weld line strength increased for melt temperatures above 210 °C. However, whereafter melt temperature reaches 210 °C, weld line strength is decreased at 260 °C. Since thermal degradation occurs at high melt temperature.

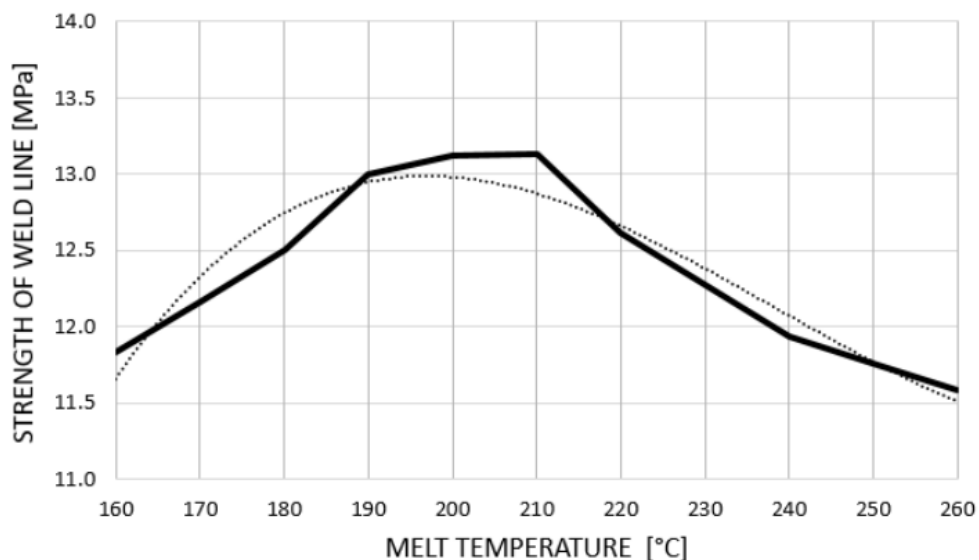


Figure 3.1: Relationship between melt temperature and strength of weld line and a third-order polynomial trend line [19]

Taguchi method is a statistical analysis that allows estimating results of all tests with fewer testing sets. It can be also implemented to estimate the contribution rate of plastic injection molding factors. In the analysis, a signal-to-noise (S/N) ratio is the statistical quantity representing the power of a response signal divided by the power of the variation in the signal due to noise. If the goal of the experiments is the maximize response, the S/N ratio should be a larger value. For this reason, when melt and mold temperatures increase, the S/N ratio of weld line strength should increase.

The importance of this analysis is finding contribution rates of the parameters, the effect of the parameters, performing a fewer number of tests, and expressing and plotting experimental results. Lei and Gerhard [20] investigated the contribution of injection parameters on the weld line strength of micro parts. Injection molding parameters for PP were melt temperature, mold temperature, injection pressure, packing pressure, ejection temperature, injection speed as illustrated in Table 3.1. $L_{18}(3^7)$ orthogonal array had been implemented in the Taguchi method. As a result contribution rate for mold temperature is 42.4%, melt temperature is 19.59%, injection speed is 12.43%, ejection temperature is 11.7%, packing pressure is 7.31%, the injection pressure is 6.53% on weld line strength. It can be concluded that mold and melt temperatures have major effects on weld line strength. Another result is the S/N ratio for factor levels in Figure 3.2. The letters expressing parameters with their levels in Figure 3.2 refer to parameters and levels listed in Table 3.1. Mold temperature (B) positively affects the weld line strength as seen from Figure 3.2. However, melt temperature (A) negatively affects the weld line strength. The adverse effect of melt temperature is unexpected because it is considered that the diffusion of molecules increases with melt temperature and higher plastic degradation may result in the microscale part injection molding process. In addition, the best level of parameters is $A_1B_2C_1D_2E_2F_3$ according to Taguchi Analysis.

Table 3.1: Parameters and levels of PP in the Taguchi experiments [20]

Factors	1	2	3
A. Melt Temperature (°C)	210	230	250
B. Mold Temperature (°C)	120	140	160
C. Injection Pressure (MPa)	500	1000	2000
D. Packing Pressure (MPa)	400	800	1600
E. Ejection Temperature (°C)	40	60	80
F. Injection Speed (cm ³ /s)	60	80	100

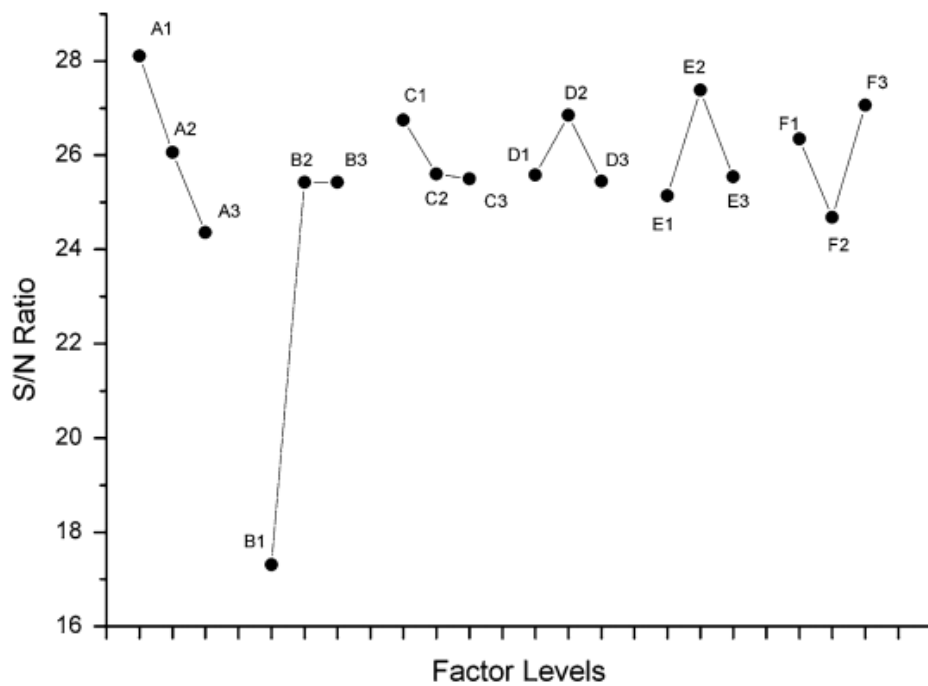


Figure 3.2: Process parameter levels S/N ratio of weld line strength in PP [20]

There are different parameters like packing time, injection acceleration, and obstacle geometry creating weld lines to enhance the mechanical properties or visual quality of weld lines. Weld line strength of general-purpose polystyrene (GPPS) is enhanced by using different six parameters that are obstacle geometry, melt injection pressure, melt temperature, packing pressure, mold temperature, and melt injection speed by Liu et al [21]. Parameters and levels of this study are illustrated in Table 3.2. The Taguchi method is applied for this study. $A_1B_3C_3D_3E_3F_2$ is the parameters and levels indicating the process conditions for maximum weld line strength. In addition, when melt and

mold temperature increase, weld line strength also increases as illustrated in the S/N ratio plot in Figure 3.3.

The melt temperature, mold temperature, and packing pressure contribute to the weld line tensile strength of ABS with percentages of 67.46%, 17.72%, and 13.39, respectively. The effect of obstacle geometry, melt injection speed, and melt injection pressure on weld line tensile strength are inconsiderable. Weld line strength is affected by other parameters but melt and mold temperatures still have the highest contribution rate of weld line strength in this study.

Table 3.2: Parameters and levels of GPPS in the Taguchi experiments [21]

	Level 1	Level 2	Level 3
A. Obstacle Geometry	Circle	Square	Rhombus
B. Melt Injection Pressure (MPa)	84	92	100
C. Melt Temperature (°C)	205	215	225
D. Packing Pressure (MPa)	60	70	80
E. Mold Temperature (°C)	40	50	60
F. Melt Injection Speed (%)	50	60	70

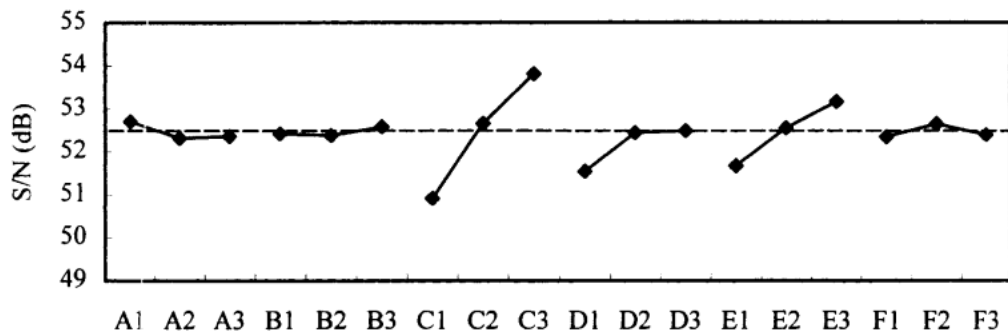


Figure 3.3: Process parameter levels S/N ratio of weld line strength in GPPS [21]

Increasing mold temperature generally improves the weld line strength. However, like mold temperature increases, non-weld line strength may decrease because of the formation of plastic degradation. Even if it increases weld line strength with mold temperature, the strength of any non-weld line region may decrease. So, if it has a

complex part or it should be a durable part, there may be problems with the strength. Effect of mold temperature on weld line and non-weld line strength are examined with the natural rubber (NR) filled filler contents (phr) 30 carbon black material by Chookaew et al [22]. Mold temperatures are adjusted as three different levels which are 140 °C, 150 °C, and 160 °C in this study. When mold temperatures are 140 °C, 150 °C, and 160 °C, weld line strength of NR filled phr 30 carbon black is 20.85 MPa, 24.75 MPa, and 26.27 MPa, respectively. Weld line strength improves with mold temperature but non-weld line strengths are 33.4 MPa, 31.7 MPa, and 28.81 MPa, respectively. A comparison of maximum tensile strength is depicted in Figure 3.4. In these results, non-weld line strength decreases with mold temperature. It can be explained that it is strongly prone to reversion at high-temperatures. So, the strengths of parts cannot be improved with mold temperature all the time.

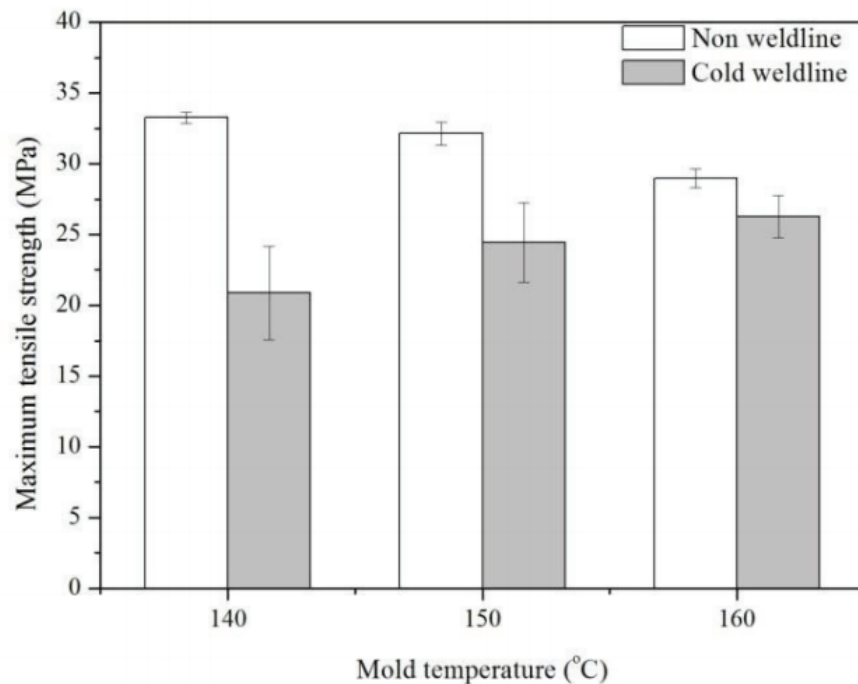
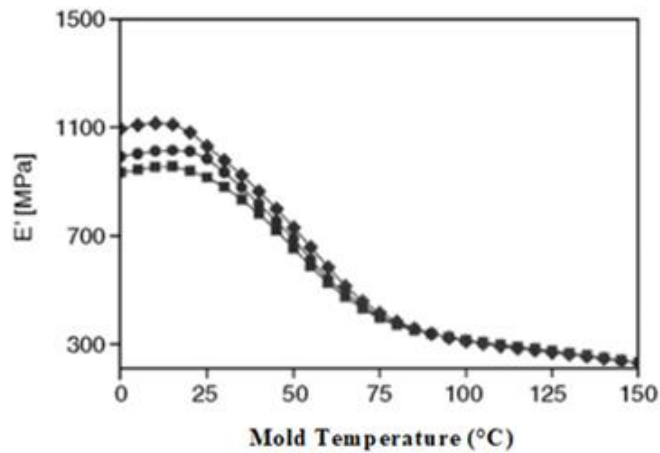


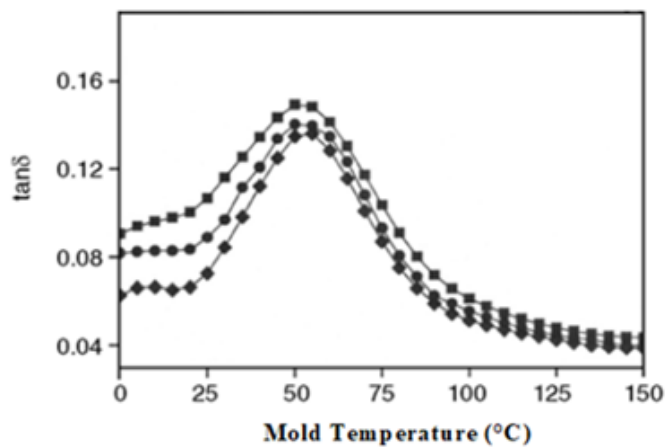
Figure 3.4: Comparison of maximum tensile strength for non-weld line and cold-weld line specimens at 140 °C, 150 °C, and 160 °C mold temperatures [22]

To fully evaluate the behavior of a plastic part, it is necessary to examine the other mechanical properties. Some of these mechanical properties are storage modulus and loss modulus. The storage modulus (E') is an indication of hydrogel's ability to store

deformation energy elastically. The loss modulus (E'') highlights the viscous properties of a polymeric-based material and represents energy lost as heat or dissipated during one cyclic load. Loss factor ($\tan \delta$) is the ratio of E''/E' [23]. At different mold, temperatures are investigated mechanical properties of polybutylene terephthalate (PBT) by Banik [24]. Storage modulus is decreasing after mold temperature exceeds room temperature. The loss factor is increasing until mold temperature exceeds 52 °C. However, after that temperature, the loss factor is decreasing; consequently, if it is necessary to high mold temperature, mechanical properties of plastic part can decrease. Change of storage modulus and loss factor related to mold temperatures is illustrated in Figure 3.5.



(a)



(b)

Figure 3.5: Effect of mold temperature on (a) Storage modulus (E') and (b) Loss factor ($\tan \delta$) of PBT (■PBT14, ●PBT40, ◆ PBT60) [24]

The temperature of molten plastics that recombined in the mold should be high for interdiffusion. For this, the mold temperature or the melt temperature must increase. However, entire mold or molten plastics have high-temperatures, after which plastic degradation can occur in an injection molding process. Even though weld line strength may be meaningfully improved, the strength of other regions of the plastic may typically decrease. In this study, it has been considered to fix an aluminum insert having a high heat transfer coefficient for the weld line region so that only the welding line region can be heated without heating the mold or molten plastic and thus the plastic does not deteriorate. Most studies have investigated the influence of mold temperature, melt temperature, injection pressure, or other injection parameters, but few studies have investigated the influence of local heating or gate design for weld line strength. This study aims to find the optimum weld line strength without excessive cost increase using local heating and different gate designs.

The mold in this study has two cavities to compare weld line strength and non-weld line strength for different materials under the same conditions. One of the cavities has only one gate to probe the non-weld line strength, the other cavity has two gates to examine the weld line strength. To observe the effect of gate type on weld line strength, all gates have been configured in discrete geometries. Because various geometries of gates can cause diverse molecular orientations in the weld line region. Another reason is molecular orientation, which reduces weld line strength, so the gate design can improve the weld line strength.

3.2 Effects of Reinforcement and Filling Materials on the Properties of Plastics

The type of plastic material, the type, and proportions of reinforcement and filler materials have a significant effect on the strength of the part and the strength of the welding line, which is revealed in many studies. However, in some studies, it has been investigated that the filling materials do not have much or very little effect. Fillers are generally supplied to facilitate the injection molding process, reduce the cost and the shrinkage rate, increase the surface quality, hardness, and heat resistance, and reduce. They can be used to slightly increase the strength of the material. Therefore, it does not significantly affect the strength of the part and welding line considerably

Reinforcing materials are generally adjusted to increase the strength of the material. Depending on the type and ratio of the reinforcement material, it can increase the strength of the part more than twice. It also increases thermal dimensional stability, reduces the shrinkage ratio of the plastic materials, and reduces the number of sink marks. Therefore, the effect of reinforcement materials on the strength of plastic materials is significantly high.

In the weld line region, the orientation of the fibers develops perpendicular to the flow direction as shown in Figure. 3.6. All fiber types are brittle in the weld line region and their strength is very low, as the fiber arrays enhance the strength in the flow direction. For this reason, the strength loss in the welding line region is less in the parts where reinforcement and filling materials are mixed.

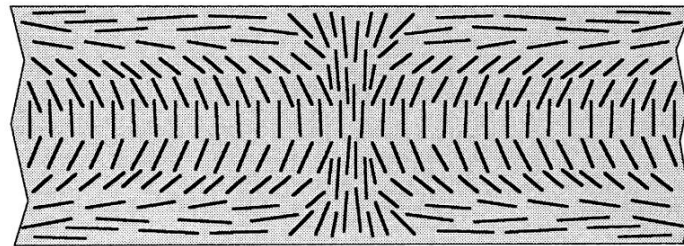


Figure 3.6: Orientation of reinforcement material in the weld line region [8]

3.2.1 Effect of Reinforcement Materials on Plastics

Glass fiber, carbon fiber, and aramid fiber are widely consumed in thermoplastic materials as reinforcement materials. Glass fiber is the most widely used reinforcement material due to its cost and ease of manufacture. It can be found in the original raw material in the desired ratio or it can be added to the raw material as an extra from the outside. As the glass fiber ratio increases, the strength of the material increases, but on the contrary, the weld line strength and ductility decrease. Takayama [25] found the joint mark strength and elongation of the material by adding 10%, 20%, 30%, and 40% glass fiber, carbon fiber, and aramid fiber to the PP, respectively. As fiber ratios increase, the weld line strength and elongation decrease significantly in all test results.

Figure 3.7 shows the stress-strain diagram of the weld line strength of 10%, 20%, 30%, and 40% of glass, carbon, and aramid fibers.

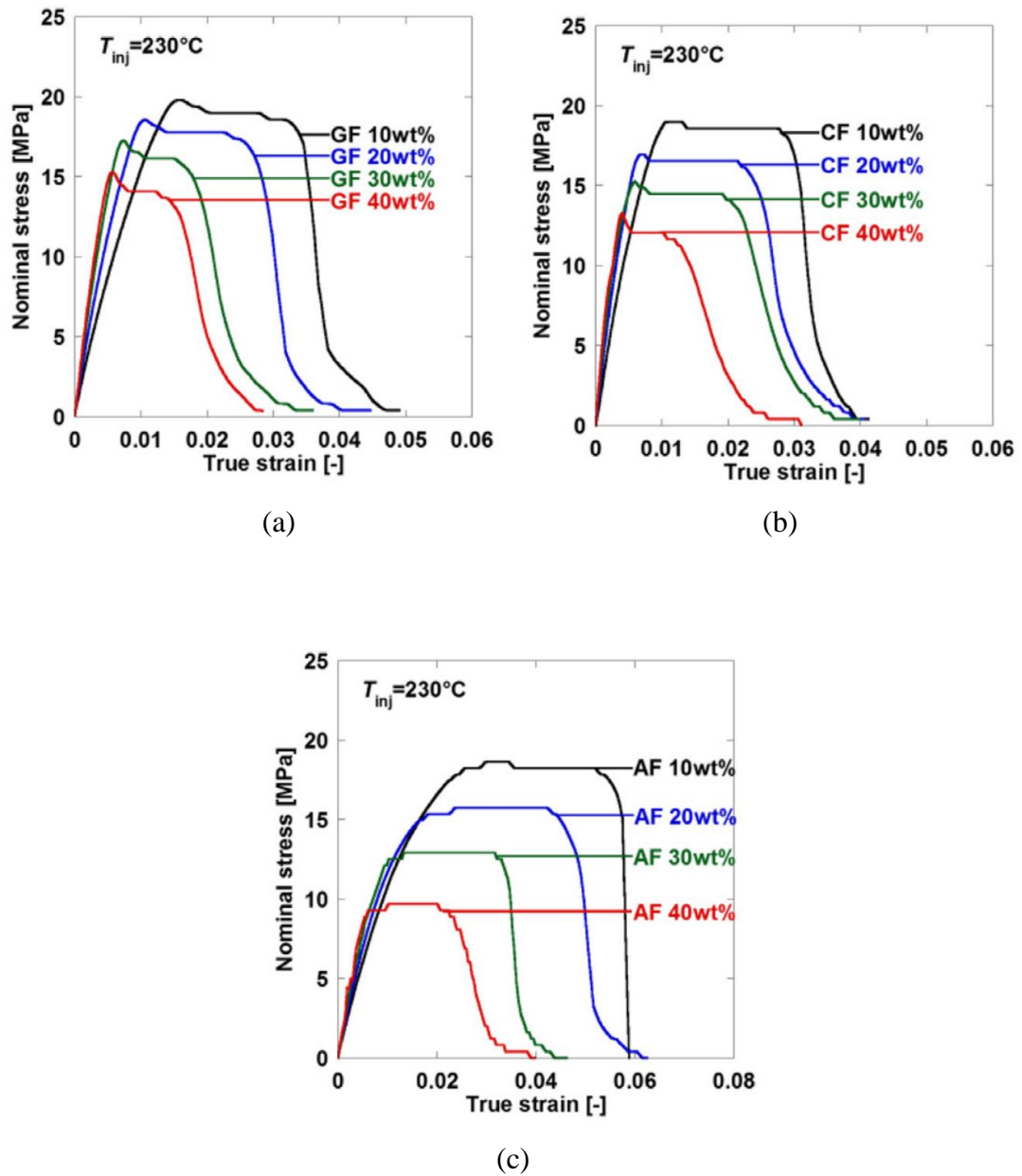


Figure 3.7: Stress-strain graph in the weld line region of fiber reinforced PP composite, (a) Glass fiber, (b) Carbon fiber, (c) Aramid fiber [25]

As the fiber ratio increases, the ratio of the weld line strength to the non-weld line strength decreases. However, although the fiber ratio increases, the welding line strength does not increase similarly. Gyung-Hwan Oh et al. [26]

researched the welding line strength and non-welding line strength of materials with 0%, 10%, 20%, and 30% of glass fiber content. As a result of this research, they observed that the strength of the non-weld line specimens increased gradually as the glass fiber ratio increased. However, for 0%, 10%, 20% and 30% glass fiber content, ratio of the weld line strength to non-weld line strength decreased by 12%, 34%, 52% and 56%, respectively. In Figure 3.8, the strength values for 0%, 10%, 20%, and 30% glass fiber contents are shown in the graph.

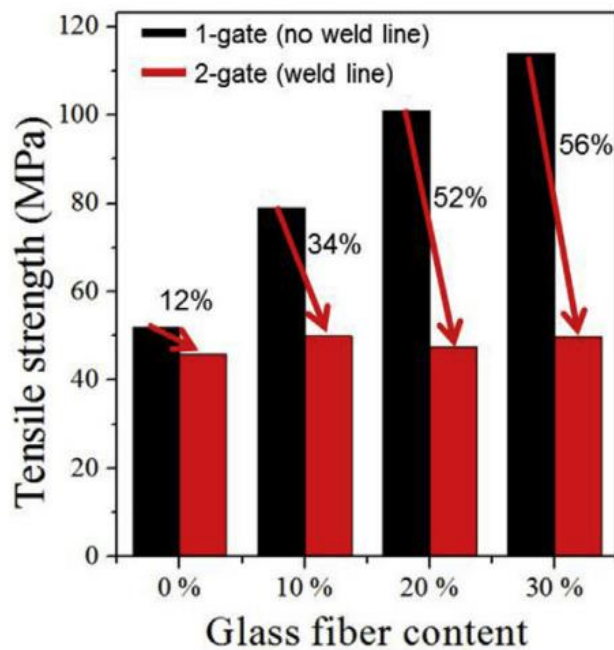


Figure 3.8: Weld line and non-weld line strengths of glass fiber parts [26]

The retention rate of weld line strength varies with the type and ratio of the reinforcement materials. Figure 3.8 shows how much the weld line strength retention rate depends on the material type at different glass fiber ratios. In the absence of reinforcement material, the retention rate of the welding line strength is approximately 80-100%. However, when there is glass fiber reinforcement, there is much more retention in strength. As seen in Table 3.3, the retention of 40% glass fiber reinforced polyphenylene sulfide (PPS) decreased to 20%. However, such retention of weld line strength has not been observed in other plastic materials. For this reason, the type of

plastic material and the ratio of the reinforcement material are very critical parameters for the strength of the weld line [27].

Table 3.3: The retention of weld line strength values [27]

Material Type	Reinforcement Type	Tensile Strength Retention (%)
Polypropylene	no reinforcement	86%
Polypropylene	20% glass fiber	47%
Polypropylene	30% glass fiber	34%
SAN	no reinforcement	80%
SAN	30% glass fiber	40%
Polycarbonate	no reinforcement	99%
Polycarbonate	10% glass fiber	86%
Polycarbonate	30% glass fiber	64%
Polysulfone	no reinforcement	100%
Polysulfone	30% glass fiber	62%
PPS	no reinforcement	83%
PPS	10% glass fiber	38%
PPS	40% glass fiber	20%
Nylon 66	no reinforcement	83-100%
Nylon 67	10% reinforcement	87-93%
Nylon 68	30% reinforcement	56-64%

3.2.2 Effect of Filler Materials on Plastics

The most accepted filling materials in the plastic injection process are calcium carbonate (CaCO_3) and silica (SiO_2). These materials are typical filling materials. Filling materials do not contribute much to the strength of the part but are often used to improve other properties of the plastic and reduce production costs. Watcharapong Chookaew et al. [22] added 0%, 15%, 30% CaCO_3 , SiO_2 , and carbon black (CB) fillers to the rubber material and tested the strength of the rubber material. They observed that CaCO_3 did not have much effect on the maximum tensile strength of the specimen with and without the weld line. However, when the ratio of SiO_2 and CB increases, the

weld line strength decreases. Especially in SiO_2 filler material, welding line strength decreases more. In Figure 3.9, the tensile strength of CaCO_3 , SiO_2 , and CB fillers in distinct ratios of the part with and without the weld line is illustrated.

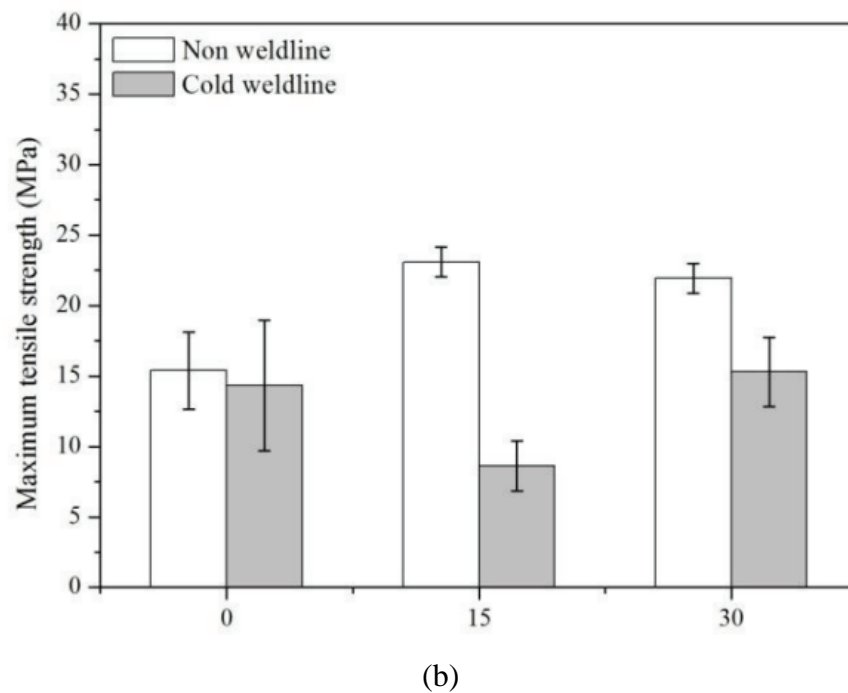
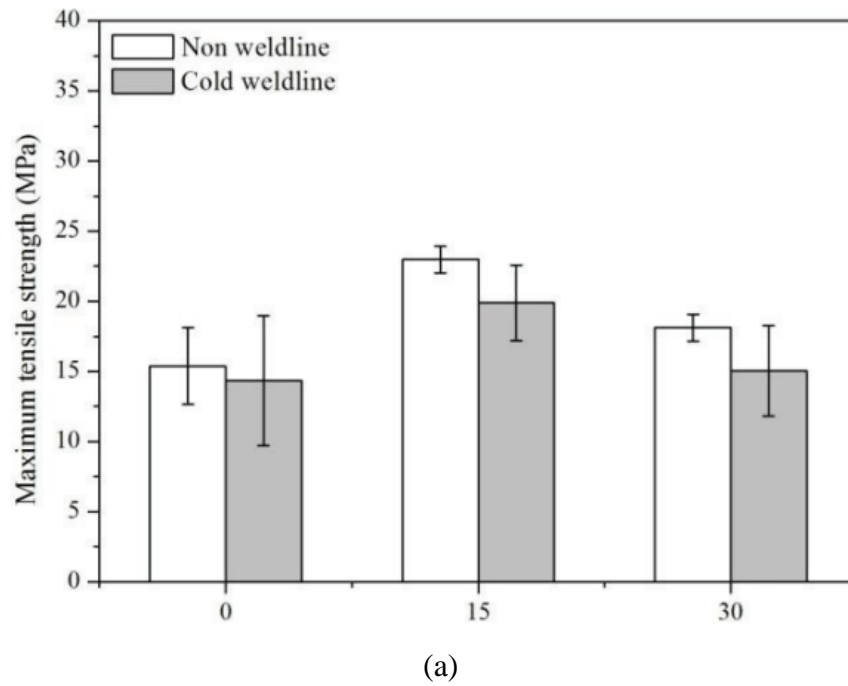
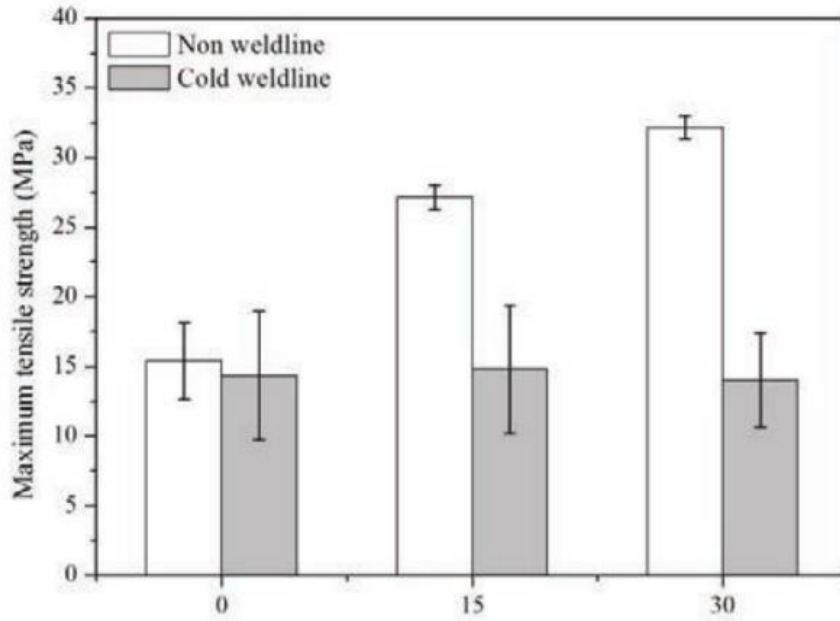


Figure 3.9: Tensile strength of CaCO_3 , SiO_2 , and CB fillers added to rubber material with and without the weld line, (a) phr of CaCO_3 , (b) phr of SiO_2 , (c) phr of CB [22]
(Continued)



(c)

Figure 3.9: (Continued)

Şahin et al. [28] investigated the mechanical and physical properties of polypropylene random copolymer (PP-R) by adding 5%, 10%, 15%, 20%, 25%, 30%, and 35% CaCO₃ fillers by volume. As a result of these investigations, it was observed that when CaCO₃ increased, the modulus of elasticity increased, but strength at yield and elongation at yield decreased. Shore D hardness value increases with increasing CaCO₃ ratio. The melt flow index (MFI) also increases with the CaCO₃ ratio. With the increase of MFI, it will be possible to fill the mold cavity by using less energy. However, the density of the material also increases. Thus, the mechanical and physical properties of plastics can be changed as desired by adding an external filling material to provide the properties expected from plastic materials. This provides an increase in the usage area of plastics. Figure 3.10 shows the density and hardness of the PP-R material at different CaCO₃ ratios.

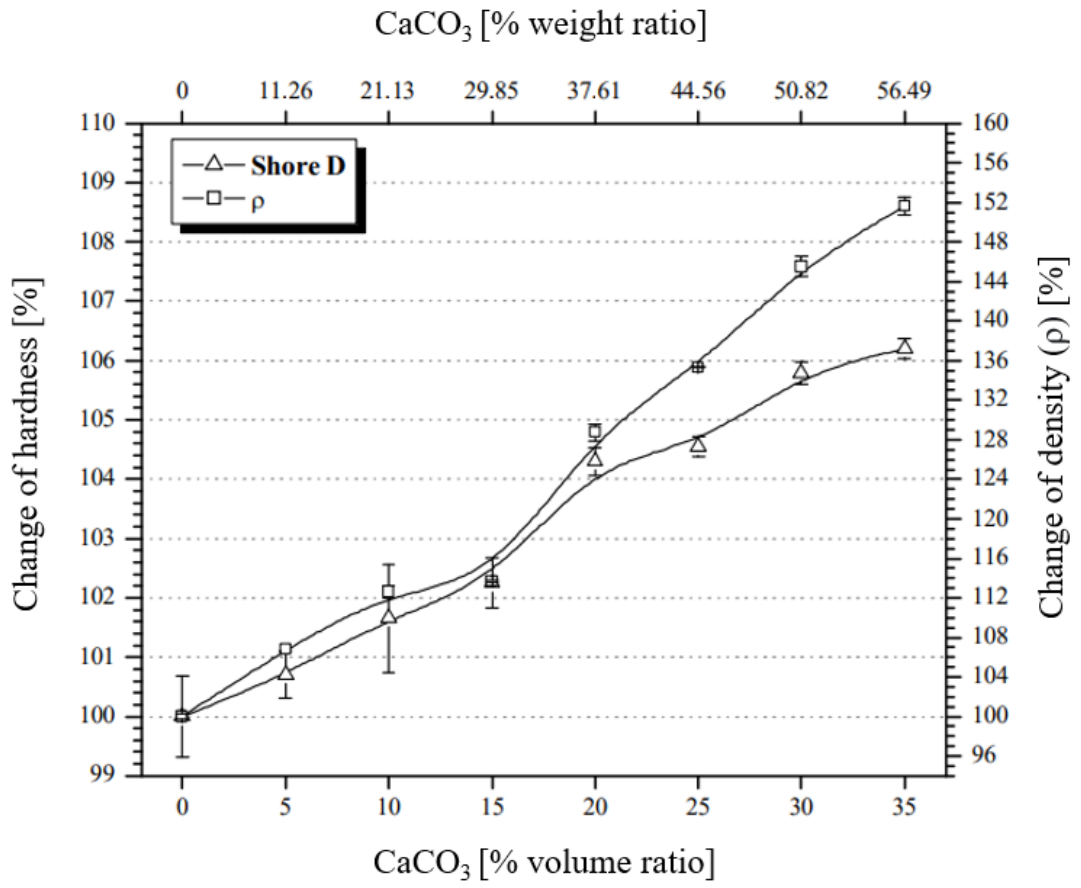


Figure 3.10: The density and hardness graph of PP-R at different CaCO₃ ratios [28]

Chapter 4

The Effect of the Plastic Parts and Mold Design on the Weld Line

One of the most important factors affecting the part design is the production method. In order to determine the production method, the part design must be functionally completed first. The most appropriate production method of the completed design should be determined. According to the selected production method, the design should be revised and made suitable for production. After the part design is completed based on both functionality and production method, prototype production should be accomplished. Prototypes can be produced with fast and low-cost production methods such as 3D printing or machining. If the part does not fulfill its function when tested in the working environment, the part design should be revised and the prototype should be produced again. This process continues until the part design is suitable for the working environment. After the part design is fully adapted, it becomes ready for mass or special production.

This process should be managed in the same way for the part to be produced with the However, after the functional design of the part is satisfactorily completed, it is difficult to redesign the part for plastic injection production. Then, many unforeseen problems may naturally occur during the plastic injection process. Some of these problems are warpage of the part, leaving the part in the mold, sink marks, air pockets or vacuum voids, weld lines, diesel effect, short shot, flow lines, flash or spew or burrs, error of measurement, ovalization problem, visual faults, ejector pin marks. Usually, the root cause of these errors is not from only one parameter. Although some errors can be corrected with a single parameter, mass production of the part will be smoother and perfect if other parameters are made suitable for the injection method.

There are four main causes of a faulty part. The first is the plastic part design, the others are mold design, injection molding machine or injection parameters, and plastic raw material. If any of these four parameters is faulty, the plastic part cannot be produced properly. Therefore, these four parameters should be designed and adjusted in the most appropriate way for production.

4.1 Improved Plastic Part Design to Reduce the Effect of the Weld Line

Part design directly affects the strength, visual appearance, suitability for mass production, injection parameters, the cost of the part, and the cost of the mold. For this reason, it requires serious experience and technical knowledge to be able to design the part produced in plastic injection. Especially if the plastic part is multifunctional and complex and has a high visual quality, the design of the part becomes even more important. Another critical point is to expect durability and visual quality from plastic parts with joint marks. Therefore, plastic part design, mold design, and injection parameters should be considered simultaneously to satisfy these conditions.

4.1.1 Ribs and Bosses Design

Weld line regions can be predicted with plastic injection analysis programs. The plastic part can then be strengthened in the design, making it more durable by employing ribs and bosses. However, in order to perform this correctly, it is necessary to make the right decision on the weld line region. The important point here is that with different injection parameters, the weld line regions can change. Therefore, it should be analyzed and interpreted by setting different injection parameters. After the location of the weld line region is estimated, the ribs and bosses can be added to the part design.

In a suitable rib and boss design for a part, there may be very low sink marks and easy to eject from the mold. In Figure 4.1, the dimensions of the rib are shown. Factors affecting the dimensions of the rib and boss are the type and thickness of the plastic part. In Figure 4.1 the range of dimensions is given based on the wall thickness (W) of the part. As the shrinkage of the plastic decreases, the amount of sink marks also

decreases. Therefore, in plastics with a high shrinkage ratio, the rib thickness should be at the lower limit of the given range of dimensions, and in plastic materials with a low shrinkage ratio, the rib thickness can be selected at the upper limit of the given range of dimension. Since the shrinkage ratio of thermoplastic materials in the semi-crystalline group such as PP, PE, and POM is high, the rib thickness should be low. But the shrinkage of thermoplastic materials in the amorphous group such as ABS, PC, and PS is low, the rib thickness can be higher. In this way, the part can be designed more durable without visual disturbances in the weld line region, depending on the type and wall thickness of the plastic material. Thus, strengthening improves the design of the plastic part both visually and functionally.

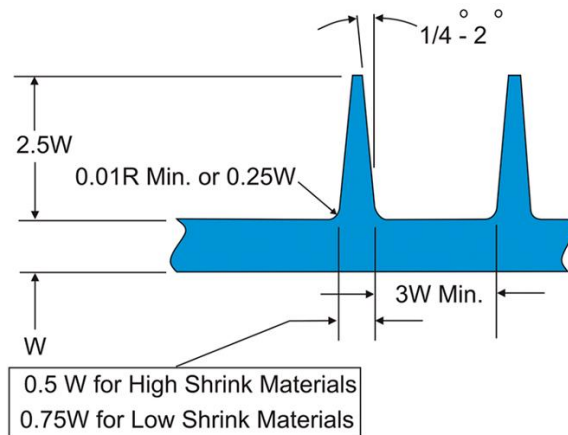


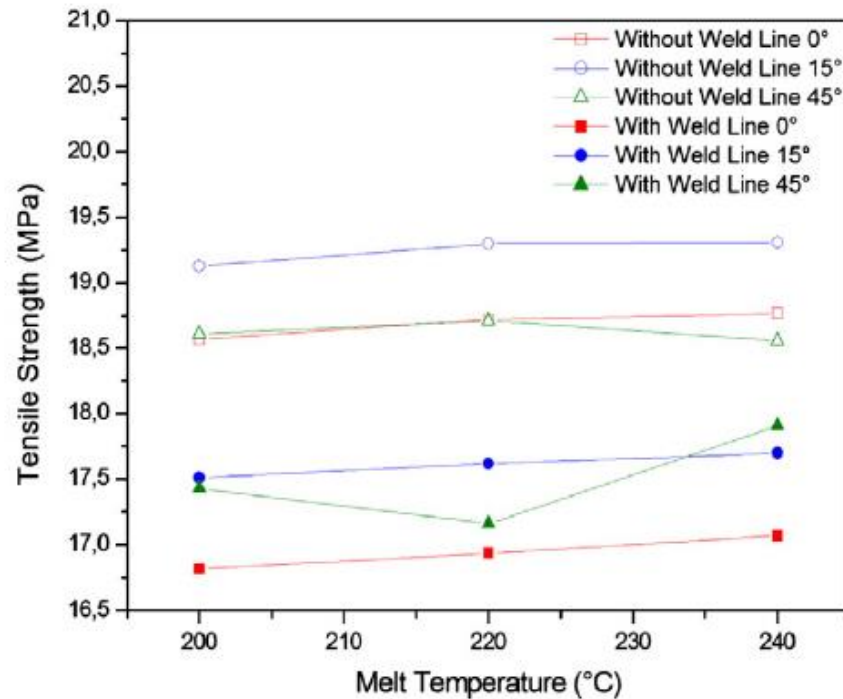
Figure 4.1: The rib dimensions [29]

4.1.2 Hole and Gap Designs

If there is a hole or gap in any area of the plastic part, a weld line will form. If there is only one gap and, the weld line can be avoided by using a diaphragm gate through this gap. This type of gate can be used in gap designs on parts to eliminate both deflection and weld line. But if there is more than one gap on the part, the weld line is inevitable. For this reason, it is important to reduce the hole and gap forms on the part as much as possible. In this way, both strength and visual quality can be increased.

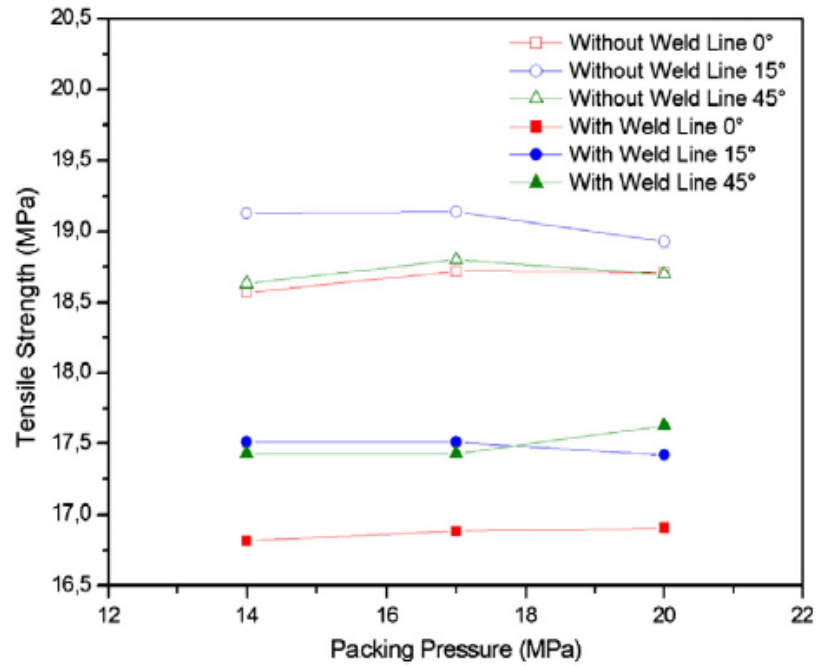
Another important element is the geometry of the hole or gap on the part. The geometry here affects both the meeting angle and the weld line length, and a more durable region

can be formed. Özçelik et al. [30] formed a gap in the PP plastic part with the obstacle geometry in the mold. The angles of these obstacle geometries are produced as 0°, 15°, and 45°. By changing the melt temperature and packing pressure at these angles, the effect on the weld line and non-weld line strength of the part was investigated. The tensile strength of the part with the obstacle geometry angle at 15° is higher than the others. However, as can be seen in Figure 4.2, the tensile strength of the part with an angle of 45° at high-temperature and pressure is higher than the others. At every temperature and pressure, the obstacle geometry at 0° has a lower tensile strength compared to the others. This is because the meeting angle of the molten plastic is lower and the weld line length is longer.



(a)

Figure 4.2: Tensile strength of specimens with/without weld line for obstacle edge angle, (a) Melt temperature, (b) Packing pressure [30] (Continued)



(b)

Figure 4.2: (Continued)

4.2 Improved Mold Design to Reduce the Effect of the Weld Line

The changes that can be made in the mold design to improve the strength and visibility in the weld line region are more than the plastic part design. Since the plastic part is designed for visibility or functionality, it may not be possible to make too many changes. Accordingly, improvements can be achieved with mold design according to needs and requests.

The parameters that enable the development of the mold design in the weld line region are the gate type and location, the vent channels, cooling or heating channels. Among these, the most effective solution is the gate type, location, and number. While the vent channels and cooling or heating channels are optimizing the weld line region, the weld line can be eliminated with the gate type and location. Therefore, if any improvement is to be made in the weld line region, it should first be started with the gate type and

location. Consequently, if the part is to be any improved for the welding, improvement should first start with the gate type and location.

4.2.1 The Gate

A gate is a channel opened for the filling of the plastic part. There are many different types of gates. The selection of the gate type is made with the design of the plastic part, the design of the mold, and the features expected from the plastic part. The gate region is weak in plastics and this region has visual defects. For this reason, the gate of the plastic part should be positioned from the region that is not important in terms of visual and strength. If it cannot be located in an insignificant region or there is no such region in the plastic part, the gate region should be as small as possible. This can be accomplished with the cold runner system, but the best results are achieved in this region by using the hot runner system that is generally used for transparent visual parts. There are three main reasons for using the hot runner system. The first is to minimize the gate scar, the second is to keep the temperature and pressure of the molten plastic in the mold, and the third is to eliminate the runner scrap. Thus, the best result is obtained for the visual quality, mechanical strength properties, and cost of the plastic part.

The gate type, location, and number directly affect the formation of the weld line. This effect varies according to the design of the plastic part. In some cases, the joint scar can be completely removed with gate type change, while in some cases only minor improvements can be achieved. As a result of the plastic filling analysis, the final decision is to determine the type, position, and the number of the gate that provides the best result showing the meeting angle, temperature, location, and length of the weld line.

It is possible to prevent the weld line with the type of the gate. But it may not possible for every plastic part. Especially in designs with more than one hole or gap in the part, there will be a definite weld line formed. For parts with these features, the best is to try to optimize the weld line. As a result of the plastic filling analysis, the position of the weld line should be moved to the desired region, the meeting angle should be large, the meeting temperature should be high and the weld line length should be low. Then, the gate type and location are determined.

For round parts, the weld line can be avoided with the diaphragm or ring gate type. The characteristic of these gate types is that the part is not point filling, so the filling of the part is uniform in the round parts. In addition, it is provided for measurement accuracy, predictable shrinkage, low distortion, low deflection, and uniform flow, apart from preventing the weld line in diaphragm and ring runner round parts [31]. The disadvantage is that since the runner is broken after the injection, there will be a scar in the broken area, and that area will be of poor quality visually. However, in point gates, there will be the weld line on the opposite side of the gate as it diametrically encircles the part during filling. And in this type of part, the weld lines are formed as much as the number of gates. The diaphragm gate is shown in Figure 4.3.a and the ring gate in Figure 4.3.b.

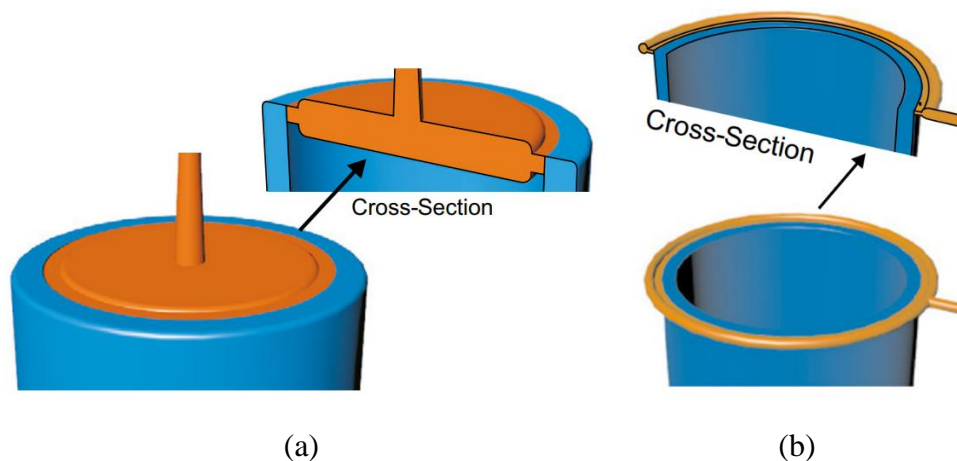


Figure 4.3: (a) Diaphragm gate and cross-section (b) Ring gate and cross-section [31]

For flat, wide, and large plastic parts, using a fan gate can prevent the weld line formation without adding multiple gates. Other advantages are slow and uniform filling, reducing the jetting defect, and reducing the stress in the gate region. It also reduces deflection and warpage in large parts and increases measurement accuracy. The disadvantage is that it is cut manually like the diaphragm and the ring gate. Therefore, the visual quality of the cut area is poor in the fan gate. The fan gate type is shown in Figure 4.4.

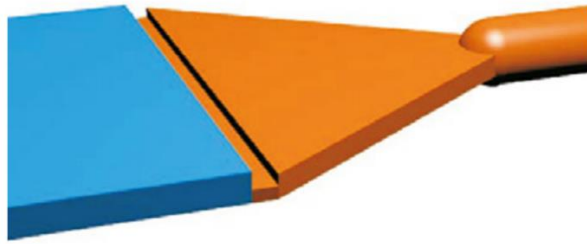


Figure 4.4: Fan gate [31]

Since the fan gate has a wide cross section area, the speed of molten plastic slows down in this cross section during the injection. This situation directly affects the filling and packing stage of the plastic part. While it has a positive effect on the filling of the plastic part, it has a negative effect on the packing. Because plastic flow has a low velocity in narrow spaces, the molten plastic loses heat energy and cools. And if the molten plastic cools further, it freezes and the pressure applied during the packaging stage does not reach the mold cavity, which may cause malfunctions in the part. Then, it is necessary to increase the thickness of narrow sections in the mold. It is not appropriate to increase the gate thickness because the area to be cut will increase. For this reason, a more effective design can be achieved by thickening the area of the gate that does not contact the part. However, the molten plastic enters the dead zone before it enters the first mold cavity during the injection stage. Then the molten plastic at the back first enters the mold cavity. It fills the mold cavity more easily because the heat energy of the molten plastic at the back is higher. This dead zone should also be present in all other runner types so that the molten plastic with low heat energy does not enter the mold cavity. Improved fan gate design is shown in Figure 4.5.

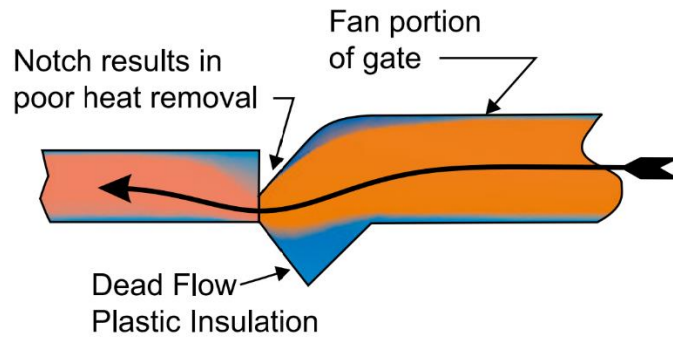


Figure 4.5: Improved the fan gate design [31]

For runners, this area is called cold slug well shown in Figure 4.6. Typical cold slug well dimensions are approximately 1.5 to 2.0 times the diameter or width of the feed runner. The important thing is that the molten plastic with low heat energy in the front does not enter the mold cavity.

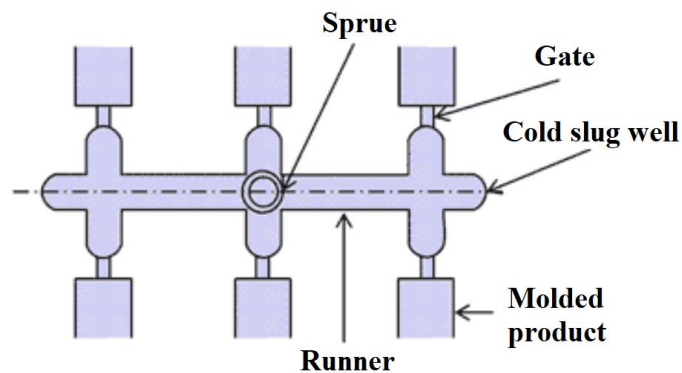


Figure 4.6: Cold slug well design

4.2.2 Air Vent Channel

While the molten plastic is filling the mold cavity, the air inside the mold cavity cannot be evacuated. Afterward, the air is trapped in the last filled volumes of the mold cavity and may cause short shots, staining, and burn marks in that region [32]. Air traps are often seen in regions such as the ribs and bosses, the last filled volumes of the mold, and the weld line. The occurrence of the air trap defect is illustrated in Figure 4.7.

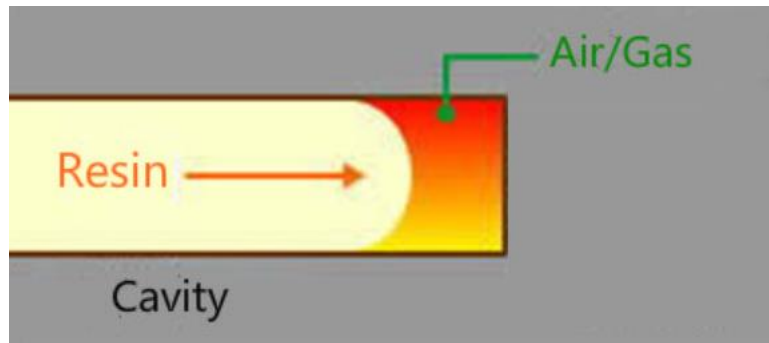


Figure 4.7: Air Trap

It creates a diesel effect with the air trap and causes the plastic to burn in that area. As a result, this results in a visual appearance problem on the plastic part surface. In Figure 4.8, defects on the plastic due to the air trap are shown. In addition, since the air pressure created by the air trap will create a pressure opposite to the injection pressure, molten plastic becomes so hot that it causes burnt spots on the plastic. At the end of the flow path or individual areas of the molded part plastic will not be fully formed and locally black discolorations of the molded part occur in the area of the weld lines. It can also be the case that changes appear on the mold surface. As a result, a decrease in strength and visual quality will be observed. In particular, the air compression in the weld line considerably reduces the strength of that region. Because defects caused by both the welding line and the air trap weaken that area considerably. For this reason, it is necessary to prevent air trapping the parts that are visually important and desired to be durable.

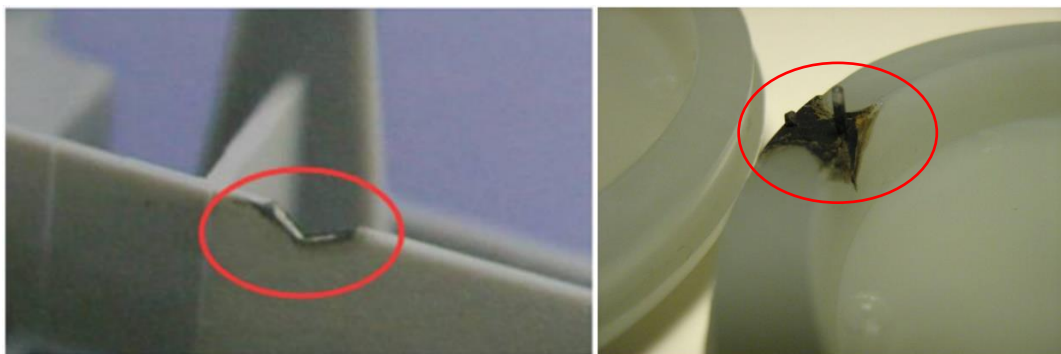


Figure 4.8: Samples of the air trap defect

There are certain methods of completely avoiding air traps. The basis of several different methods is to machine a gap in the region where there is an air trap located and to release the trapped air from that gap. First, the channel can be machined in the region where there is an air trap between the core and cavity mold. Second, the diameter of the ejector pin can be machined 0.02 mm smaller than the ejector pin hole. The last one is the parting lines of the mold is the natural air vent channel [33]. But there are typically two main points when performing these gapping operations. The first is the depth and width dimensions of the air vent channel and the possible second is the correct determination of the region where the air trap is instantly formed.

The proper depth of the air vent channel varies according to the specific type of plastic, the melt temperature of the plastic, the temperature of the mold, the injection and packing pressure. The significant issue is that the air trap must be able to pass through the channel, but the molten plastic must not be able to pass through this channel. In general, accordingly, the depth measure that will provide this varies between 10-60 μm . Miranda et al. [34] studied process efficiency with changes in injection parameters and mold design using general-purpose polystyrene (GPPS). In their study, the design of the air vent channel on the mold is shown in Figure 4.9. The air vent channel is machined 20 mm in length, 10 mm in width, and 0.025 mm in depth. In the continuation of the air vent channel, a 1 mm depth channel is machined after 20 mm length to facilitate the gas escape from the mold cavity. Thus, the air vent is provided without any problems.

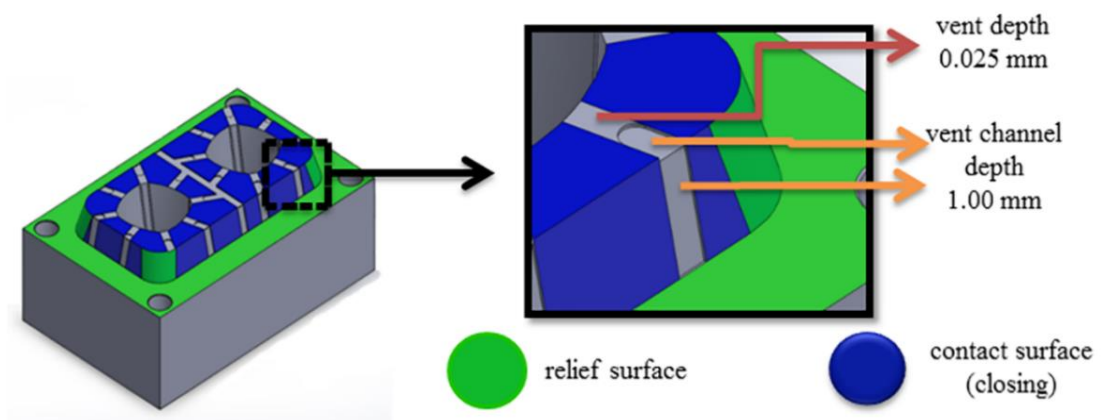


Figure 4.9: The design of the air vent channel [34]

Another critical consideration is to find the region where the air trap. The locations of the defects can be detected with plastic filling analysis. Since air will be trapped in regions such as ribs and bosses, the mold should be designed to have an air vent channel in these locations. However, since the position of the air trap may change with the injection parameters, the air vent channels can be machined after the first injection is completed. Thus, the locations of the air vent channels machined after the experimental test will be more accurate. Alternatively, after the injection parameters are set in the plastic filling analysis programs, air trap regions can be determined and then machined directly on the mold material. Thus, the mold can be produced more cost-effectively and in a shorter time.

4.2.3 Cooling System

The cooling process in the plastic injection process accounts for about eighty percent of the cycle time. Fast and uniform cooling both reduces the cost of the part and ensures a higher quality of the part. Also, the well-designed cooling system prevents differential shrinkage, internal stresses, warpage, ejector marks problems, and redundant cycle time [35].

In plastic injection molds, the cooling system design comprises a key factor for the defect-free production of the plastic part. Because in the shaping process of the parts in the mold cavity by solidifying the molten plastic, the properties of the plastic part are determined. Consequently, the mold must be cooled uniformly during the solidification process of the molten plastic. To achieve this, the mold and plastic part materials and design and injection parameters must be carefully considered.

There are many possible reasons why the cooling system is a critical parameter. For instance, the cooling system affects and determines the mechanical properties of the plastic part, shrinkage, deflection, warping, cycle time, sink marks, transparency, flow, the weld line, and cost. The cooling time is directly proportional to the square of the wall thickness of the plastic material [36]. For this reason, the cooling process should be more intense, especially in regions with high wall thickness. Since the thin and thick wall thicknesses of the plastic part solidify at the same time, the cooling time will decrease and the cost will reduce. It also prevents possible defects such as sink marks, deflection, warping, and dimensional errors.

Mold temperature, which directly affects the welding line, is also controlled by the cooling system. Therefore, the defect in the weld line can be improved by changing the mold temperature. Cheng-Hsien Wu et al. [37] found that the contribution rate of the mold temperature to the weld line strength was 13.00%. Figure 4.10 shows the effect of different mold temperatures on the weld line factor for PP. The weld line factor is the ratio of the weld line strength to the non-weld line strength of the test specimen with the same geometry and material. No.1, 2, 3, 4, and 5 identify test specimens with various widths and thicknesses in Figure 4.10. Thus, it is possible to improve the weld line defect by increasing or decreasing the mold temperature. In other studies, the effect of mold temperature on the weld line strength varies between 5.84% and 42.40%.

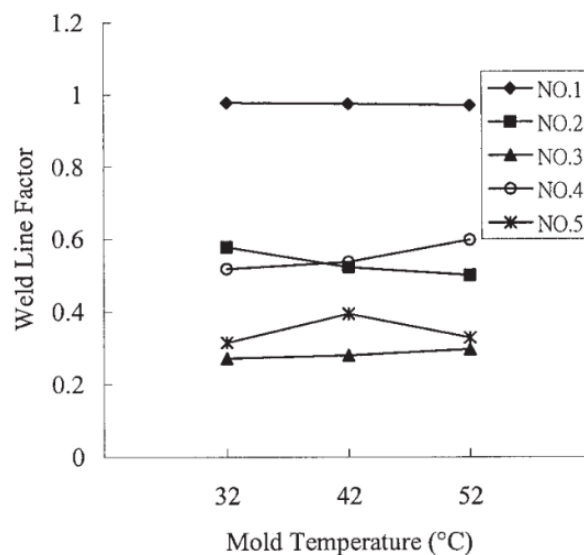


Figure 4.10: The effect of the mold temperature on the weld line factor for PP [37]

As can be seen from Figure 4.10, there are cases where the mold needs not only cooling but also heating. Heating is also needed for reasons such as preventing welding line formations and the surface quality requirements. The heating process is applied in the same way as the cooling process. The mold temperature can be increased up to 90-95 °C by connecting hot water from the cooling channels machined on the mold, and up to 200 °C by connecting hot oil. However, the connectors in the hot water system and especially in the hot oil system should be installed attentively. Threaded polyurethane

nipples should never be practiced in hot systems. The hose fittings may come loose or break as the mounting system loosens with the increase in mold temperature. Therefore, durable connectors such as quick-release connector plugs are recommended.

Another important scrutiny in the mold cooling system is heat transfer. The increasing rate of heat transfer will bring about faster and more uniform cooling or heating. Heat transfer can be improved in two ways. First, the hose diameter in the cooling system must be selected larger than the diameter of the cooling channels. As a result, the flow velocity is increased by reducing the area in the flow path. Thus, turbulent flow is achieved with a higher Reynolds number, which means a higher transfer rate [38]. For this reason, the cooling channels should be designed in such a way as to obtain a turbulent flow. There are various cooling channel alternatives to be configured in mold design. The four commonly installed cooling channel configurations are starkly illustrated in Figures 4.11, 4.12 4.13, and 4.14.

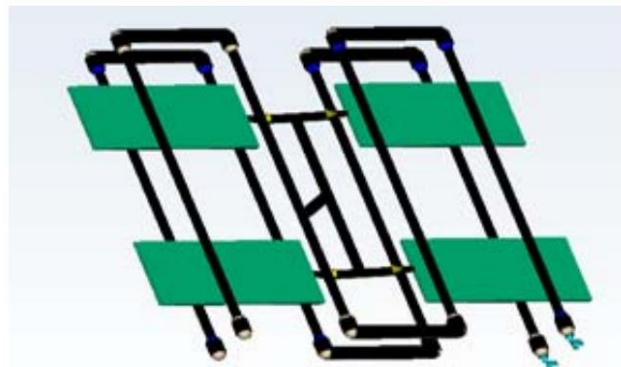


Figure 4.11: In line transverse cooling channel [38]

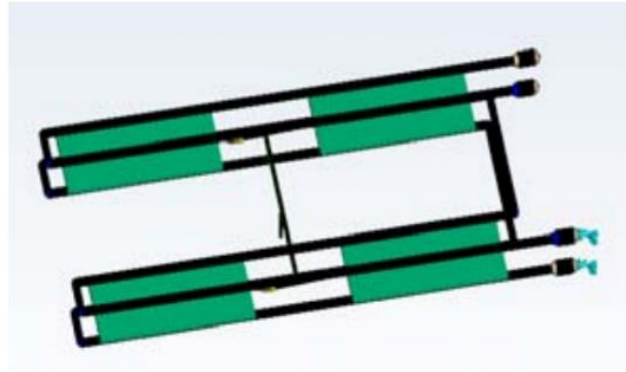


Figure 4.12: In line longitudinal cooling channel [38]

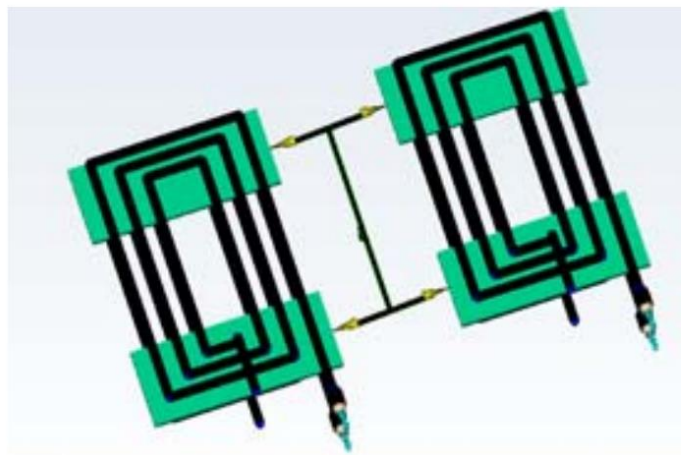


Figure 4.13: Spiral cooling channel [38]

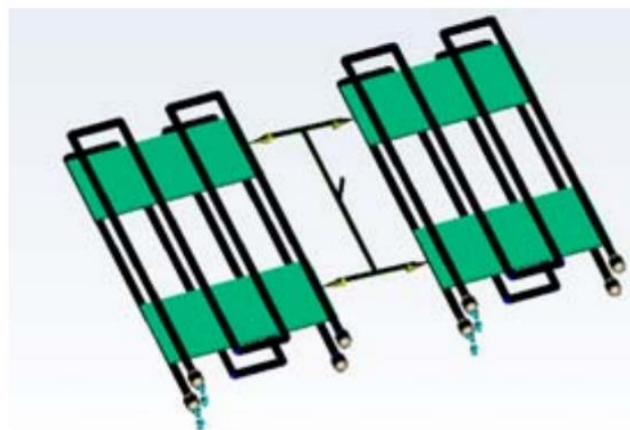


Figure 4.14: Zig-zag cooling channel [38]

Another way to increase heat transfer is to change the mold materials. Copper beryllium (CuBe) alloy is the most regularly consumed material when high heat transfer is required in the mold. This alloy is frequently supplied because its strength properties are close to steel and the heat transfer coefficient is quite high. For example, the properties of the copper-beryllium alloy Alloy 25 (C17200) Strip material can achieve a heat transfer coefficient of up to 105 W/mK, the ultimate tensile strength of up to 1520 MPa, and hardness of up to 421 HB. Tensile strength values differ for various tempering processes. As a disadvantage, the cost of the copper-beryllium alloy is very high. Due to its high cost, it is only fixed in regions where it is very necessary and essential.

The most commonly employed mold material is tool steel because of its high strength, low cost, and ferromagneticity. For example, 40CrMnNiMo 8-6-4 (1.2738 tool steel) is one of the most commonly used tool steel. 40CrMnNiMo 8-6-4 has a heat transfer coefficient of between 33-34 W/mK, the ultimate tensile strength of 950-1100 MPa, and hardness of 280-325 HB. However, the ultimate tensile strength can be increased up to 1920 MPa and hardness up to 54 HRC by heat treatment.

Aluminum is also frequently used as a mold material. Aluminum has some properties that are superior to other metals. They are a very high heat transfer coefficient, a low density of approximately 2.5 times, low cost, and easy machinability. But, the mechanical strength of aluminum is low. For this reason, it is generally set in molds of low production numbers or parts that do not require strength. 7075-T6 aluminum series with the highest mechanical properties among aluminum materials can be considered as the most accustomed mold material having a heat transfer coefficient of 130 W/mK, the ultimate tensile strength of 572 MPa, and hardness of 150 HB. Since the heat transfer is very high and the mechanical properties are low, aluminum can be chosen as the insert material in the mold without a cooling system can be chosen.

In order to increase the effectiveness of the cooling system on the weld line strength, the turbulent flow should be provided in the cooling channels, the Reynolds number should be increased and the mold material with a high heat transfer coefficient should be selected. The mold temperature is ensured to be kept uniform by giving cold water, hot water, or hot oil from the cooling channels. As a result, it is possible to reduce the

effect of the weld line, improve the surface quality, increase the dimensional accuracy and reduce the cycle time.

Chapter 5

Materials and Methods

5.1 Materials

LG ABS HI121H and Ravago PP 20% glass fiber (PP GF20) were consumed as plastic raw materials. The reason for using these materials is to test both amorphous and semi-crystalline thermoplastic materials. In addition, the weld line can be examined in both reinforced and non-reinforced thermoplastic materials. Thus, it is possible to examine the behavior in the weld line.

5.2 Methods

5.2.1 Plastic Injection Molding

The injection molding machine is Arburg Allrounder 470 C Golden Edition. The specifications of the injection machine: The clamping force is 1470 kN, the screw diameter is 40 mm and the injection capacity is 201 cm³. The width and length distance between the columns of the injection molding machine is 470x470 mm. The Arburg Allrounder 470C Golden Edition plastic injection molding machine is shown in Figure 5.1.



Figure 5.1: Arburg Allrounder 470C Golden Edition plastic injection molding machine

5.2.2 Tensile Testing Machine

Both the tensile and bending tests were performed on a 100 kN capacity SHIMADZU AG-IC machine. Bending tests were performed by changing the equipment of the testing machine.

5.2.3 Mold Temperature Controller

The mold temperature controller was instrumented to control the core, the cavity, and the insert temperatures. Rhong RTC 950 series mold temperature controller was used. It provides heating with oil. It has a power of 9 kW and the cooling method is indirect cooling. The RTC 950 series mold temperature controller is demonstrated in Figure 5.2.



Figure 5.2: RTC 950 series oil type mold temperature controller

5.2.4 Temperature Control Module

The temperature of the core, the cavity, and the insert were measured with a thermocouple. Temperature measurements were gauged by connecting the thermocouple to the temperature control module. Opkon HCC-4 hot runner control module was attached to the molding system (Figure 5.3).

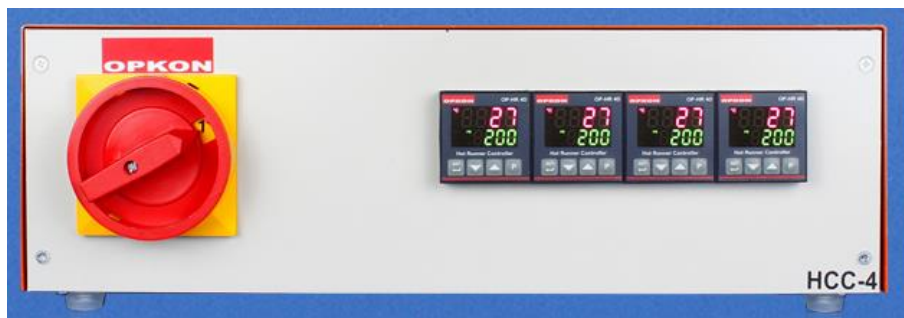


Figure 5.3: Opkon HCC-4 hot runner control module

Chapter 6

Experiments

This study aims to improve the strength of the weld line region by local heating or cooling. In this case, the core and cavity should not be affected too much by local heating or cooling here. The insert for the mold is configured according to the local heating and cooling principle. Thus, the temperature of the weld line region is altered independently from the mold and adjusted to the desired temperature set. In this way, the mold temperature is not affected by the insert temperature, the mechanical properties of the plastic part and the mechanical properties of the joint track can be adjusted as desired.

In the experimentation, the insert temperature, mold temperature, and melt temperature were changed and their mechanical properties were examined. Tensile and bending tests were performed to investigate its mechanical properties. As a result of the tests, the tensile strength and bending strengths at the breaking point were found. In this experimental study, the Taguchi method was carried out. Thus, the optimum sets of process parameters were found by reducing the experimental sets.

6.1 Design of Experiments

In the experiments, ABS and PP GF20 were tested as two different plastic materials. For each three process parameters with three levels for plastic injection molding have been studied. There are 27 experimental sets for each plastic material. Since it is very costly and time-consuming to complete all test sets, Taguchi L₉ (3⁴) orthogonal array was selected to reduce the experimental trials for plastic injection molding from 27 sets to 9 sets. For analyzing experimental data, Minitab 19.1 statistical software was

implemented. The process parameters and levels arranged for ABS and PP GF20 are listed in Table 6.1 and Table 6.2, respectively.

Table 6.1: The process parameters and levels for ABS

Parameter	Symbol	Unit	Level 1	Level 2	Level 3
Insert Temperature	A	°C	45	60	75
Mold Temperature	B	°C	45	55	65
Melt Temperature	C	°C	200	225	250

Table 6.2: The process parameters and levels for PP GF20

Parameter	Symbol	Unit	Level 1	Level 2	Level 3
Insert Temperature	A	°C	30	50	70
Mold Temperature	B	°C	30	50	70
Melt Temperature	C	°C	190	215	240

The experimental sets of ABS and PP GF20 with Taguchi L_9 (3^4) orthogonal array design are presented in Table 6.3 and Table 6.4 respectively. 16 test specimens have been fabricated for each experimental set. Of these, eight were spent for the tensile tests, and the other eight were used for the bending tests. Four of them have the weld line, and the other four are specimens without the weld line. The temperatures for each parameter were controlled and adjusted with a tolerance of ± 1 °C. A certain period has been expected for temperature changes to reach temperature set values. After waiting, 5 to 10 pieces of specimens were not treated as a test specimen and were scrapped. This is because the barrel and nozzle of the injection molding machine must be cleaned and waited for the mold to a steady state. Thus, the previous process conditions will not affect the specimens to be produced in new process conditions.

Table 6.3: $L_9 (3^4)$ orthogonal array of the parameters and levels of ABS

Experiment No.	Parameters		
	A	B	C
	Insert Temperature (°C)	Mold Temperature (°C)	Melt Temperature (°C)
1	45	45	200
2	45	55	225
3	45	65	250
4	60	45	225
5	60	55	250
6	60	65	200
7	75	45	250
8	75	55	200
9	75	65	225

Table 6.4: $L_9 (3^4)$ orthogonal array of the parameters and levels of PP GF20

Experiment No.	Parameters		
	A	B	C
	Insert Temperature (°C)	Mold Temperature (°C)	Melt Temperature (°C)
1	30	30	190
2	30	50	215
3	30	70	240
4	50	30	215
5	50	50	240
6	50	70	190
7	70	30	240
8	70	50	190
9	70	70	215

All the injection molding process parameters other than insert, mold, and melt temperatures were kept constant. The constant injection parameters of ABS and PP GF20 specimens are tabulated in Table 6.5 and Table 6.6, respectively.

Table 6.5: Plastic injection parameters and levels kept constant for ABS

Processing Parameter	Unit	Level
Injection Pressure	bar	750
Injection Speed	cm ³ /s	20
Injection Time	s	2
Packing Pressure	bar	500
Packing Speed	cm ³ /s	10
Packing Time	s	3
Cooling Time	s	35
Cycle Time	s	45
Dosing Volume	cm ³	45
Switch Over Point	cm ³	19

Table 6.6: Plastic injection parameters and levels kept constant for PP GF20

Processing Parameter	Unit	Level
Injection Pressure	bar	700
Injection Speed	cm ³ /s	15
Injection Time	s	2
Packing Pressure	bar	500
Packing Speed	cm ³ /s	10
Packing Time	s	2
Cooling Time	s	35
Cycle Time	s	44
Dosing Volume	cm ³	45
Switch Over Point	cm ³	22

Signal-to-noise ratio (SNR or S/N) is a measure handled in science and engineering that compares the level of the desired signal to the level of background noise. S/N is defined as the ratio of signal power to noise power. Note that these S/N ratios are described on a decibel scale. Equation (6.1) would be expressed if the objective is to reduce variability around a specific target, Equation (6.2) would be used if the system is optimized when the response is as large as possible, and

Equation (6.3) would be introduced if the system is optimized when the response is as small as possible [39]. In this study, Equation (6.2) was used because the largest value of stress gives the best result.

$$S/N = 10 \log \left(\frac{\bar{y}}{s_y^2} \right) \quad (6.1)$$

$$S/N = 10 \log \left(\frac{1}{n} \sum_{i=1}^n \frac{1}{y_i^2} \right) \quad (6.2)$$

$$S/N = 10 \log \left(\frac{1}{n} \sum_{i=1}^n y_i^2 \right) \quad (6.3)$$

\bar{y} : average of test data, s_y^2 : variance of y, n: number of tests and y_i : the value of output characteristic for the test.

The sum of squares is the sum of the square of variation, where variation is defined as the spread between each value and the mean. To determine the sum of squares, the distance between each data point and the line of best fit is squared and then summed up.

In probability theory and statistics, variance is the expectation of the squared deviation of a random variable from its population mean or sample mean. Variance is a measure of dispersion, meaning it is a measure of how far a set of numbers is spread out from their average value.

Analysis of variance (ANOVA) is a statistical tool provided to detect differences between experimental group means. ANOVA is warranted in experimental designs with one dependent variable that is a continuous parametric numerical outcome measure, and multiple experimental groups within one or more independent variables [40].

Statistically, the Fisher test, called the F-test, is a tool handled to find out which design parameters have a significant impact on the quality characteristics. The F-test allows checking the null hypothesis that there are no deviations in the average values of each factor level. Fisher test, as a phase of the statistical analysis, the Fisher test is employed to assess the degree of significance of parameters. A larger F-value displays that the variation of the injection molding process parameters produces a significant change in

the effectiveness [41]. There are intermediate levels commonly adjusted for the F-test and they are tabulated for significance levels of 0.5%, 1%, and 5%.

In statistics, the number of degrees of freedom is the number of values in the final calculation of a statistic that are free to vary.

The contribution rate (P_A) is the ratio of the parameter net sum of squares of factor A to the total sum of squares. Thus, the effect of parameters on the strength of the part is found as a percentage. The formula of the contribution rate is depicted in Equation (6.4).

SS'_A : Net sum of squares of factor A

SS'_T : Total sum of squares

$$P_A = \frac{SS'_A}{SS'_T} \times 100 \quad (6.4)$$

6.2 The Mold and Plastic Part Design

The mold for test specimens was fabricated in a two-cavity configuration, one for a weld line and the other for a non-weld line specimen. Thus, in a single production, both the weld line and non-weld line specimens are obtained. The tensile test specimen mold was borrowed from the Plastic Technology Laboratory of Ege Vocational High School at Ege University. Cavity, core, and inserts have been reworked. Some revisions have been machined on the tensile test specimen mold. However, the earlier version of the mold was also kept for later use, the original tensile test specimen can be still fabricated.

Two different materials were machined as mold material. The first is 6000 series aluminum for mold insert and the second is 1045 steel for other parts of the mold.

1045 steel is weak among tool steels, but it is a durable material compared to other metals. The reason for using 1045 steel grade is because of the low number of productions, there is no need to use more durable tool steel. Because the cavity has a parting line, different metal with low strength is not consumed. The parting line is the separating line for the mold halves. Even if the number of productions is low, the cavity

can be deformed during the pressurized injection process or clamp force application. Afterward, undesirable flashes may form on the plastic part.

6000 series aluminum has higher mechanical strength and high heat transfer coefficient compared to other metals. Subsequently, it was machined as the insert material. Even if the insert has a parting line, the risk of flash formation and inserts deformation is low because it is a small piece in the local area.

The mold cavity is machined on one side to facilitate mold production. The other side of the mold has a flat surface. This has benefited to simplifying mold making, reducing the risk of flash, and increasing measurement accuracy. The mold configuration is illustrated in Figure 6.1.

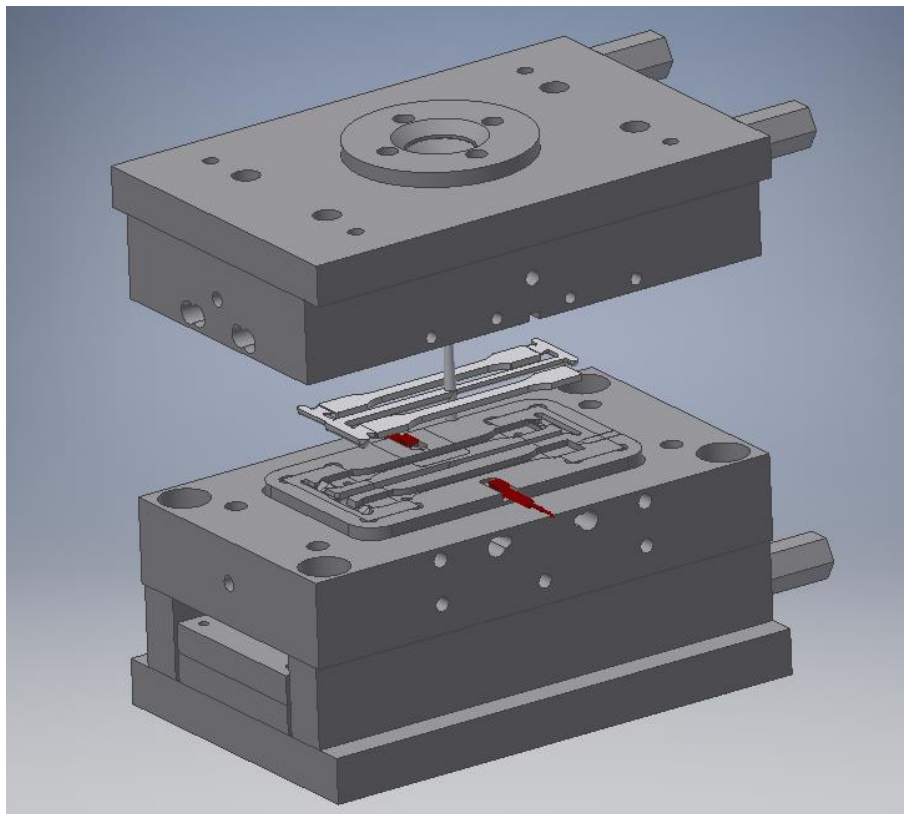


Figure 6.1: The mold of the tensile test specimen

The cavity side of the mold design are depicted in Figure 6.2. The mold design was detailed in the Autodesk Inventor Professional 2018 program. The cavity parts

designated by the numbers in Figure 6.2 are tabulated in Table 6.7. Figure 6.3 shows the image of the cavity side of the mold attached to the injection molding machine.

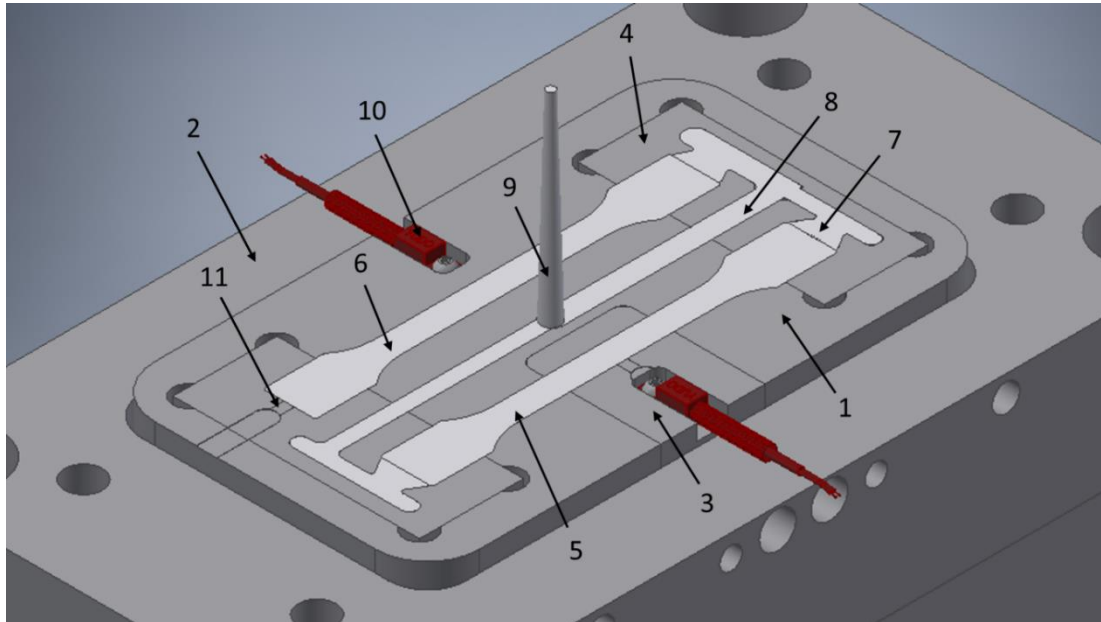


Figure 6.2: Design of the cavity side of the mold

Table 6.7: Part names of the cavity side

Part Names of Cavity Side	No.
Cavity	1
Cavity Plate	2
Insert 1	3
Insert 2	4
Weld Line Specimen	5
Non-Weld Line Specimen	6
Gate	7
Runner	8
Sprue	9
Thermocouple	10
Air Vent Channel	11



Figure 6.3: The cavity side of the mold

“Insert 1” is embedded for independent temperature control in the weld line region. The reason for placing “Insert 2” is that it is planned to examine the effect of changing the gate type on the weld line region in future studies. Therefore, two “Insert 2” have been fastened on the cavity side.

The gate was machined vertically from both sides of the weld line specimen, so the weld line have been formed in the middle of the tensile test specimen. In non-weld line specimen, the gate is formed vertically on one side, so there will be no weld line. Fan gate has been preferred as the gate type. The runner type has a parabolic geometry. The sprue is in the form of a conical hole inside the standard cold runner part. Two thermocouples were installed. Two thermocouples were used, one measuring the temperature of “Insert 1” and the other measuring the temperature of the cavity. In this way, temperature control of the insert and cavity temperatures can be performed independently.

The air vent channels were machined for both specimens. Since air trapped occurs in different regions, one is opened into the end zone and the other is opened into the middle zone. The core side of mold design are depicted in Figure 6.4. The core parts designated by the numbers in Figure 6.4 are listed in Table 6.8. Figure 6.5 shows the image of the core side of the mold on the injection molding machine.

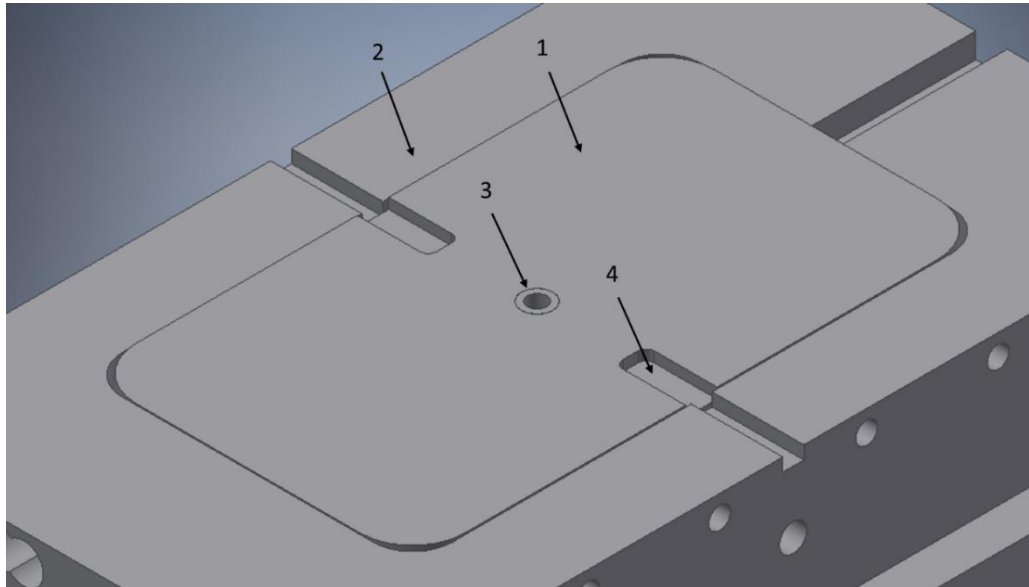


Figure 6.4: Design of the core side of the mold

Table 6.8: Part names of the core side

Part Names of Core Side	No.
Core	1
Core Plate	2
Cold Runner	3
Gap for the Thermocouple	4



Figure 6.5: The core side of the mold

The reason for making the cavities for the thermocouple is to prevent the thermocouples from being crushed between the core and the cavity when the mold is closed.

The heat transfer by conduction is directly proportional to the contact area. If the area of contact of the insert with the cavity is reduced, then the heat transfer is reduced. Therefore, to reduce the contact area, a 1 mm channel was machined on the insert. Thus, inserts and cavities at different temperatures will affect each other less. The insert geometry is illustrated in Figure 6.6. It should be noted here that a very small contact area can cause a flash on the plastic part and a centering problem of the insert. Therefore, the thickness of the contact area is 10 mm, and the minimum thickness is 6 mm.

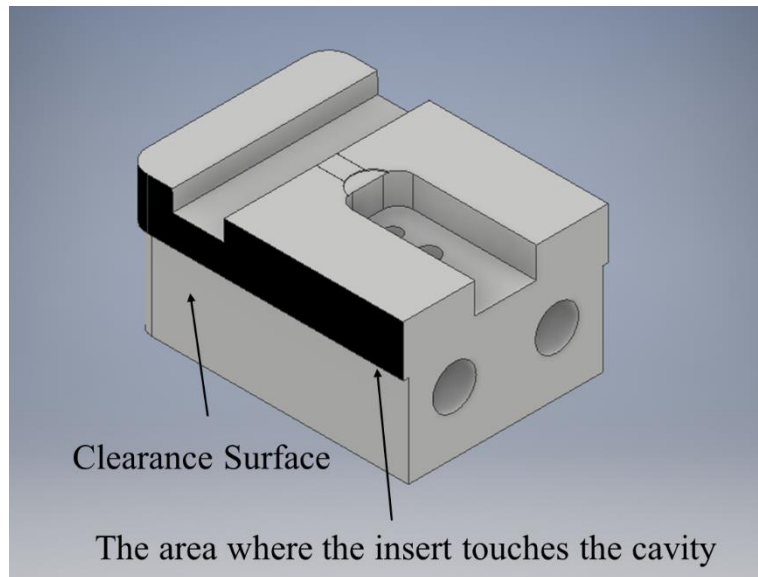


Figure 6.6: The insert design

Plastic parts made of ABS and PP GF20 are shown in Figure 6.7 and Figure 6.8, respectively. A close-up view of the weld line region is given in Figure 6.9.

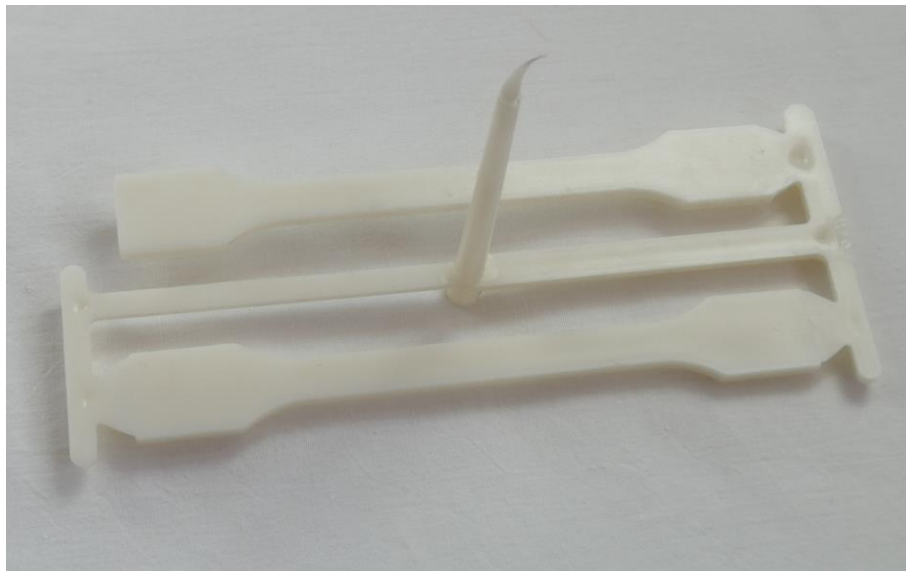


Figure 6.7: ABS specimens

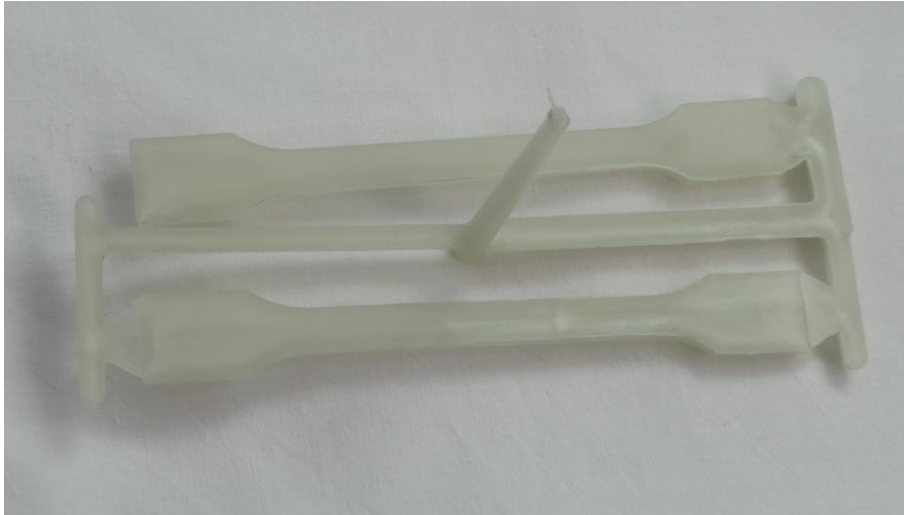


Figure 6.8: PP GF20 specimens

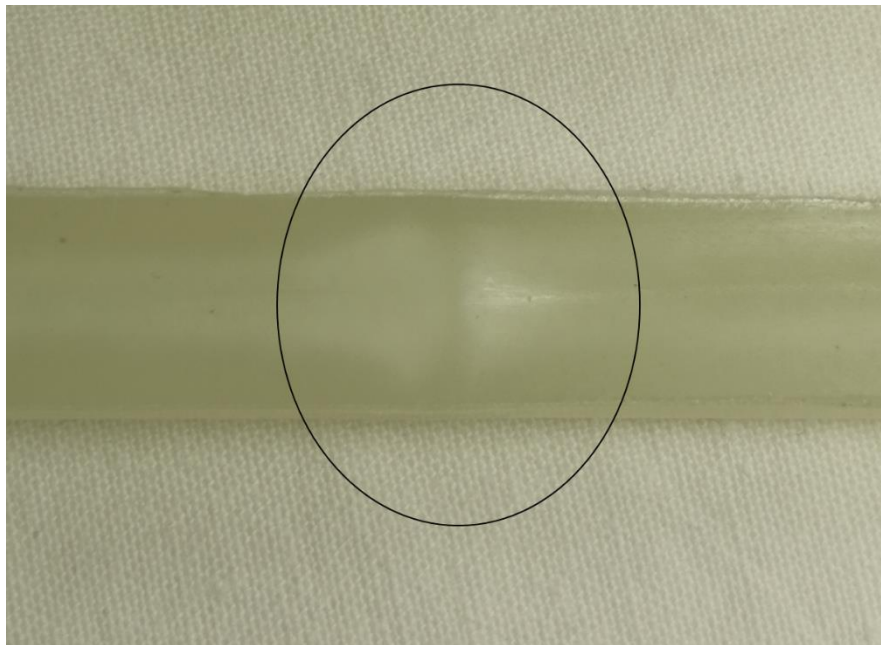


Figure 6.9: The weld line region of PP GF20

6.2.1 Design of Gates and Runners

6.2.1.1 Gates

The gates of the two specimens are fan gate types in the vertical direction. The main reason for this is that the filling of melt plastic is uniform during the injection. In this

way, it is aimed that there are no injection defects on the test specimens other than the welding line. The modeling of the gate is demonstrated in Figure 6.10.

The dimensions of all the gates are different from each other. Because there are two important points to be considered while the filling of these specimens. The first important issue is that, both the specimens must be filled at the same time. If a cavity fills up earlier, the injection and packing pressure may have less effect on this cavity. This is because the gate of the specimen may solidify or the injection and packing pressure may only have an effect upon the other cavity. The second is that the weld line should be in the middle region in the specimen with two gates because the insert temperature must affect the weld line. Otherwise, the insert will remain in the defect-free zone of the plastic part.

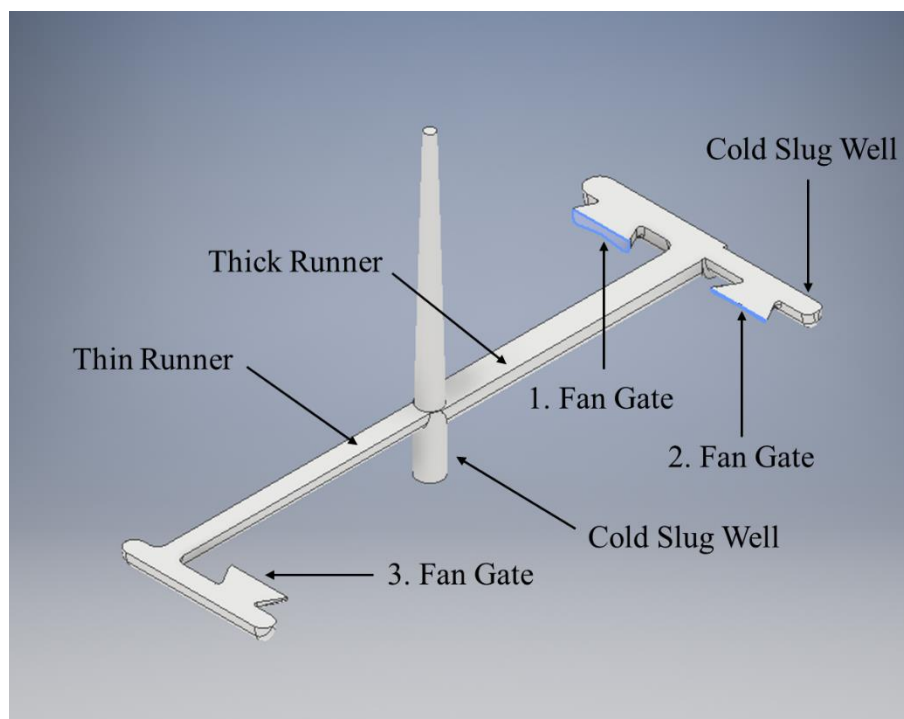


Figure 6.10: The fan gate design

The millimetric dimensions of the fan gates 1, 2, and 3 are illustrated in Figure 6.11, Figure 6.12, and Figure 6.13, respectively. With the plastic injection filling analysis program, the dimensions of the gates provide the molten plastic to fill the cavities at the same time and the welding line to be formed in the middle.

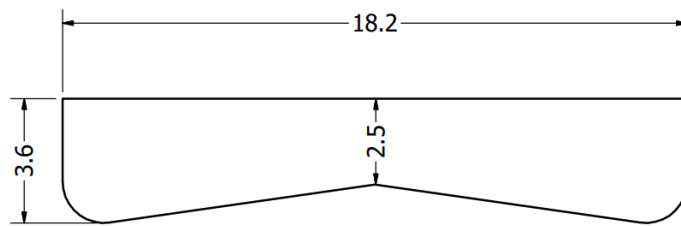


Figure 6.11: Dimension of 1. fan gate

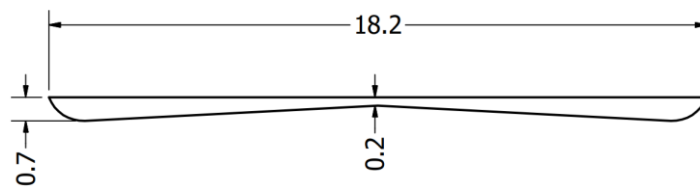


Figure 6.12: Dimension of 2. fan gate

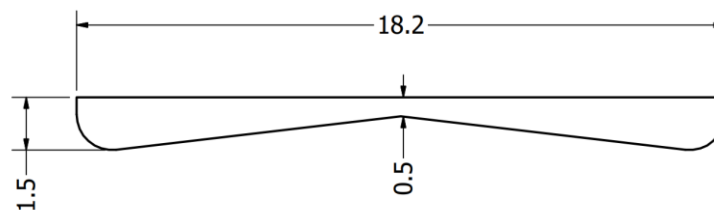


Figure 6.13: Dimension of 3. fan gate

6.2.1.2 Runners

Parabolic geometry has been preferred as the cross-section of the runner. If the ratio of the cross-sectional area of the runner to its circumference is greater, the flow of molten plastic will be easier and less energy will be lost. For this reason, a parabolic runner, which is one of the largest types of runners with this ratio, was equipped. Filling the cavities simultaneously and meeting the molten plastic fronts in the middle could not be achieved by simply changing the size of the gate. The dimensions of the runners were also arranged to satisfy these conditions. Two different parabolic runner

sizes were set. In Figure 6.10, thin and thick runners can be distinguished. The dimensions of the runner cross-sections in millimeters are geometrized in Figure 6.14.

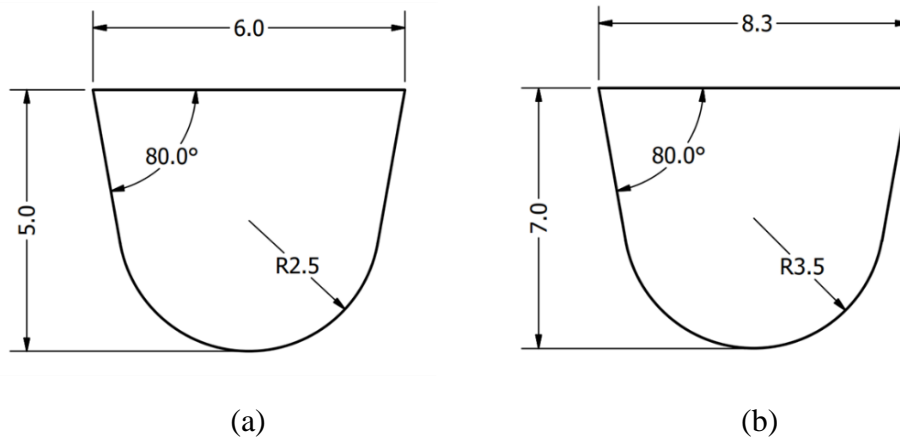


Figure 6.14: Runner dimensions, (a) Thin runner, (b) Thick runner

With the cold slug well, molten plastic with low heat energy cannot get into the mold cavity. The cold slug well configurations are shown in Figure 6.10.

6.2.2 The Cooling Channel Design

In the process, water was fed as a cooling and heating fluid. A separate cooling system has been installed for the insert. The cooling channels of the insert are illustrated in Figure 6.15. The water connection of the cavity and core was provided through the same hose. In this way, the same coolant will pass through both, ensuring that the cavity and core have the same temperature. The cooling channels of the cavity and core are demonstrated in Figures 6.16 and 6.17, respectively.

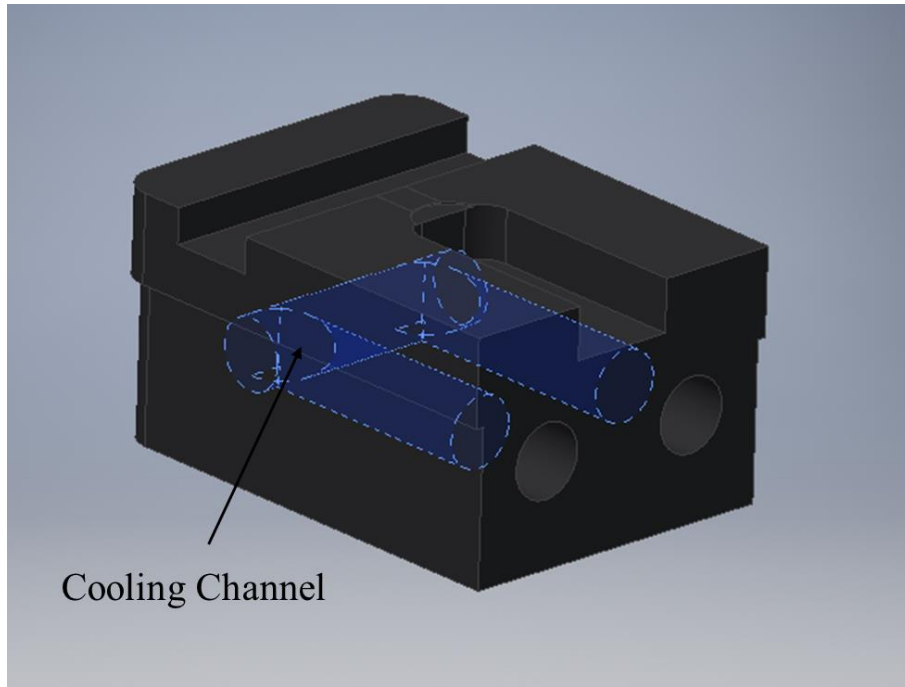


Figure 6.15: Cooling channel design of the insert

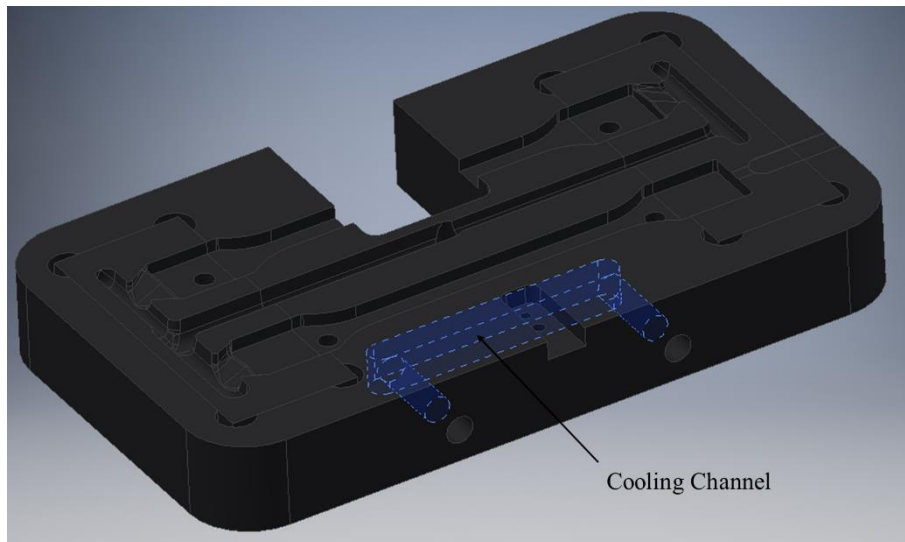


Figure 6.16: Cooling channel design of the cavity

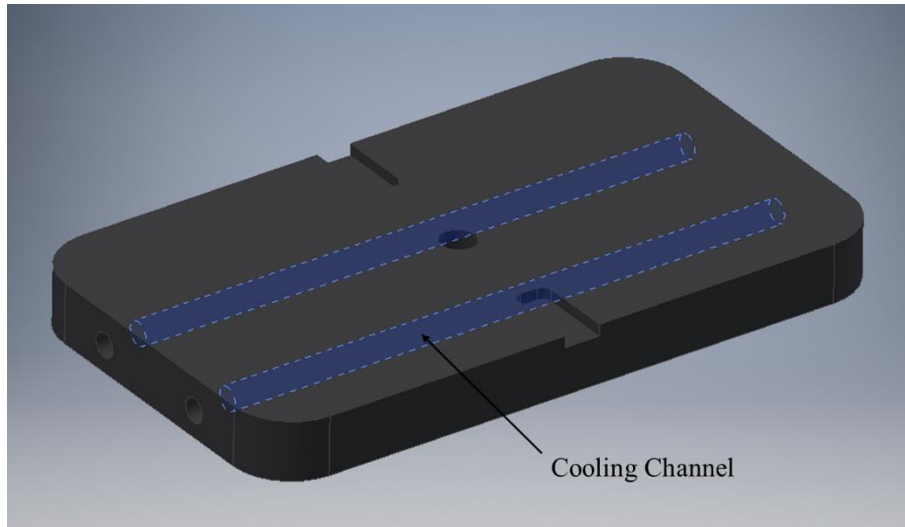


Figure 6.17: Cooling channel design of the core

The cooling channels were drilled into the insert and core with a diameter of 8 mm size. But cooling channel of the cavity was machined with a width of 8 mm, a height of 14 mm, and a length of 80 mm.

6.2.3 The Air Vent Channel Design

The air vent channels should be located in the last filled areas of the mold. Because of this, the air vent channel was machined in the farthest point from the entrance in the mold cavity of the non-weld line specimen. However, since the meeting of the molten plastic fronts will be in the middle of the weld line specimen, the air vent channel has been machined in the midpoint. All dimensions are similar for both channels. Air vent channels were sized as 0.03 mm in depth, 4 mm in width, and 5 mm in length. After that, a second channel with a depth of 0.2 mm and a width of 8 mm was opened for easy passage of air. The air vent channel of the insert is shown in Figure 6.2.

6.3 Tensile Tests and Bending Tests

6.3.1 Tensile Tests

Tensile test procedures are carried out by DIN EN ISO-527-2:2012 standards [42]. The images of the weld line and non-weld line specimens made of PP GF20 after tensile testing are depicted in Figure 6.18 and Figure 6.19. The dimensions taken from the tensile test standard are shown in Figure 20. Type 1A specimen size was appropriate for testing. Because type 1A is for specimens produced by injection molding, while type 1B is for machined specimens from pressed or injection molded sheets. A tensile test was performed with a speed of 5 mm/s. The tensile testing machine is demonstrated in Figure 6.21.

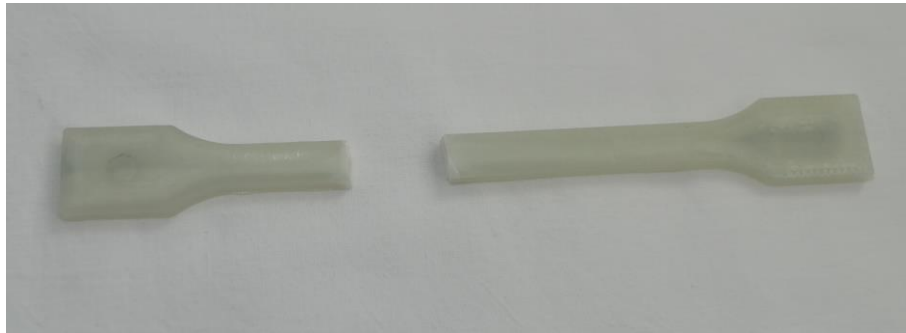
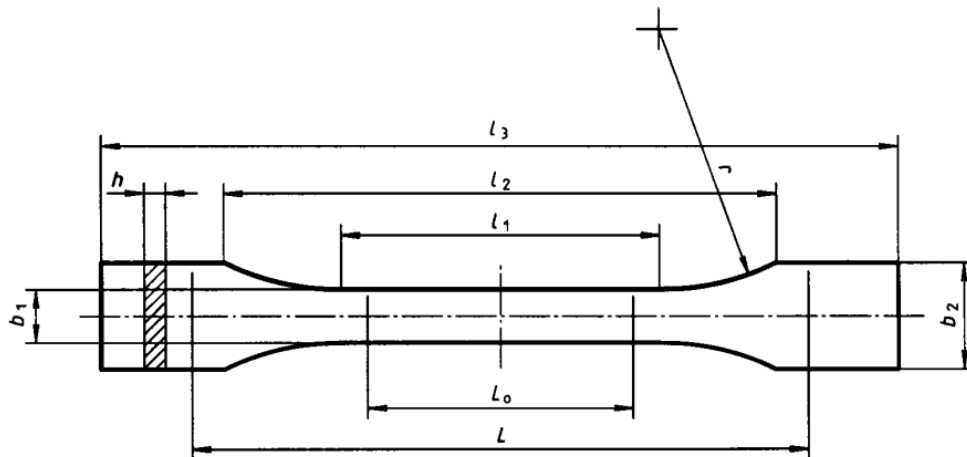


Figure 6.18: The weld line specimen made of PP GF20 after tensile test



Figure 6.19: The non-weld line specimen made of PP GF20 after tensile test



Dimensions in millimetres

Specimen type	1A	1B
l_3 Overall length	≥ 150 ¹⁾	
l_1 Length of narrow parallel-sided portion	80 ± 2	$60,0 \pm 0,5$
r Radius	20 to 25	≥ 60 ²⁾
l_2 Distance between broad parallel-sided portions	104 to 113 ³⁾	106 to 120 ³⁾
b_2 Width at ends	$20,0 \pm 0,2$	
b_1 Width of narrow portion	$10,0 \pm 0,2$	
h Preferred thickness	$4,0 \pm 0,2$	
L_0 Gauge length	$50,0 \pm 0,5$	
L Initial distance between grips	115 ± 1	l_2 ⁵⁾

Figure 6.20: Dimensions of the specimen in DIN EN ISO 527-2 standard [42]

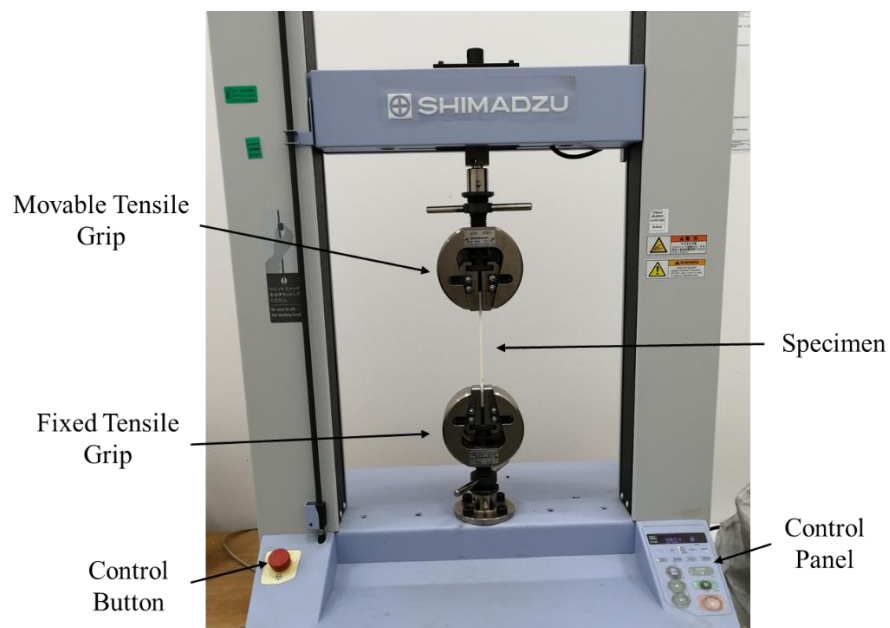


Figure 6.21: The tensile testing machine

As a result of the tensile test, force (N) – elongation (mm) data were measured and recorded. Stress (MPa) – strain (mm/mm) results were found by using Equation (6.5) and Equation (6.6)

$$\sigma = \frac{F}{A} \quad (6.5)$$

$$\varepsilon = \frac{Lf - Lo}{Lo} \quad (6.6)$$

6.3.2 Bending Tests

The three-point bending test procedures are carried out by DIN EN ISO 178-2019 standards [43]. The image of the weld line specimen made of PP GF20 after bending testing is given in Figure 6.22. The dimensions of the bending test standard are shown in Figure 6.23. The length is 80 mm, the width is 10 mm, the thickness is 4 mm, and the length of the span between supports is 64 mm. An injection mold cavity for the bending test specimen has not been fabricated. The bending test specimens were cut from the tensile test specimens with a size of 80 mm and a tolerance of ± 0.2 mm. The bending test speed is 5 mm/s. The bending test machine is illustrated in Figure 6.24.



Figure 6.22: The weld line specimen made of PP GF20 after bending testing

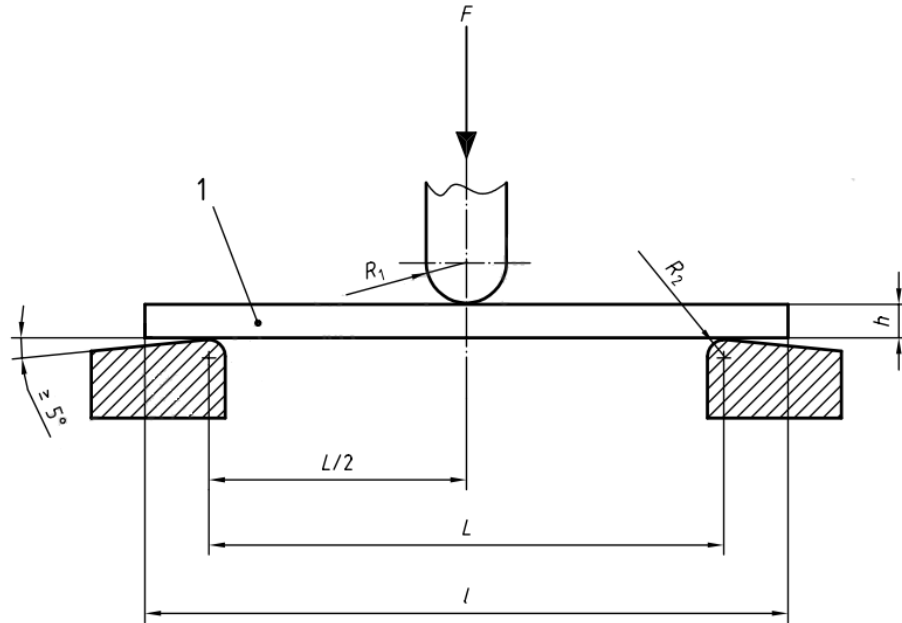


Figure 6.23: Dimensions of the specimen in DIN EN ISO 178-2019 standard [43]

Dimension of the length of the span between supports is equal to 16 times the thickness in DIN EN ISO 178-2019 standard. The measurements given in Figure 6.23 are as follows.

- 1: Test specimen
- F: Applied force
- R_1 : Radius of loading edge
- R_2 : Radius of supports
- h: Thickness of specimen
- l : Length of specimen
- L: Length of the span between supports

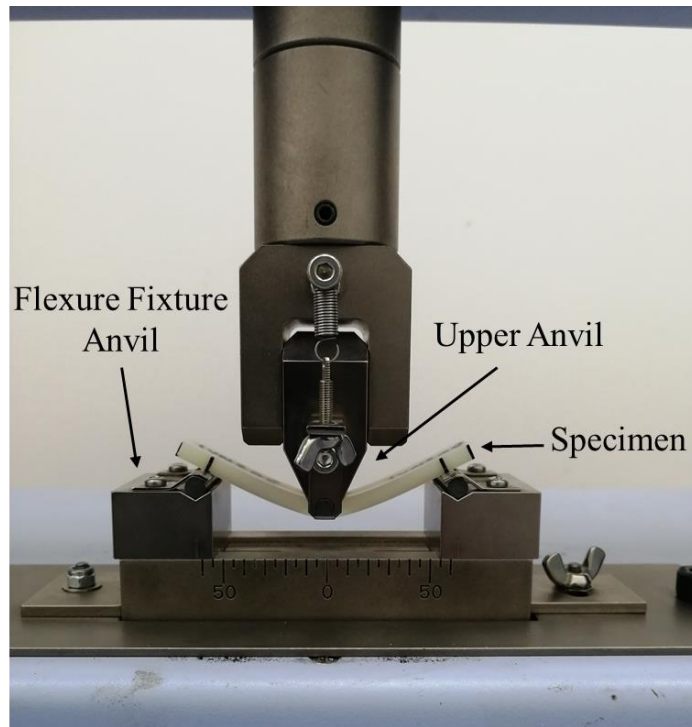


Figure 6.24: The three-point bending test machine

As a result of the bending test, force (N) – elongation (mm) data were measured. Stress (MPa) – strain (mm/mm) results were found by using Equation 6.7 and Equation 6.8

$$\sigma_e = \frac{3FL}{2bd^2} \quad (6.7)$$

$$\varepsilon = \frac{6Dd}{L^2} \quad (6.8)$$

Equation (6.9) was deployed in both calculations of the weld line factor for bending and tensile strength.

$$\text{Weld Line Factor} = \frac{\text{Weld Line Strength}}{\text{Non-Weld Line Strength}} \quad (6.9)$$

Chapter 7

Analyses and Results

7.1 Plastic Injection Filling Analysis

The plastic filling was simulated and analyzed within the Moldex3D 2020 program. As a result of the analysis, it was decided to reconfigure the runners, gates, and cooling channels in the mold. In particular, an iterative method was executed by performing multiple filling analysis with different dimensions of the runners and gates. Then, the runner and the gate sizes were preferred, which allow the cavities to be filled at the same time and meet in the middle of the weld line specimen.

In the Moldex3D program, five layers of boundary layer mesh (BLM) were selected in the solid mesh as the mesh type. As the number of layers on the surface increase, the number of meshes increases. The reason why five-layer BLM is preferred is for a more detailed plastic filling analysis. The total number of solid meshes is 1.145.785, and the number of surface meshes is 49.692.

In the plastic filling analysis, plastic part, mold base, mold insert, runner, gates, cooling channels, and cooler inlets/outlets were defined. The plastic filling analysis on the mold model in the Moldex3D program is demonstrated in Figure 7.1.

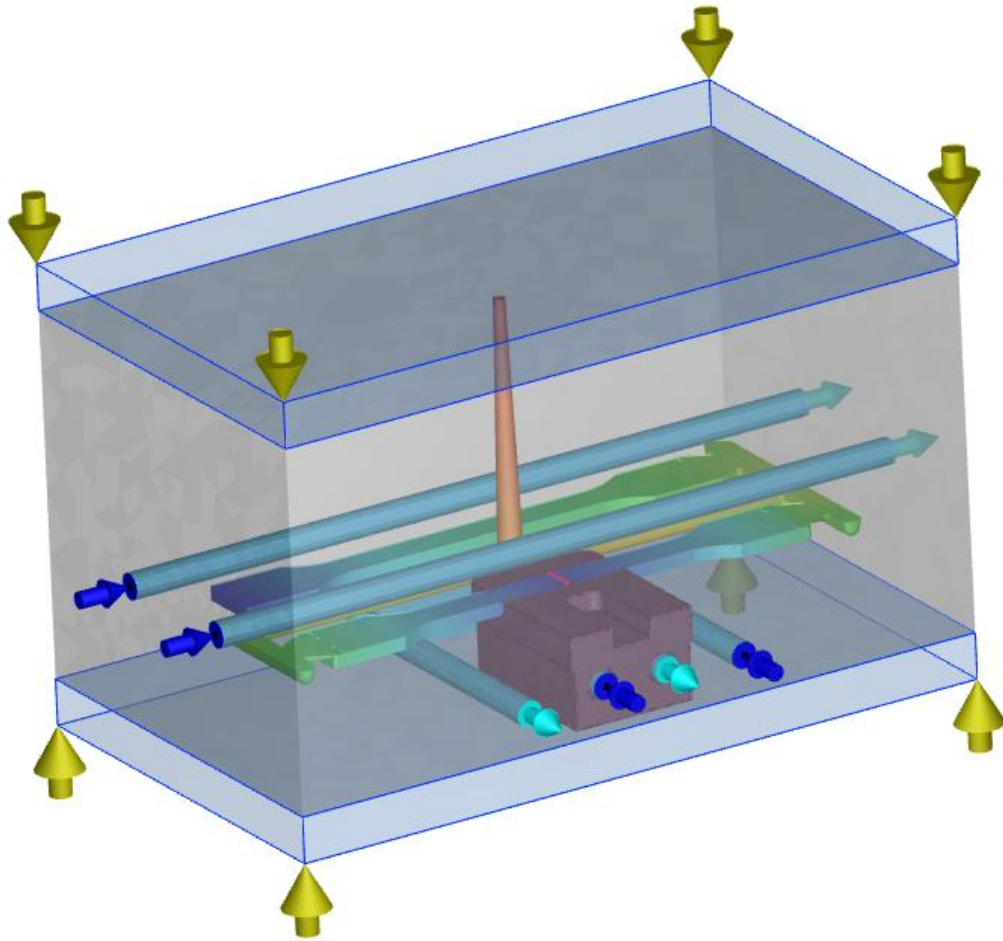


Figure 7.1: The plastic filling analysis in the Moldex3D program

7.1.1 Plastic Filling Analysis of ABS

The filling time of 50%, 95%, and 100% for ABS is illustrated in Figure 7.2, Figure 7.3, and Figure 7.4, respectively. The rectangle line that remains in the middle of the part is the weld line. As shown in Figure 7.3, the cavities of the test specimens were filled simultaneously and there was a meeting of flow frontlines in the middle of the weld line specimen. In the plastic filling analysis carried out for ABS, the insert temperature was 75 °C, the mold temperature was 65 °C and the melt temperature was 250 °C.

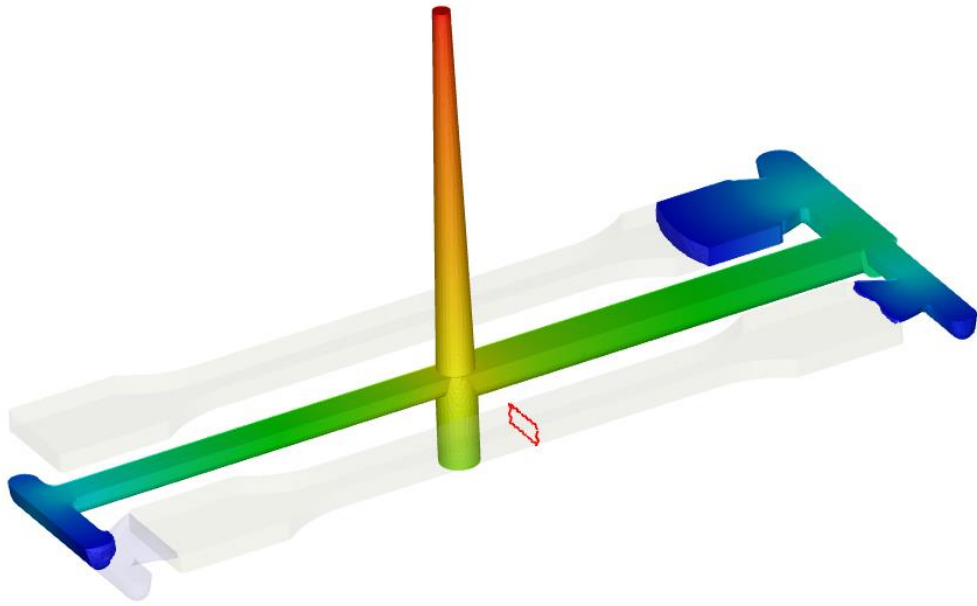


Figure 7.2: Filling ABS in 50% time

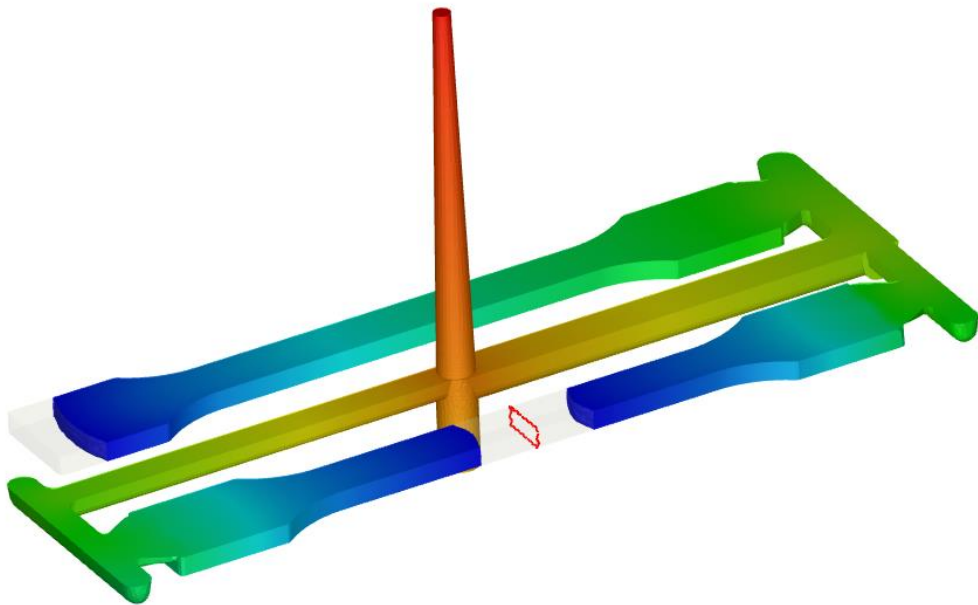


Figure 7.3: Filling ABS in 95% time

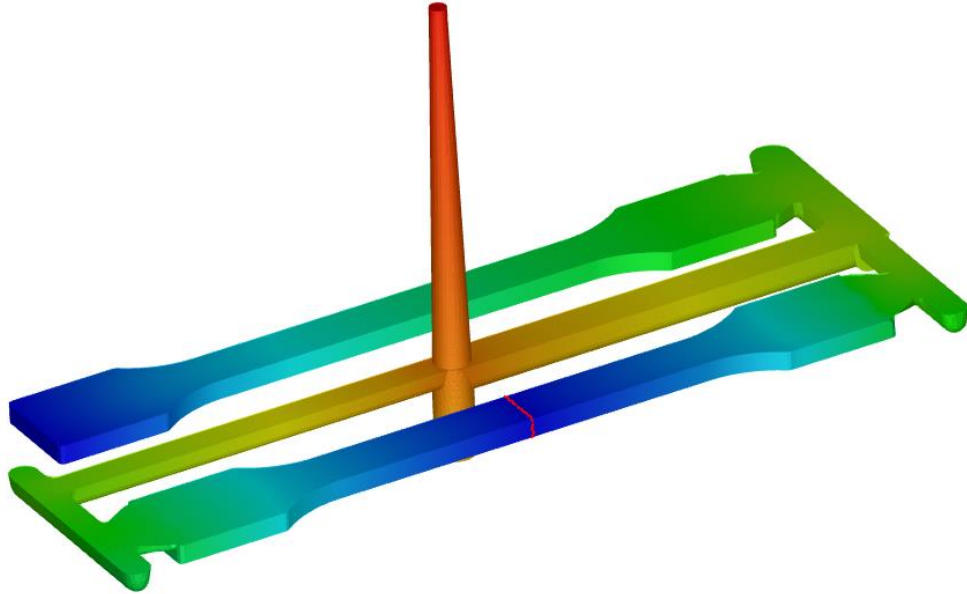


Figure 7.4: Filling ABS in 100% time

7.1.2 Plastic Filling Analysis of PP GF20

The filling time of 50%, 95%, and 100% for PP GF20 is demonstrated in Figure 7.5, Figure 7.6, and Figure 7.7, respectively. Figure 7.6 shows that the cavities of the test specimens were filled simultaneously and flow frontlines met in the middle of the weld line specimen. In the plastic filling analysis for PP GF20, the insert, mold, and melt temperatures were 50, 30, and 240 °C.

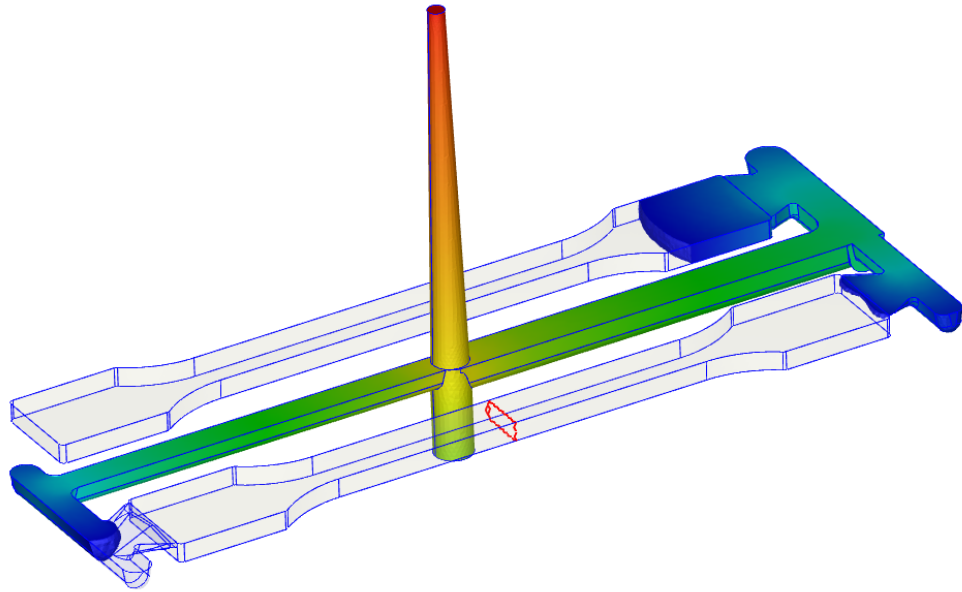


Figure 7.5: Filling PP GF20 in 50% time

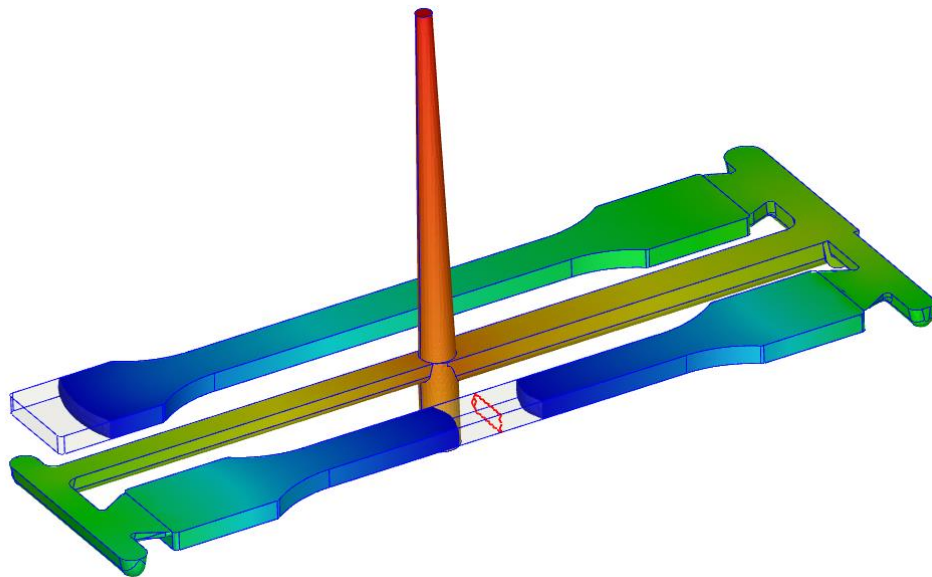


Figure 7.6: Filling PP GF20 in 95% time

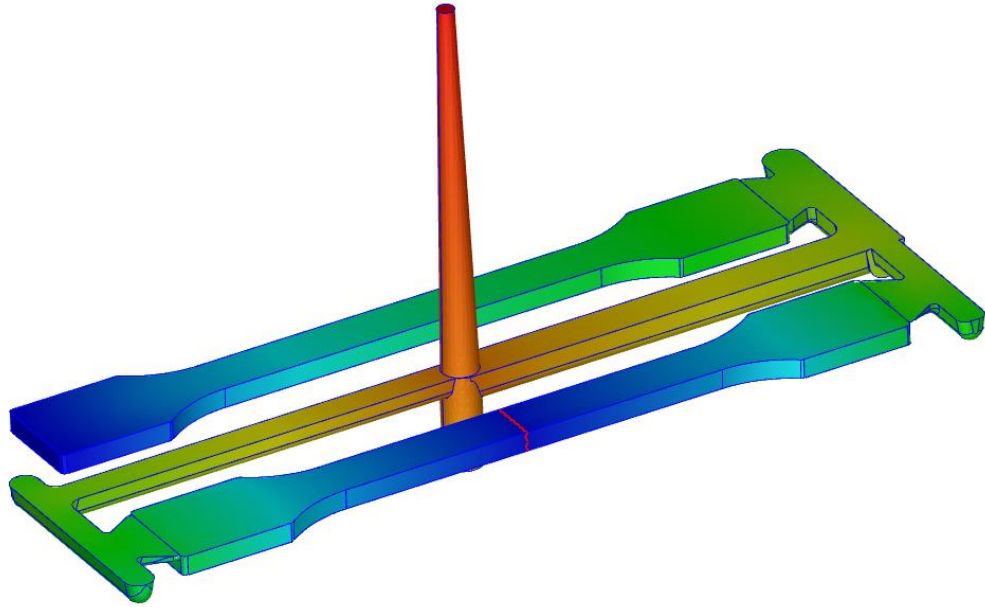


Figure 7.7: Filling PP GF20 in 100% time

7.2 Tensile and Bending Properties

7.2.1 Results of ABS

7.2.1.1 Results of the Tensile Tests for ABS

The weld line and non-weld line tensile strengths of ABS are depicted for nine experimental sets in Table 7.1. The average weld line factor of the tensile test was calculated as 0.98, which is not far from unity because the tensile strength of the weld line and the non-weld line specimens are very close to each other. The fact that the ABS is amorphous and not reinforced with additives can explain this situation.

Table 7.1: The weld line and the non-weld line tensile strength for ABS

Experiment No.	Parameters			Mean Weld Line Tensile Strength (MPa)	Mean non-Weld Line Tensile Strength (MPa)	Weld Line Factor (MPa/MPa)
	A	B	C			
	Insert Temp. (°C)	Mold Temp. (°C)	Melt Temp. (°C)			
1	45	45	200	43.5	45.0	0.97
2	45	55	225	49.1	49.6	0.99
3	45	65	250	43.8	43.7	1.00
4	60	45	225	48.7	49.5	0.98
5	60	55	250	43.9	44.2	0.99
6	60	65	200	44.2	44.9	0.98
7	75	45	250	43.5	44.3	0.98
8	75	55	200	43.2	45.1	0.96
9	75	65	225	49.0	49.7	0.98
Average				45.4	46.2	0.98

The main effects plots for S/N ratios for the insert temperature, mold temperature, and melt temperature of the weld line tensile strength are presented in Figure 7.8, Figure 7.9, and Figure 7.10, respectively. The S/N ratios of the insert, mold, and melt temperatures have been found as the highest at 60 °C, 65 °C, and 225 °C, respectively.

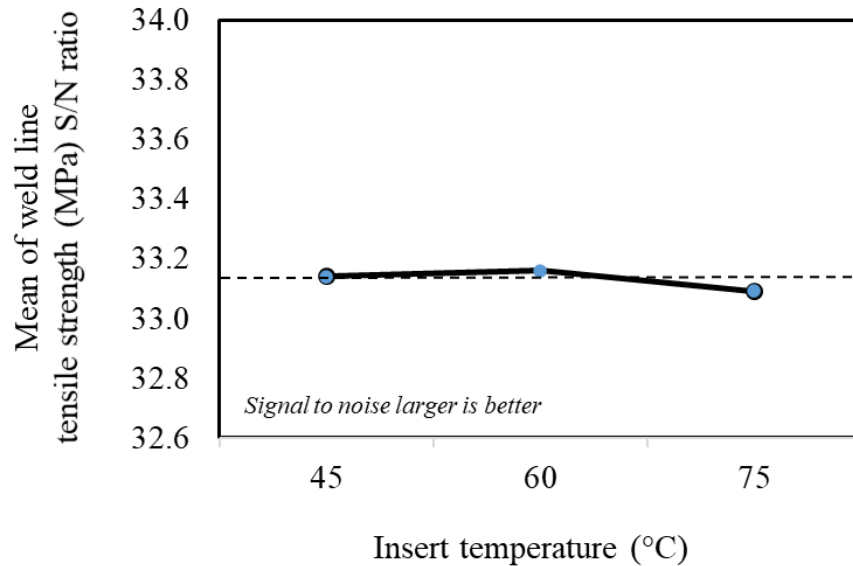


Figure 7.8: Main effects plot for S/N ratios: insert temperature vs. weld line tensile strength for the weld line for ABS

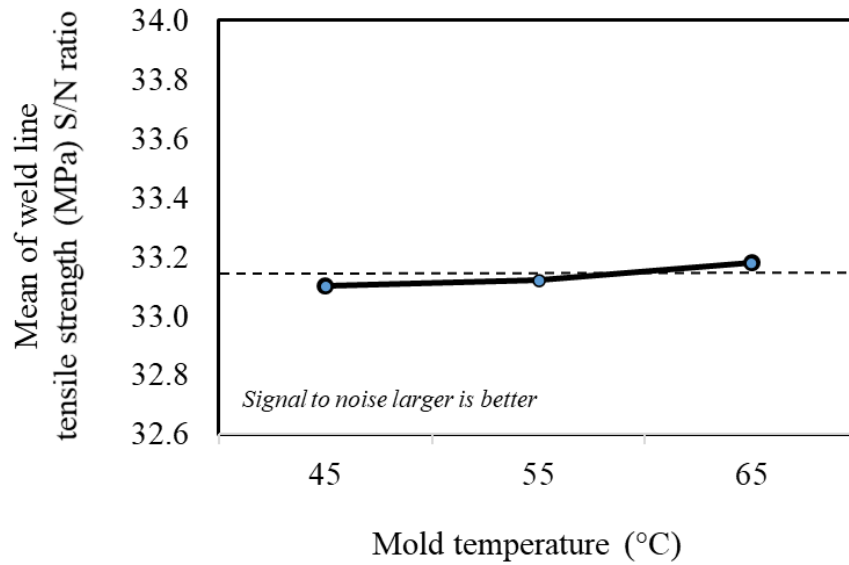


Figure 7.9: Main effects plot for S/N ratios: mold temperature vs. weld line tensile strength for the weld line for ABS

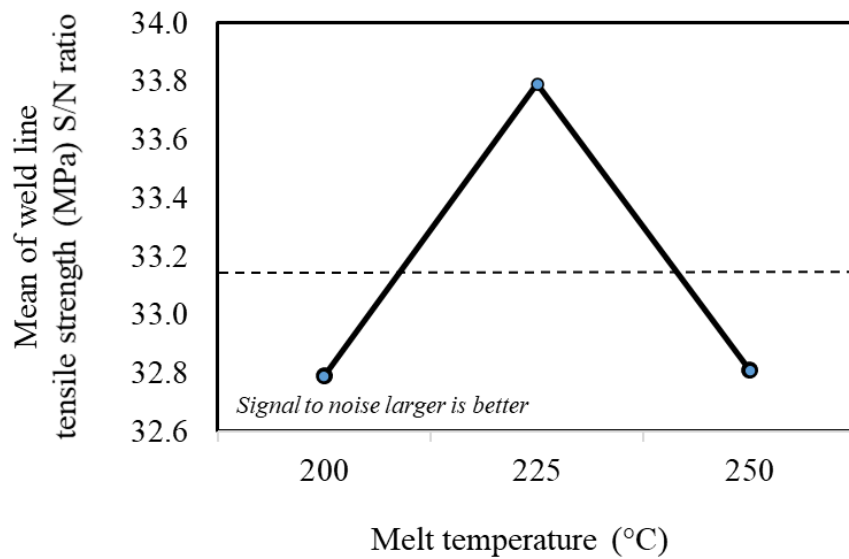


Figure 7.10: Main effects plot for S/N ratios: melt temperature vs. weld line tensile strength for the weld line for ABS

The optimum process parameters for weld line tensile strength of ABS can be designated as $A_2B_3C_2$. The predicted value of the optimum weld line tensile strength (WT_p) is formulated in Equation (7.1). T_m is the average strength. The predicted value of the optimum weld line tensile strength is illustrated in Table 7.2.

$$WT_p = A_2 + B_3 + C_2 - 2T_m \quad (7.1)$$

$$WT_p = 45.6 + 45.6 + 48.9 - 2(45.4)$$

$$WT_p = 49.3 \text{ MPa}$$

Table 7.2: The predicted value of the weld line tensile strength for ABS

Parameters	Symbol	Levels	The Predicted Value	
Insert Temp.	A	2	60 °C	49.3 MPa
Mold Temp.	B	3	65 °C	
Melt Temp.	C	2	225 °C	

In Table 7.3, the signal-to-noise (S/N) ratio of the weld line specimens for ABS is listed in the form of a response table. Since the melt temperature has the highest delta of S/N ratio, it has been observed that the melt temperature is the most effective parameter for the weld line tensile strength. The second most effective parameter is the mold temperature, and the least effective one is the insert temperature.

Table 7.3: Response table for signal-to-noise (S/N) ratios for the weld line tensile strength for ABS

Parameters	Symbol	S/N ratio						Rank
		Level 1	Level 2	Level 3	Max.	Min.	Delta	
Insert Temp.	A	33.14	33.16	33.09	33.16	33.09	0.07	3
Mold Temp.	B	33.10	33.12	33.18	33.18	33.10	0.08	2
Melt Temp.	C	32.79	33.79	32.82	33.79	32.79	1.00	1

The ANOVA results for ABS specimens with the weld line are shown in Table 7.4. The melt temperature has the highest contribution rate of 99.72%. The insert temperature and the mold temperature have a contribution rate of 0.40% and 0.49%,

respectively. The melt temperature has the greatest influence on the tensile strength of the weld line.

Table 7.4: ANOVA results for weld line tensile strength for ABS

Parameter	Symbol	Degree of Freedom	Sum of Squares	Mean Squares (Variance)	Variance Ratio	Contribution
Factor		f	S	V	F	P (%)
Insert Temp.	A	2	0.00787	0.00393	0.99	0.40
Mold Temp.	B	2	0.00964	0.00964	1.22	0.49
Melt Temp.	C	2	1.95753	0.97876	247.41	98.72
Error	e	2	0.00791	0.00396		0.40
Total		8	1.98295			100.00

The Fisher test values for $F(2,2)$ used to compare with the variance ratios in Table 7.4 are shown in Table 7.5. In the table, α is the significance level, f_1 and f_2 represent the degree of freedom for variable and error factor respectively. By comparing the variance ratios of the process parameters with the $F(2,2)$ values, it was deduced that the insert and mold temperatures had a confidence level of below 95% and the melt temperature had a confidence level of over 99.5%.

Table 7.5: Fisher test value for $F(2,2)$

$F_\alpha (f_1, f_2)$	Significance Level (%)	Confidence Level (%)	Fisher Test Value
$F_{0.005} (2,2)$	0.5	99.5	199.0
$F_{0.01} (2,2)$	1.0	99.0	99.0
$F_{0.05} (2,2)$	5.0	95.0	19.0

7.2.1.2 Results of the Bending Tests for ABS

The weld line and non-weld line bending strengths of ABS are listed in Table 7.6. Similar to the tensile test results, the results of bending tests of the weld line and the non-weld line specimens are almost the same, so the average weld line factor of the

bending test is also calculated very close to unity, approximately 0.95. The same fact that the ABS is amorphous and not reinforced with additives can explain this situation.

Table 7.6: The weld line and the non-weld line bending strength for ABS

Experiment No.	Parameters			Mean Weld Line Bending Strength (MPa)	Mean non-Weld Line Bending Strength (MPa)	Weld Line Factor (MPa/MPa)
	A Insert Temp. (°C)	B Mold Temp. (°C)	C Melt Temp. (°C)			
1	45	45	200	82.6	89.2	0.93
2	45	55	225	84.4	88.1	0.96
3	45	65	250	84.3	85.8	0.98
4	60	45	225	83.0	87.8	0.94
5	60	55	250	83.3	85.2	0.98
6	60	65	200	82.2	87.8	0.94
7	75	45	250	81.4	84.9	0.96
8	75	55	200	80.3	87.5	0.92
9	75	65	225	82.4	84.9	0.97
Average				82.7	86.8	0.95

The main effects plots for S/N ratios for the insert, mold, and melt temperatures of the weld line bending strength are shown in Figure 7.11, Figure 7.12, and Figure 7.13, respectively. The S/N ratios of the insert, mold, and melt temperatures have been identified as the highest at 45 °C, 65 °C, and 225 °C, respectively.

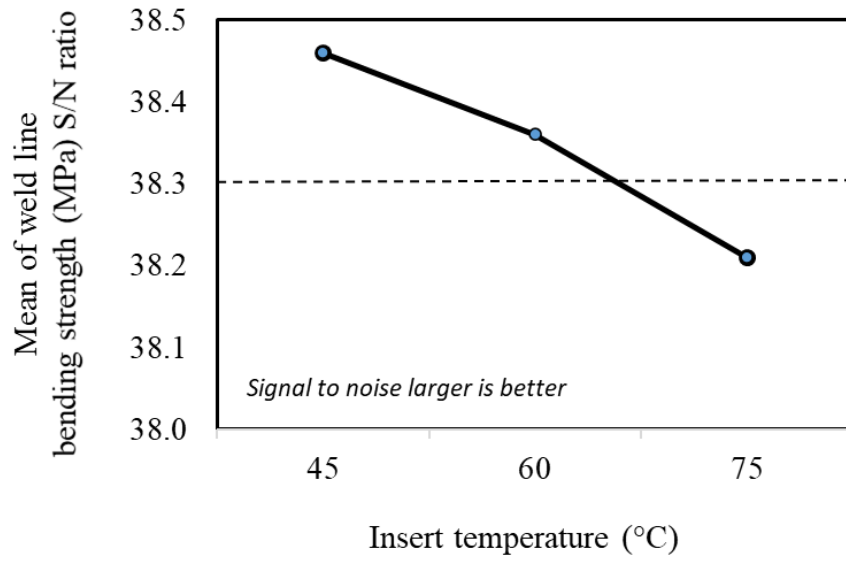


Figure 7.11: Main effects plot for S/N ratios: insert temperature vs. weld line bending strength for the weld line for ABS

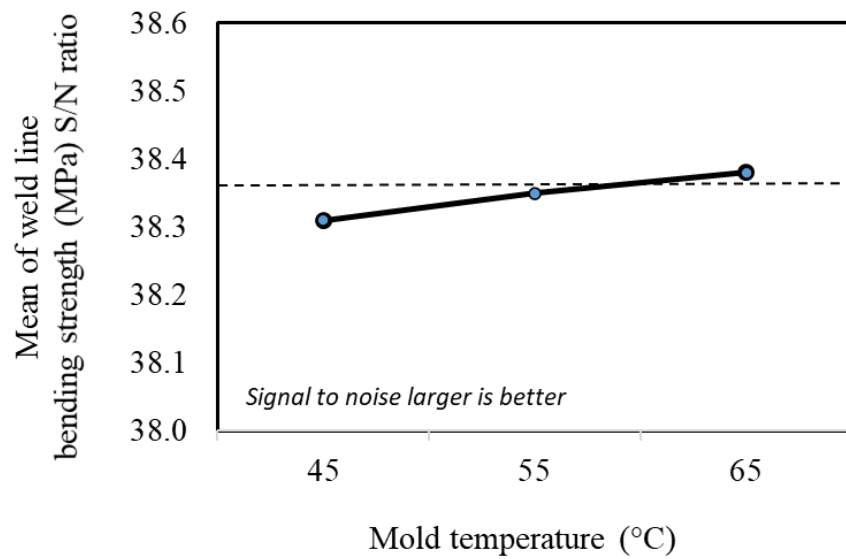


Figure 7.12: Main effects plot for S/N ratios: mold temperature vs. weld line bending strength for the weld line for ABS

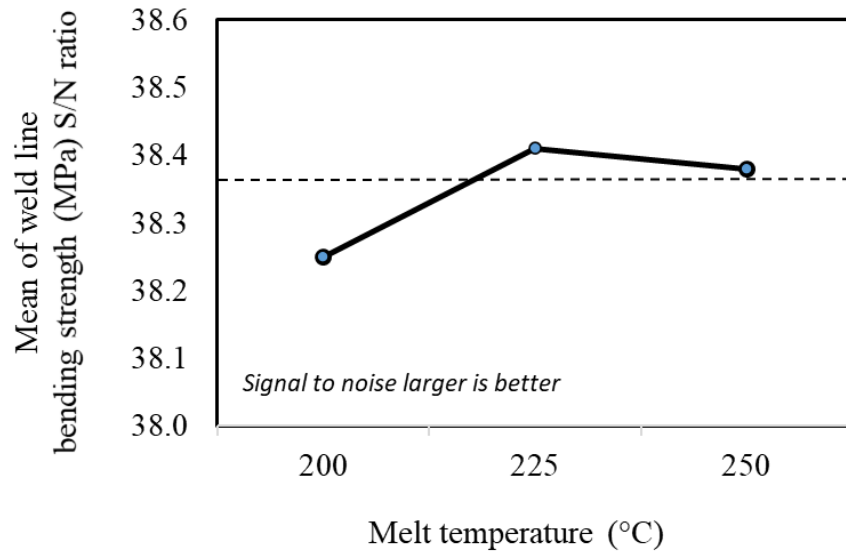


Figure 7.13: Main effects plot for S/N ratios: melt temperature vs. weld line bending strength for the weld line for ABS

The optimum process parameters for weld line tensile strength of ABS can be labeled as $A_1B_3C_2$. The predicted value of the optimum weld line bending strength (WB_p) is expressed in Equation (7.2). The predicted value of the optimum weld line bending strength is illustrated in Table 7.7.

$$WB_p = A_1 + B_3 + C_2 - 2T_m \quad (7.2)$$

$$WB_p = 83.8 + 83.0 + 83.3 - 2(82.7)$$

$$WB_p = 84.7 \text{ MPa}$$

Table 7.7: The predicted value of the weld line bending strength for ABS

Parameters	Symbol	Levels	The Predicted Value	
Insert Temp.	A	1	45 °C	84.7 MPa
Mold Temp.	B	3	65 °C	
Melt Temp.	C	2	225 °C	

In Table 7.8, the signal-to-noise (S/N) ratio of the weld line specimens for ABS is tabulated in the form of a response table. Since the insert temperature has the maximum delta of S/N ratio, it has been noticed that the insert temperature is the most effective parameter for the bending strength of the weld line specimens. The second most effective parameter is the mold temperature, and the most ineffective one is the mold temperature.

Table 7.8: Response table for signal-to-noise (S/N) ratios for the weld line bending strength for ABS

Parameters	Symbol	S/N ratio						
		Level 1	Level 2	Level 3	Max.	Min.	Delta	Rank
Insert Temp.	A	38.46	38.36	38.21	38.46	38.21	0.25	1
Mold Temp.	B	38.31	38.35	38.41	38.41	38.31	0.10	3
Melt Temp.	C	38.25	38.41	38.38	38.41	38.25	0.16	2

The ANOVA results for ABS specimens with the weld line are summarized in Table 7.9. The insert temperature has the highest contribution rate of 64.97%. The mold and melt temperatures have contribution rates of 4.55% and 29.59%, respectively. The insert temperature is most influential on the weld line bending strength.

By comparing the variance ratios of the process parameters with the $F(2,2)$ values from Table 7.5, it was deduced that the insert and melt temperatures had a confidence level over 95% and the mold temperature had a confidence level below 95%.

Table 7.9: ANOVA results for weld line bending strength for ABS

Parameter	Symbol	Degree of Freedom	Sum of Squares	Mean Squares (Variance)	Variance Ratio	Contribution
Factor		f	S	V	F	P (%)
Insert Temp.	A	2	0.09917	0.04959	72.70	64.97
Mold Temp.	B	2	0.00695	0.00347	5.09	4.55
Melt Temp.	C	2	0.04517	0.02258	33.11	29.59
Error	e	2	0.00136	0.00068		0.89
Total		8	0.15265			100.00

7.2.2 Results of PP GF20

7.2.2.1 Results of the Tensile Tests for PP GF20

The weld line and non-weld line tensile strengths of PP GF20 are shown in Table 7.10. The average weld line factor of the tensile test was calculated as 0.57. The most important reason why its value is so low is that PP GF20 contains glass fiber additives. The fibers are spread vertically in the weld line region of the glass fiber test specimen produced by plastic injection. As a result, the strength decreases in a considerable amount in the weld line region, as the fibers provide strength in the direction in which they are aligned.

Table 7.10: The weld line and the non-weld line tensile strengths for PP GF20

Experiment No.	Parameters			Mean Weld Line Tensile Strength (MPa)	Mean non-Weld Line Tensile Strength (MPa)	Weld Line Factor (MPa/MPa)
	A Insert Temp. (°C)	B Mold Temp. (°C)	C Melt Temp. (°C)			
1	30	30	190	38.8	57.9	0.67
2	30	50	215	35.0	62.3	0.56
3	30	70	240	39.9	63.2	0.63
4	50	30	215	32.8	61.1	0.54
5	50	50	240	36.4	63.3	0.58
6	50	70	190	31.0	59.9	0.52
7	70	30	240	38.2	62.3	0.61
8	70	50	190	31.7	59.5	0.53
9	70	70	215	30.1	62.5	0.48
Average				34.9	61.3	0.57

The main effects plots for S/N ratios for the insert temperature, mold temperature, and melt temperature of the weld line tensile strength are illustrated in Figure 7.14, Figure 7.15, and Figure 7.16, respectively. The S/N ratio of the insert temperature has been identified as the highest at 30 °C. Thus, the weld line tensile strength has reached the highest value at the temperature of the insert at 30 °C. As for the mold temperature, the result was similar to the insert temperature. The weld line strength has the highest value at the mold temperature of 30 °C. But the results are not the same for the melt

temperature. The weld line strength at the melt temperature of 240 °C is the highest tensile strength value of the weld line.

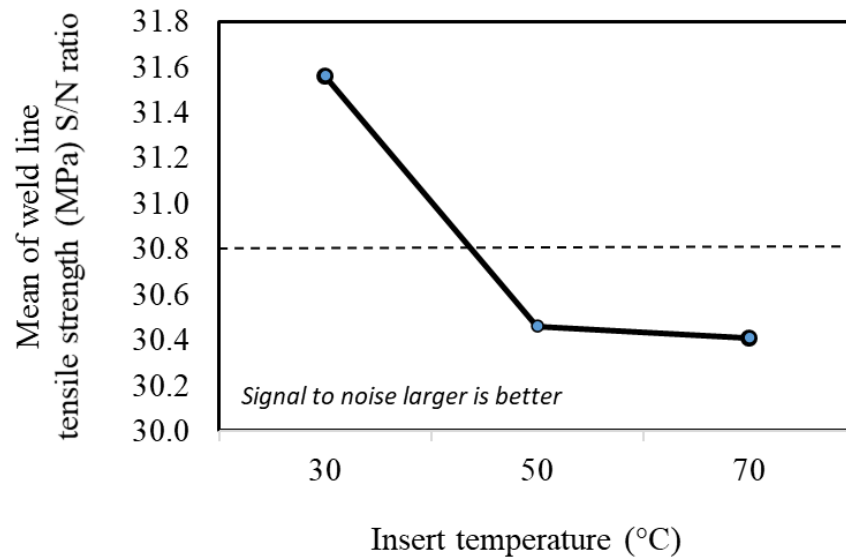


Figure 7.14: Main effects plot for S/N ratios: insert temperature vs. weld line tensile strength for the weld line for PP GF20

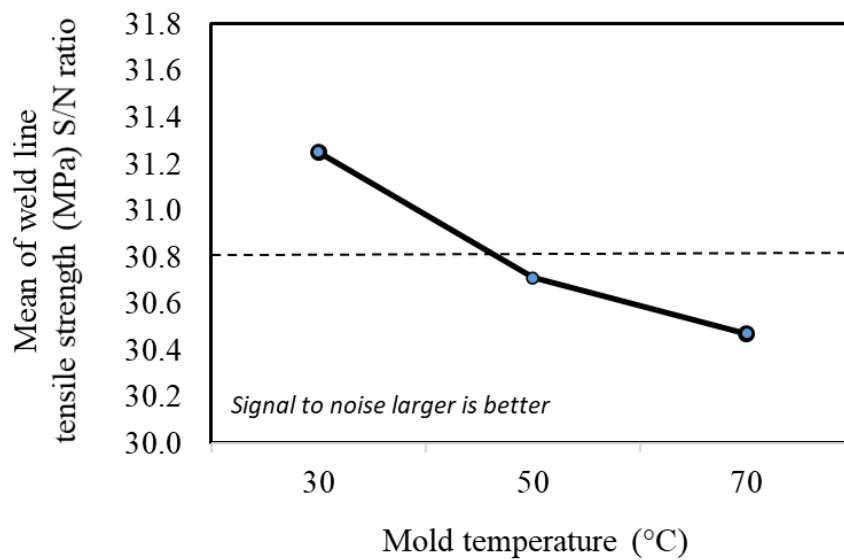


Figure 7.15: Main effects plot for S/N ratios: mold temperature vs. weld line tensile strength for the weld line for PP GF20

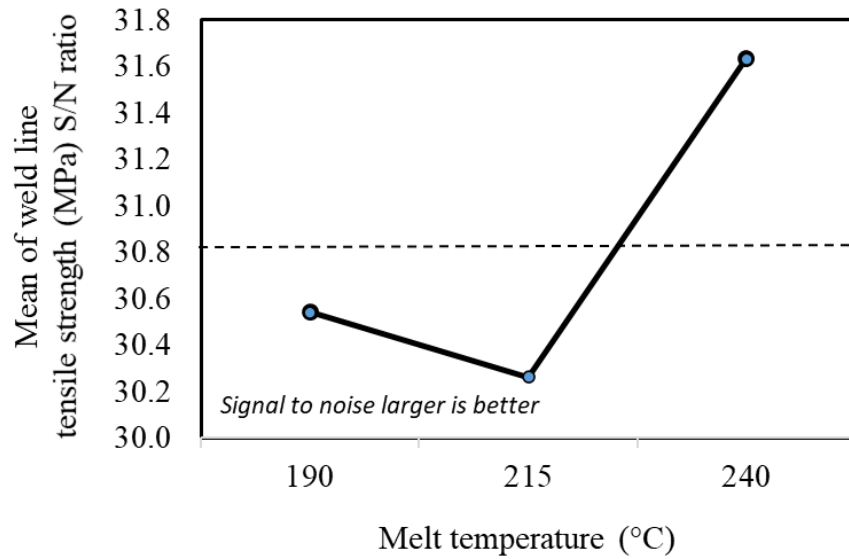


Figure 7.16: Main effects plot for S/N ratios: melt temperature vs. weld line tensile strength for the weld line for PP GF20

The optimum process parameters for weld line tensile strength of PP GF20 is $A_1B_1C_3$. The predicted value of the optimum weld line tensile strength (WT_p) for PP GF20 is shown in Equation (7.3). T_m is the average strength. The predicted value of the optimum weld line tensile strength is illustrated in Table 7.11.

$$WT_p = A_1 + B_1 + C_3 - 2T_m \quad (7.3)$$

$$WT_p = 37.9 + 36.6 + 38.2 - 2(34.9)$$

$$WT_p = 42.9 \text{ MPa}$$

Table 7.11: The predicted value of the weld line tensile strength for PP GF20

Parameters	Symbol	Levels	The Predicted Value
Insert Temp.	A	1	30 °C
Mold Temp.	B	1	30 °C
Melt Temp.	C	3	240 °C
$A_1B_1C_3$ 42.9 MPa			

In Table 7.12, the response table for the signal-to-noise (S/N) ratio of the weld line specimens in PP GF20 is listed. Since melt temperature has the highest delta of S/N ratio, it has been noted that the melt temperature is the most forceful parameter for the weld line tensile strength. The second most effective parameter is the insert temperature, and the least effective parameter is the mold temperature.

Table 7.12: Response table for signal-to-noise (S/N) ratios for the weld line tensile strength for PP GF20

Parameters	Symbol	S/N ratio						
		Level 1	Level 2	Level 3	Max.	Min.	Delta	Rank
Insert Temp.	A	31.56	30.46	30.41	31.56	30.41	1.15	2
Mold Temp.	B	31.25	30.71	30.47	31.25	30.47	0.78	3
Melt Temp.	C	30.54	30.26	31.63	31.63	30.26	1.37	1

The ANOVA results for PP GF20 specimens with the weld line are shown in Table 7.13. The melt temperature has the highest contribution rate of 47.36%. The insert temperature and the mold temperature have contribution rates of 38.31% and 14.18%, respectively.

By comparing the variance ratios of the process parameters with the Fisher test values for F(2,2) from Table 7.5, it was deduced that the insert and melt temperatures had a confidence level over 99.5% and the mold temperature had a confidence level above 95%.

Table 7.13: ANOVA results for weld line tensile strength for PP GF20

Parameter	Symbol	Degree of Freedom	Sum of Squares	Mean Squares (Variance)	Variance Ratio	Contribution
Factor		f	S	V	F	P (%)
Insert Temp.	A	2	2.54	1.270	224.47	38.31
Mold Temp.	B	2	0.94	0.470	90.61	14.18
Melt Temp.	C	2	3.14	1.570	302.49	47.36
Error	e	2	0.01	0.005		0.15
Total		8	6.63			100.00

The main effects plots for S/N ratios for the mold and melt temperatures of the non-weld line specimen are demonstrated in Figure 7.17, and Figure 7.18, respectively. There is no insert part in the middle of the non-weld line cavity. Because there will be no weld line, there is no need for extra heating or cooling in the mold. The S/N ratio of the mold and melt temperatures have been found as the maximum at 70 °C and 240 °C, respectively. Thus, the non-weld line strength has reached its highest value at the mold temperature at 70 °C and the melt temperature at 240 °C. As both mold and melt temperatures increase, the tensile strength of the non-weld line increases.

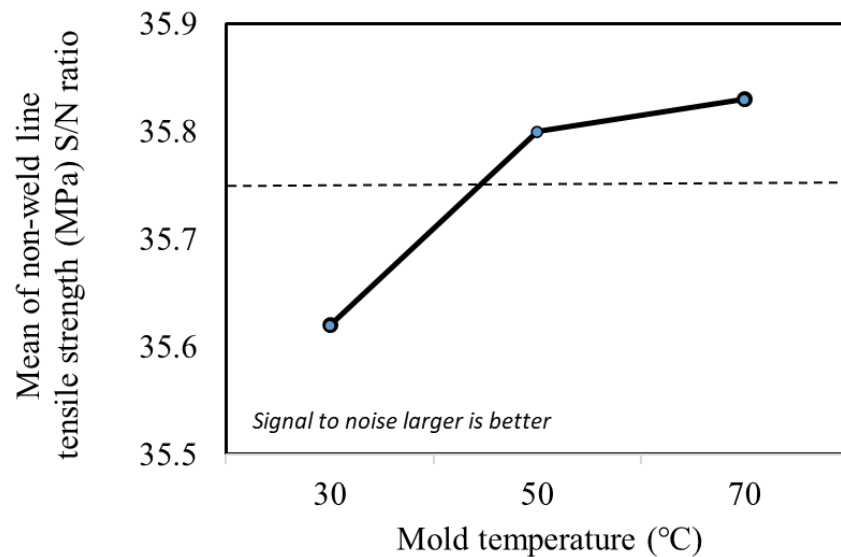


Figure 7.17: Main effects plot for S/N ratios: mold temperature vs. non-weld line tensile strength for the non-weld line for PP GF20

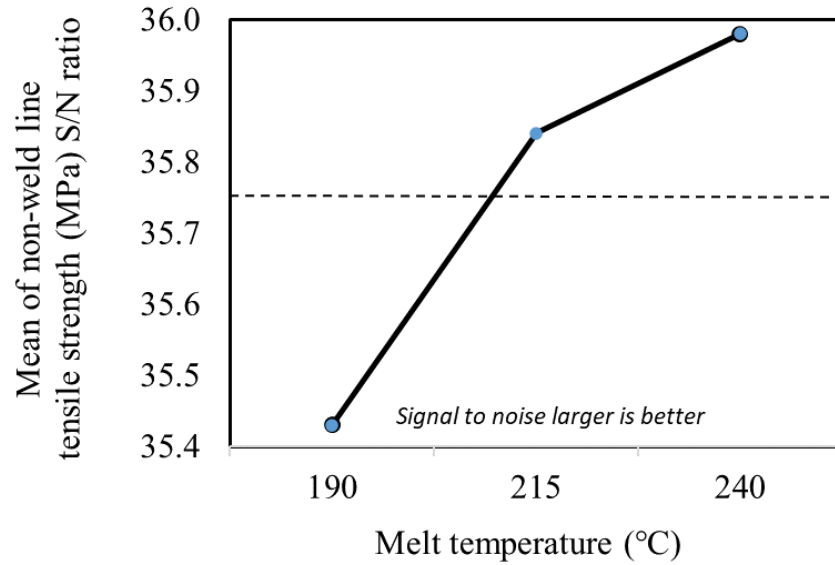


Figure 7.18: Main effects plot for S/N ratios: melt temperature vs. non-weld line tensile strength for the non-weld line for PP GF20

The optimum process parameter for non-weld line tensile strength of PP GF20 can be labeled as B_3C_3 . Since the optimum process set is already in the experimental set, B_3C_3 test results can be easily read as 63.2 MPa from Table 7.10. It is very close to the predicted value of the tensile strength (63.5 MPa). The predicted value of the optimum non-weld line tensile strength (nWT_p) for PP GF20 is depicted in Equation (7.4). T_m is the average strength. The predicted value of the optimum non-weld line tensile strength is illustrated in Table 7.14.

$$nWT_p = B_3 + C_3 - T_m \quad (7.4)$$

$$nWT_p = 61.9 + 62.9 - 61.3$$

$$nWT_p = 63.5 \text{ MPa}$$

Table 7.14: The predicted value of the non-weld line tensile strength for PP GF20

Parameters	Symbol	Levels		The Predicted Value
Mold Temp.	B	3	70 °C	B_3C_3 63.5 MPa
Melt Temp.	C	3	240 °C	

In Table 7.15, the responses for the signal-to-noise (S/N) ratio of the non-weld line specimens in PP GF20 are listed. Since melt temperature has the highest delta of S/N ratio, it has been observed that the melt temperature is the most effective parameter for the non-weld line tensile strength. The effect of the mold temperature was found to be less.

Table 7.15: Response table for signal-to-noise (S/N) ratios for the non-weld line tensile strength for PP GF20

Parameters	Symbol	S/N ratio						
		Level 1	Level 2	Level 3	Max.	Min.	Delta	Rank
Mold Temp.	B	35.62	35.80	35.83	35.83	35.62	0.21	2
Melt Temp.	C	35.43	35.84	35.98	35.98	35.43	0.55	1

The ANOVA results for PP GF20 specimens with the non-weld line are shown in Table 7.16. The melt temperature has a maximum contribution rate of 85.41%. ANOVA gives the contribution rate of the mold temperature as 13.36%.

By checking the variance ratios of the process parameters with the F(2,4) values from Table 7.17, it was concluded that the melt temperatures had a confidence level of over 99.5% and the mold temperature had a confidence level of over 99%.

Table 7.16: ANOVA results for non-weld line tensile strength for PP GF20

Parameter	Symbol	Degree of Freedom	Sum of Squares	Mean Squares (Variance)	Variance Ratio	Contribution
Factor		f	S	V	F	P (%)
Mold Temp.	B	2	0.076	0.038	20.35	13.36
Melt Temp.	C	2	0.486	0.243	130.83	85.41
Error	e	4	0.007	0.002		1.23
Total		8	0.569			100.00

Table 7.17: Fisher test values for F(2,4)

$F_{\alpha} (f_1, f_2)$	Significance Level (%)	Confidence Level (%)	Fisher Test Value
$F_{0.005} (2,4)$	0.5	99.5	26.28
$F_{0.01} (2,4)$	1.0	99.0	18.00
$F_{0.05} (2,4)$	5.0	95.0	6.94

7.2.2.2 Results of Bending Tests for PP GF20

The weld line and non-weld line bending strengths of PP GF20 are tabularized in Table 7.18. The average weld line factor of the bending test was calculated as 0.91. The weld line factor of the bending test strength was recorded as higher than the weld line factor of the tensile test strength. The main reason for this is that the force applied in the bending test in both the weld line zone and the non-weld line zone is perpendicular to the fiber array direction. For this reason, the bending strengths of the weld line and the non-weld line are close to each other.

Table 7.18: The weld line and the non-weld line bending strength for PP GF20

Experiment No.	Parameters			Mean Weld Line Bending Strength (MPa)	Mean non-Weld Line Bending Strength (MPa)	Weld Line Factor (MPa/MPa)
	A Insert Temp. (°C)	B Mold Temp. (°C)	C Melt Temp. (°C)			
1	30	30	190	81.8	88.4	0.93
2	30	50	215	81.5	92.0	0.89
3	30	70	240	82.2	94.6	0.87
4	50	30	215	83.8	91.5	0.92
5	50	50	240	82.0	93.3	0.88
6	50	70	190	83.6	90.4	0.92
7	70	30	240	84.9	92.7	0.92
8	70	50	190	82.8	88.8	0.93
9	70	70	215	84.7	93.5	0.91
Average				83.0	91.7	0.91

The main effects plots for S/N ratios for the insert temperature, mold temperature, and melt temperature of the weld line bending strength are shown in Figure 7.19, Figure 7.20, and Figure 7.21, respectively. The S/N ratio of the insert temperature has been

identified as the highest at 70 °C. Thus, the weld line bending strength has reached the highest value at the temperature of the insert at 70 °C. The weld line bending strength is the highest at mold temperatures of 30 °C. But the results are not the same for the melt temperature. The weld line strength has the highest value at the melt temperature of 215 °C. The lowest weld line bending strength was observed at the melt temperature of 190 °C.

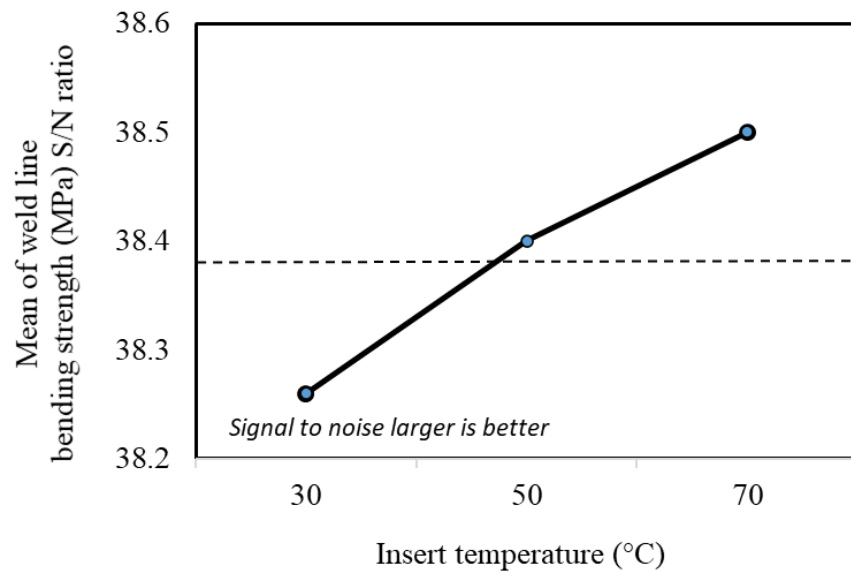


Figure 7.19: Main effects plot for S/N ratios: insert temperature vs. weld line bending strength for the weld line for PP GF20

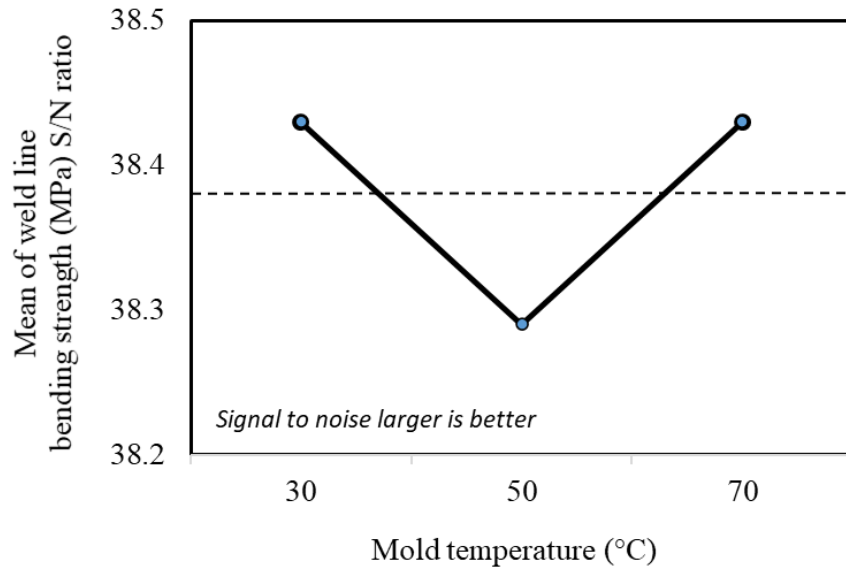


Figure 7.20: Main effects plot for S/N ratios: mold temperature vs. weld line bending strength for the weld line for PP GF20

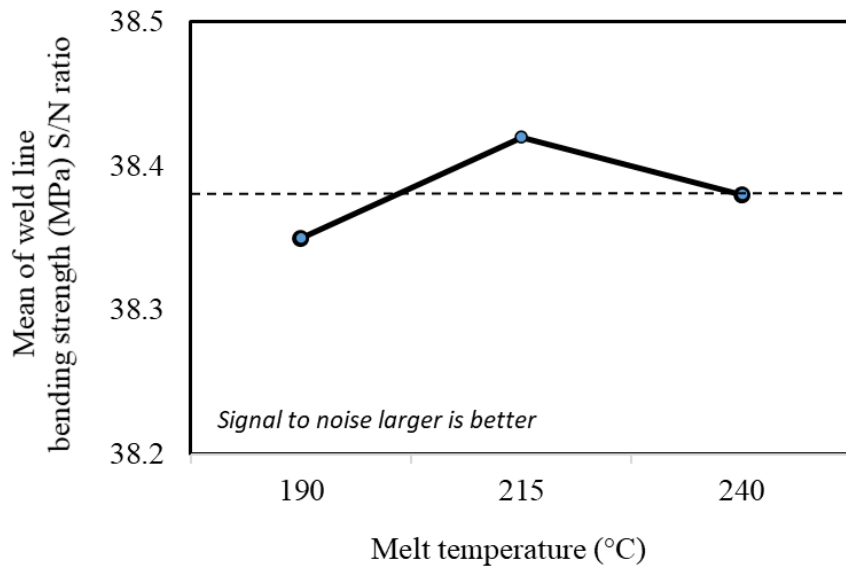


Figure 7.21: Main effects plot for S/N ratios: melt temperature vs. weld line bending strength for the weld line for PP GF20

The optimum process parameters for weld line bending strength of PP GF20 is $A_3B_1C_2$. The predicted value of the optimum weld line bending strength (WB_p) for PP GF20 is depicted in Equation (7.5). T_m is the average strength. The predicted value of the optimum weld line bending strength is illustrated in Table 7.19.

$$WB_p = A_3 + B_1 + C_2 - 2T_m \quad (7.5)$$

$$WB_p = 84.1 + 83.5 + 83.3 - 2(83.0)$$

$$WB_p = 84.9 \text{ MPa}$$

Table 7.19: The predicted value of the weld line bending strength for PP GF20

Parameters	Symbol	Levels	The Predicted Value	
Insert Temp.	A	3	70 °C	$A_3B_1C_2$ 84.9 MPa
Mold Temp.	B	3	30 °C	
Melt Temp.	C	2	215 °C	

In Table 7.20, the response table for the signal-to-noise (S/N) ratio of the non-weld line bending strength in PP GF20 is listed. Since it has the highest delta of S/N ratio, it has been noticed that the insert temperature is the most effective parameter for the weld line bending strength. The second most effective parameter is the mold temperature, and the least effective parameter is the melt temperature.

Table 7.20: Response table for signal-to-noise (S/N) ratios for the weld line bending strength for PP GF20

Parameters	Symbol	S/N ratio						Rank
		Level 1	Level 2	Level 3	Max.	Min.	Delta	
Insert Temp.	A	38.26	38.40	38.50	38.50	38.26	0.24	1
Mold Temp.	B	38.43	38.29	38.43	38.43	38.29	0.14	2
Melt Temp.	C	38.35	38.42	38.38	38.42	38.35	0.07	3

ANOVA results for the bending strength of PP GF20 specimens with the weld line are shown in Table 7.21. The insert temperature has the highest contribution rate of 62.05%. The mold and melt temperatures have contribution rates of 30.67% and 4.07%, respectively.

By comparing the variance ratios of the process parameters with the Fisher test values for $F(2,2)$ from Table 7.5, it was concluded that the insert temperature had a confidence level of over 95%, and the mold and melt temperatures had a confidence level of below 95%.

Table 7.21: ANOVA results for weld line bending strength for PP GF20

Parameter	Symbol	Degree of Freedom	Sum of Squares	Mean Squares (Variance)	Variance Ratio	Contribution
Factor		f	S	V	F	P (%)
Insert Temp.	A	2	0.0870	0.0440	19.30	62.05
Mold Temp.	B	2	0.0430	0.0210	9.47	30.67
Melt Temp.	C	2	0.0057	0.0029	1.28	4.07
Error	e	2	0.0045	0.0023		3.21
Total		8	0.1402			100.00

The main effects plots for S/N ratios for the mold temperature, and the melt temperature of the non-weld line specimen are depicted in Figure 7.22 and Figure 7.23, respectively. The S/N ratio of the mold temperature and melt temperature has been found the highest at 70 °C and 240 °C, respectively. Thus, the non-weld line bending strength has reached the highest value at the mold temperature at 70 °C and the melt temperature at 240 °C. As the mold temperature and melt temperature increase, the bending strength of the non-weld line increases.

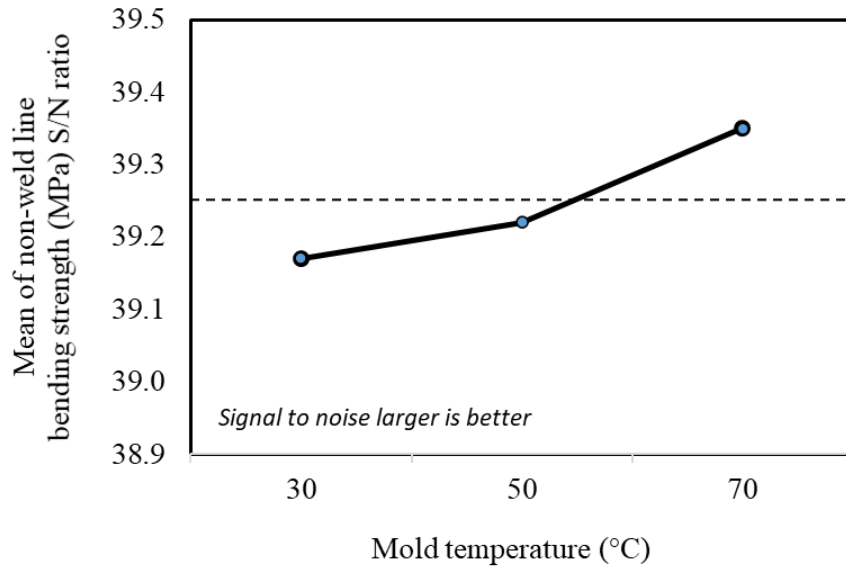


Figure 7.22: Main effects plot for S/N ratios: mold temperature vs. non-weld line bending strength for the non-weld line for PP GF20

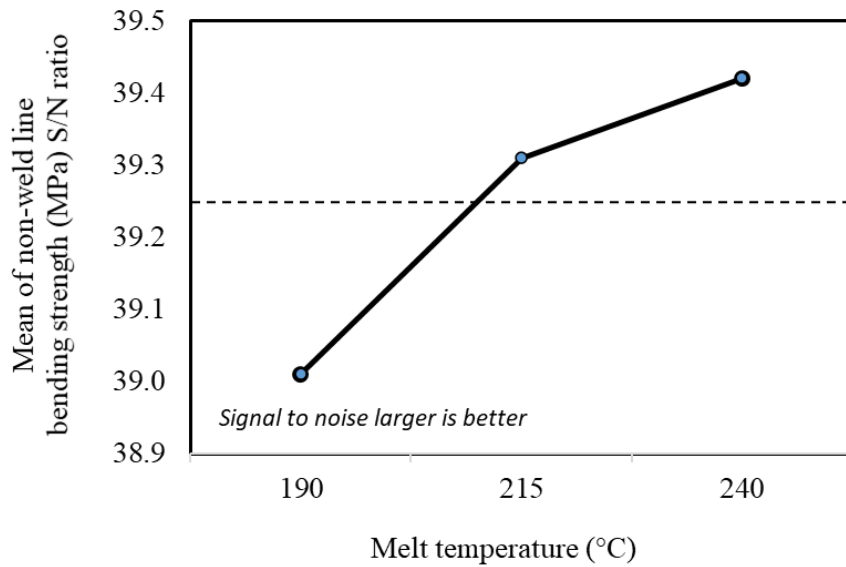


Figure 7.23: Main effects plot for S/N ratios: melt temperature vs. non-weld line bending strength for the non-weld line for PP GF20

The optimum process parameter for the non-weld line bending strength of PP GF20 is B_3C_3 . Since the optimum process set is already in the experimental set, B_3C_3 test results can be easily read as 94.6 MPa from Table 7.10. The predicted value of the optimum non-weld line bending strength (nWB_p) for PP GF20 is depicted in Equation (7.6). T_m

is the average strength. The predicted value of the optimum non-weld line bending strength is illustrated in Table 7.22.

$$nWB_p = B_3 + C_3 - T_m \quad (7.6)$$

$$nWB_p = 92.8 + 93.5 - 91.7$$

$$nWB_p = 94.6 \text{ MPa}$$

Table 7.22: The predicted value of the non-weld line bending strength for PP GF20

Parameters	Symbol	Levels	The Predicted Value
Mold Temp.	B	3	70 °C
Melt Temp.	C	3	240 °C
			B_3C_3 94.6 MPa

In Table 7.23, the responses for the signal-to-noise (S/N) ratio of the non-weld line bending strength in PP GF20 are listed. It has been observed that the melt temperature is the most effective parameter for the non-weld line tensile strength. The effect of the mold temperature was found to be less.

Table 7.23: Response table for signal-to-noise (S/N) ratios for the non-weld line bending strength for PP GF20

Parameters	Symbol	S/N ratio						
		Level 1	Level 2	Level 3	Max.	Min.	Delta	Rank
Mold Temp.	B	39.17	39.22	39.35	39.35	39.17	0.18	2
Melt Temp.	C	39.01	39.31	39.42	39.42	39.01	0.41	1

ANOVA results for the bending strength of PP GF20 specimens with non-the weld line are shown in Table 7.24. The melt temperature has the highest contribution rate of 82.85%. The mold temperature has a contribution rate of 17.10%. By comparing the variance ratios of the process parameters with the F(2,4) values from Table 7.17,

it was concluded that the mold and melt temperatures had a confidence level of over 99.5%.

Table 7.24: ANOVA results for non-weld line bending strength for PP GF20

Parameter	Symbol	Degree of Freedom	Sum of Squares	Mean Squares (Variance)	Variance Ratio	Contribution
Factor		f	S	V	F	P (%)
Mold Temp.	B	2	6.150	3.077	651.1	17.10
Melt Temp.	C	2	29.800	14.900	3153.1	82.85
Error	e	4	0.019	0.005		0.05
Total		8	35.969			100.00

7.3 Effects of Process Parameters on Weld Line Strength – ABS and PP GF20

7.3.1 Effect of Insert Temperature

The insert temperature affects the solidification time of the molten plastic material in the weld line specimen. By heating the insert, the solidification time of the molten plastic increases, and by cooling the insert, the solidification time decreases.

Optimum weld line tensile strength for ABS was achieved at the insert temperature of 60 °C. In addition, the contribution rate of insert temperature for tensile strength was 0.40%. In the bending test of the weld line ABS, the optimum bending strength result was obtained at the insert temperature of 56 °C with the contribution rate of 64.94%,

While the effect of the insert temperature on the weld line tensile strength is very low, the effect on the weld line bending strength is the most influential parameter.

Optimum values for weld line tensile and bending strengths were gained at the insert temperatures of 30 °C and 70 °C respectively for PP GF20 specimens. The contribution rates were 38.31% for tensile strength and 62.05% for bending strength.

The insert temperature had a different effect in the tensile test and bending test. This may be because the strength of the polymer chain structure and the direction of the glass fiber are affected by the insert temperature in the weld line region. According to the results obtained, the structure of the polymer chain is strengthened by increasing the insert temperature. However, in the weld line region, it approaches the 90° angle between the direction of the glass fiber sequence and the direction of molten plastic flow. For this reason, a high insert temperature results in better results in the bending test, while a lower insert temperature gives better results in the tensile test.

7.3.2 Effect of Mold Temperature

The mold temperature affects the cooling time of the plastic part and the filling of the molten plastic. As the mold temperature increases, the cooling time of the plastic part increases, and the filling of the molten plastic part becomes easier.

Optimum values for both weld line tensile and bending strengths were at the mold temperature of 65 °C for ABS specimens. The contribution rates were 0.49% for tensile strength and 4.55% for bending strength.

It is observed that the mold temperature does not have much effect on both the welding line tensile and bending strength of the ABS. However, the best results are obtained when the mold temperatures are raised because molten plastic can maintain its temperature and pressure until it reaches the meeting region.

In the tensile test of PP GF20, the optimum mold temperatures levels are 30 °C for the weld line and 70 °C for the non-weld line specimens. The contribution rates for weld line and the non-weld line specimens were found as 14.18% for weld line and 13.67% for the non-weld line specimens

Similar to the tensile test, the optimum mold temperatures level are 30 °C for the weld line and 70 °C for the non-weld line specimens in the bending test of PP GF20,

The contribution rates for weld line and the non-weld line specimens were found as 30.67% for weld line and 17.10% for the non-weld line specimens

The effect of mold temperature on the polymer can be the same as the insert temperature. In all tests, the optimum levels of mold temperatures were 70 °C, except for the weld line tensile and bending strength. However, the weld line bending strengths at temperatures of 30 °C and 70 °C are very close to each other. Only the angle between the force direction of the tensile test and the glass fiber sequence direction of the weld line region can be changed. In all other tests, this angle is constant. Therefore, when the mold is heated up to high-temperatures, in the weld line region, it approaches the 90° angle between the direction of the glass fiber sequence and the direction of molten plastic flow. Thus, the optimum result of the weld line tensile strength was observed at the lowest mold temperature. In other tests, since the angle between the direction of the glass fiber sequence and the direction of force is constant, the highest strength value was found at the highest mold temperature by strengthening the polymer chain structure with increasing mold temperature.

7.3.3 Effect of Melt Temperature

The melt temperature affects the cooling time of the plastic part and the filling of the molten plastic. As the melt temperature increases, the cooling time of the plastic part increases, and the filling of the molten plastic part becomes easier.

Both optimum weld line tensile and bending strengths for ABS were achieved at the melt temperature of 225 °C. The contribution rates were 98.72% for tensile strength and 29.59% for bending strength.

The melt temperature of ABS causes an intense effect on both weld line tensile and bending strength. However, thermal degradation will take place if the melting temperature continues to be increased. A low melt temperature application results in a reduction in tensile and bending strengths because there will be cold flow frontlines in the weld line region. Therefore, the optimum result was properly obtained at a moderate temperature.

In the tensile test of PP GF20, the optimum melt temperature levels for both weld line tensile and bending strength are 240 °C. The contribution rates are 47.36% for the weld line and 85.41% for the non-weld line.

In the bending test of PP GF20, the optimum mold temperatures levels are 215°C for the weld line and 240 °C for the non-weld line specimens. The contribution rates for weld line and the non-weld line specimens were calculated as 4.07% for weld line and 82.85% for the non-weld line specimens

The increasing the melt temperature increases the tensile and bending strengths of both the weld line and the non-weld line region. This is because the melt temperature strengthens the polymer chain structure. Only in the bending test of the non-weld line specimens, the melt temperature level of the highest bending strength was 215 °C. This is because the contribution rate of the melt temperature is low in this test. But the melt temperature generally has a serious contribution rate and effect on the mechanical properties of plastics.

Chapter 8

Conclusion

In this study, the effects of the insert temperature, the mold temperature, and the melt temperature on weld line strength and non-weld line strength in ABS and PP GF20 were investigated by the Taguchi experimental design method.

The parameter effects of the ABS with the insert temperatures of 45, 60, and 75 °C, the mold temperatures of 45, 55, and 65 °C, and the melt temperatures of 210, 225, and 240 °C were experimentally studied.

The parameter effects of PP GF20 with insert temperatures of 30, 50, and 70 °C, mold temperatures of 30, 50, and 70 °C and melt temperatures of 190, 215, and 240 °C have been examined experimentally.

With the Taguchi method, time-saving and experimental efficiency were achieved by reducing the number of experiments. The L₉ orthogonal array, the S/N ratio, and the use of ANOVA are combined. Statistical significance and the contribution rate of each parameter to the weld line and the non-weld line strength were evaluated by statistical analysis of experimental data.

Dimensions and geometries of the runners and gates were selected after ensuring both cavities were filled simultaneously and the weld line appeared at the middle of specimen geometry in the Moldex3D plastic filling analysis program.

The weld line factors for the ABS specimens were found to be approximately 0.98 for tensile strength and 0.95 for bending strength. Since the values of the weld line strength and non-weld line strength are so close to each other, it was reasonably concluded that the weld line caused an inconsiderable effect on both tensile and bending strengths of the ABS specimens.

The weld line factors for the PP GF20 specimen were calculated as 0.57 for tensile strength and 0.91 for bending strength. Then, it was deduced that while the effect of the welding line on the tensile strength of the PP GF20 specimens was predominant, its effect on the bending strength was not as much as the tensile strength.

For the weld line tensile strength of PP GF20, the best results were observed at the low insert and low mold temperatures, and the high melt temperature. The experimental results were best at the high mold and high melt temperatures for non-weld line tensile strength.

For the weld line bending strength of PP GF20, the best results were achieved at the high insert temperature, the low or high mold temperature, and the low melt temperature for the weld line bending strength. The best results were found at the high mold temperature and the high melt temperature for the non-weld line bending strength.

The following conclusions for ABS can be drawn from the experimental results of the Taguchi method:

- According to the ANOVA results, the insert, mold, and melt temperatures contribute to the weld line tensile strength of ABS with percentages of 0.4, 0.49, and 98.72, respectively.
- Rates of contribution to the weld line bending strength of ABS are 64.97%, 4.55%, and 29.59% for the insert, mold, and melt temperatures, respectively.
- The insert temperature and mold temperature have confidence levels of below 95% and the confidence level of the melt temperature is over 99.5% for the weld line tensile tests.
- The insert and melt temperatures have confidence levels of over 95% and the confidence level of the mold temperature is below 95% for the weld line tensile tests.
- For ABS the optimum parameters are $A_2B_3C_2$ for weld line tensile strength and $A_1B_3C_2$ for weld line bending strength.
- The error factor was 0.40% in the tensile test and 0.89% in the bending test. For this reason, the results of the strengths are quite reliable.

Similarly, reasonable conclusions below can be derived from the experimental results for PP GF20:

- Based on the ANOVA results, the insert temperature of 38.31%, the mold temperature of 14.18%, and the melt temperature of 47.36% contribute to the weld line tensile strength of PP GF20. The mold temperature of 13.36% and the melt temperature of 85.41% contribute to the non-weld line tensile strength.
- The insert temperature of 62.05%, the mold temperature of 30.67%, and the melt temperature of 4.07% contribute to the weld line bending strength of PP GF20. The mold temperature of 17.10% and the melt temperature of 82.85 contribute to the non-weld line bending strength.
- Fisher test was performed on the tensile strength of PP GF20 and results above the 99% confidence level were found for each parameter. A 95% confidence level was found in the bending strength, other than the mold and melt temperature of the weld line specimens. Thus, it was proved that the experimental design was successful.
- The optimum parameters of weld line tensile strength in PP GF20 are $A_1B_1C_3$ in the experimental set. The optimum parameters of the non-weld line tensile strength are B_3C_3 .
- The optimum parameters of weld line bending strength in PP GF20 are $A_3B_1C_2$ in the experimental set. The optimum parameters of the non-weld line bending strength are B_3C_3 .
- With the increase of the insert temperature in PP GF20, the weld line tensile strength decreases, the weld line bending strength increases.
- As the mold temperature increases in PP GF20, the weld line tensile strength decreases the non-weld line tensile strength increases, and the non-weld line bending strength increases. A high result in weld line bending strength was observed when the mold temperature was low or high.
- With the increase of melt temperature in PP GF20, the welding line tensile strength, the non-welded line tensile strength, and the non-welded line bending strength were increased. The weld line bending strength typically reached the highest result at an average melt temperature.
- The error factor was 0.15%, 3.21% in the tensile test and bending test, respectively. Therefore, the results of the strengths are trustworthy

As a result of this experimental study, it has been observed that local heating or cooling has a significant effect on both weld line tensile and bending strengths.

Chapter 9

Future Work

After performing the plastic filling analysis, the strength analysis can also be performed using the finite element method and confirmed by further experimental studies.

The effect of changing the types of the runner and gate on the weld line with computer-aided analysis programs can be examined and compared with the experimental study.

The weld line effect of local heating can be investigated experimentally and verified by computer analysis for various types of thermoplastics, diverse reinforcing materials, and particular filler materials.

After local heating, the weld line microstructure can be inspected with a scanning electron microscope (SEM) and transmission electron microscopy (TEM). The effect of local heating on fiber and polymer orientation can be observed in the weld line region.

References

- [1] Groover MP. *Fundamentals of Modern Manufacturing Materials, Processes, and Systems*, 5. edition. Wiley; 2012.
- [2] Marmillo J. *Persistence of defects during class-A sheet thermoforming of thermoplastic olefins (master's thesis)*. Bethlehem: Lehigh University; 2008.
- [3] Belcher SL. *Blow Molding, Applied Plastics Engineering Handbook: Processing, Materials, and Applications*, 2. edition. 2017.
- [4] Plastics Europe Association of Plastics Manufacturers “World Plastics Production 1950-2015,” 2015.
- [5] Klein R. *Laser Welding of Plastics*, Wiley-VCH; 2012.
- [6] Mazumdar SK. *Composites manufacturing materials, product, and process engineering*, CRC Press LLC; 2002.
- [7] Güney ZH. *The evaluation of different fillings in thermoplastic materials shaping in injection to weld line (master's thesis)*. Sakarya: Sakarya University; 2011.
- [8] Malloy RA. *Plastic part design for injection molding: an introduction*, 2. edition. Hanser; 2010.
- [9] Lan P, Nunez EE, Polycarpou AA. *Advanced Polymeric Coatings and Their Applications: Green Tribology. Reference Module in Materials Science and Materials Engineering* 2019; 1-14. doi.org/10.1016/B978-0-12-803581-8.11466-3
- [10] Goodship V. *Practical Guide to Injection Moulding*, Arburg; 2004.

- [11] Kale PD, Darade PD, Sahu AR. A literature review on injection molding process based on runner system and process variables. *Materials Science and Engineering* 2021; 1017: 1-8. doi:10.1088/1757-899X/1017/1/012031
- [12] Xie L, Shen L, Jiang B. Modelling and Simulation for Micro Injection Molding Process. *Computational Fluid Dynamics Technologies and Applications* 2011; 317-332. DOI:10.5772/16283
- [13] Rosato DV, Rosato DV, Rosato MG. *Injection molding handbook*. Kluwer Academic Publishers; 2000.
- [14] Onken J, Hopmann C. Prediction of weld line strength in injection-molded parts made of unreinforced amorphous thermoplastics. *International Polymer Science and Technology* 2016; 69: 574–580.
- [15] Rajasekaran K. *Fracture Failure and Influence of Process Parameters, Material Selection and Moisture Content on Weld Lines* (master's thesis). Municipality: Department of Mechanical Engineering Blekinge Institute of Technology; 2014.
- [16] Bociąga E, Skoneczny W. Characteristics of injection molded parts with the areas of weld lines. *Polimery* 2020; 65(5): 337–345.
- [17] Bociąga E, Jaruga T. Experimental investigation of polymer flow in injection mold, *Archives of Materials Science and Engineering* 2007; 28(3): 165-172.
- [18] Dzulkipli AA, Azuddin M. Study of the Effects of Injection Molding Parameter on Weld Line Formation. *Procedia Engineering* 2017; 184: 663–672.
- [19] Raz K, Sedlacek F. Effect of melt temperature on weld line strength. *Key Engineering Materials* 2019; 801: 264–269.
- [20] Xie L, Ziegmann G. Influence of processing parameters on microinjection molded weld line mechanical properties of polypropylene (PP). *Microsystem Technol* 2009; 15: 1427–1435.
- [21] Liu SJ, Wu JY, Chang JH. An experimental matrix design to optimize the weldline strength in injection molded parts. *Polymer Engineering and Science* 2000; 5: 1256-1262.

- [22] Chookaew W, Mingbunjurdsuk J, Jittham P, Ranong NN, Patcharaphun S. An investigation of weldline strength in injection molded rubber parts. *Energy Procedia* 2013; 34: 767-774.
- [23] Boparai KS, Singh R. Thermoplastic Composites for Fused Deposition Modeling Filament: Challenges and Applications. Reference Module in Materials Science and Materials Engineering 2018; 0-12.
- [24] Banik K. Effect of mold temperature on short and long-term mechanical properties of PBT. *Express Polymer Letters* 2008; 111–117.
- [25] Takayama T. Weld strength of injection molded short fiber reinforced polypropylene, *Mechanics of Materials* 2019.
- [26] Oh GH, Jeong JH, Park SH, Kim HS. Terahertz time-domain spectroscopy of weld line defects formed during an injection molding process. *Composites Science and Technology* 2018; 157: 67-77.
- [27] Simas R. The effect of recycle history and processing temperature on the weld line strength of a polypropylene (master's thesis). Lowell: University of Massachusetts; 2004.
- [28] Şahin T, Şahin Ş. Kalsiyum karbonat mineral dolgu maddesinin polipropilen random kopolimer bore malzemesinin performansına etkisi. *Proceedings of 8th International Fracture Conference* 2007; 269-279.
- [29] Beaumont J. Plastic part design to use ribs or not to use ribs – That is the question, American Injection Molding Institute 2016. http://read.nxtbook.com/wiley/plasticsengineering/october2016/atoystory_playingwithplastic.html
- [30] Özçelik B, Kuram E, Topal MM. Investigation the effects of obstacle geometries and injection molding parameters on weld line strength using experimental and finite element methods in plastic injection molding. *International Communications in Heat and Mass Transfer* 2012; 39(2): 275–281.
- [31] Beaumont JP. *Runner and Gating Design Handbook*. 3rd edition. Hanser; 2019.

- [32] Kapila A, Singh K, Arora G, Agarwal N. Effect of Varying Gate Size on the Air Traps in Injection Molding. *International Journal of Current Engineering and Technology* 2015; 5(1): 161-165.
- [33] Khichadi RS. Injection mold design and optimization of battery air vent. *International Journal of Innovations in Engineering and Technology* 2013; 3(2): 88-93.
- [34] Miranda DAD, Nogueira AL. Simulation of an injection process using a CAE tool: Assessment of operational conditions and mold design on the process efficiency. *Materials Research* 2019; 22(2). doi.org/10.1590/1980-5373-MR-2018-0564
- [35] Zhang Y, Zhou H. Cooling simulation. Ed.: Rose TJ. *Computer Modeling for Injection Molding*. John Wiley & Sons, Inc. Published; 2013. 129-156.
- [36] Marques S, Souza AFD, Miranda J, Yadroitsau I. Design of conformal cooling for plastic injection molding by heat transfer simulation. *Polimeros* 2015; 25(6): 564-574.
- [37] Wu CH, Liang WJ. Effects of geometry and injection-molding parameters on weld-line strength, *Polymer Engineering and Science* 2005; 45(7): 1021-1030.
- [38] Poornima K, Ansari MNM. Cooling Channel Design for Multi-Cavity Plastic Injection Moulds, *International Journal of Science and Research* 2013; 2(5): 6-11.
- [39] Ulker A. Welding parameters and joint strength optimization during friction stir welding of high-density polyethylene (HDPE) using the Taguchi method. *Production-Oriented Testing* 2016; 58: 423-432.
- [40] Montgomery, DC, Runger, GC, Hubele, NF. *Engineering Statistics*, SI, 5. edition. Wiley; 2012.
- [41] Ulker A. Application of the Taguchi method for the optimization of the strength of polyamide 6 composite hot plate welds, *Materials Testing* 2015. 57.

[42] TS EN ISO 527-2 2012. Part 2 Test conditions for molding and extrusion plastics. 2012.

[43] TS EN ISO 178:2019. Plastics - Determination of flexural properties. 2019.

Appendices

Appendix A

Publications from the Thesis

Conference Papers

1. Güler M.D., Ülker A. The Effect of Local Heating on the Weld Line Formation in Plastic Injection Molding of Acrylonitrile Butadiene Styrene. 14th International Conference of Strategic Research on Scientific Studies and Education 2021: 23-37

Journal Articles

1. Güler M.D., Ülker A., Sayer S. The Effect of Local Heating on the Weld Line Formation in Plastic Injection Molding of Glass Fiber Reinforced Polypropylene (Manuscript in preparation)

Curriculum Vitae

Name Surname : Muhsin Deniz Güler

Education:

2012–2017 Dokuz Eylül University, Dept. of Mechanical Eng.

2019–2022 İzmir Kâtip Çelebi University, Dept. of Mechanical Eng.

Work Experience:

2018 – 2020 Metis Kalıp Makina Elektronik Mühendislik “. ve Tic. A.Ş

2021 – Present Kor Ev Otomasyon Sistemleri San. ve Tic. Ltd. Şti.

Publications:

1. Güler M.D., Ülker A. The Effect of Local Heating on the Weld Line Formation in Plastic Injection Molding of Acrylonitrile Butadiene Styrene. 14th International Conference of Strategic Research on Scientific Studies and Education 2021: 23-37